AD 427397

AFCRL-63-541

[redacted]

RCA VICTOR COMPANY, LTD.
RESEARCH LABORATORIES
MONTREAL, CANADA

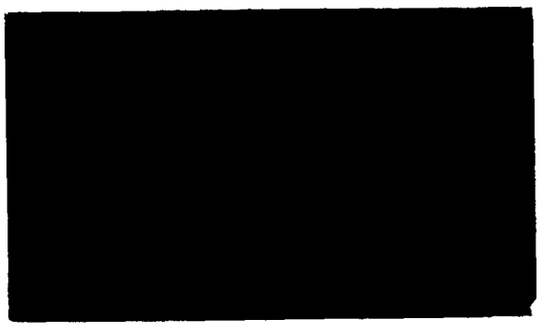

NOTICE:

Requests for additional copies by Agencies of the Department of Defense, their contractors, and other Government agenicies should be directed to the:

DEFENSE DOCUMENTATION CENTER (DDC)
CAMERON STATION
ALEXANDRIA, VIRGINIA

Department of Defense contractors must be established for DDC services or have their 'need-to-know' certified by the cognizant military agency of their project or contract. All other persons and organizations should apply to the:

U.S. DEPARTMENT OF COMMERCE
OFFICE OF TECHNICAL SERVICES
WASHINGTON 25, D.C.

AFCRL-63-541

ANALYTICAL AND EXPERIMENTAL INVESTIGATION OF THE PRESENCE OF IONIZED MEDIA ON ANTENNA PROPERTIES

M.P. Bachynski

RCA Victor Company, Ltd.
Montreal, Canada

Project 4642
Task 464201

Final Report

on

Contract AF 19(604)-7334

October 1963

Prepared by M.P. Bachynski

Approved by Director of Research

Prepared for

Air Force Cambridge Research Laboratories
Office of Aerospace Research
United States Air Force
Bedford, Massachusetts

ANALYTICAL AND EXPERIMENTAL INVESTIGATION OF THE PRESENCE OF IONIZED MEDIA ON ANTENNA PROPERTIES

M.P. Bachynski

Research Laboratories
RCA Victor Company, Ltd.
Montreal, Canada

ABSTRACT

The following research programme has been performed under Contract AF 19(604)-7334.

An experimental investigation of the behaviour of a microwave horn antenna in the presence of a plasma sheath generated in helium, has been conducted at a frequency of 9.7Gc (x-band). The effect of the plasma sheath on the far-field radiation pattern of the horn antenna is to decrease the signal level at normal incidence (by as much as 25db at "cut-off" conditions) and to redistribute the energy of the radiation pattern over angle so that at large scanning angles the sidelobe level may exceed those measured when the plasma is absent. The plasma does not, however, present a serious mismatch to the antenna indicating that the plasma is not highly reflecting.

A simplified theoretical model which considers the plasma as a uniform, infinite slab and takes into account diffraction around the edge of the experimental plasma container can be used to account for many of the significant features which are observed.

A comprehensive series of investigations designed to test the validity of various theoretical treatments of plasma properties and to assess the accuracy of various microwave systems for determining the properties of plasmas which are finite in extent using free-space microwave techniques have been performed. Theoretical results have been obtained for prediction of plasma effects such as plasma boundaries, refractive defocussing, non-uniformity of plasma and diffraction due to finite size of the plasma. Measurements on various experimental geometries demonstrated the influence of the dielectric boundaries of the plasma container, the effect of multiple reflections within the measurement system and the precautions which must be exercised both in the measurement and interpretation of the results. Measurements of plasma properties using a number of different microwave arrangements were assessed and the limitations of the various systems shown. Finally, free-space microwave determination of the properties of a plasma generated in helium and in argon have been made.

Preliminary considerations have been given to the investigation of antenna properties in the presence of a plasma sheath which is anisotropic due to the presence of a static magnetic field. A magnetic field apparatus suitable for such investigations and capable of generating magnetic field strengths in excess of 4500 gauss with a working diameter of 7" has been assembled and tested.

TABLE OF CONTENTS

I INTRODUCTION

A great deal of attention is being given at present to the performance of antennas in the presence of ionized media and in particular to the effect of a plasma sheath on communications to and from radio systems engulfed by the plasma sheath. The aim of the work performed under Contract AF 19(604)-7334 was to investigate experimentally and analytically the effect of ionized media on the properties of microwave antennas.

An experimental investigation of the influence of an isotropic plasma sheath located in front of a microwave horn antenna on the radiation pattern and impedance of that antenna was conducted. The plasma sheath was generated by a 60c/s discharge in helium contained in a cylindrical container. The effect of this plasma sheath on the radiation characteristics and impedance of the microwave horn antenna was measured in detail at a frequency of 9.7Gc using a fast-acting microwave phase and amplitude measuring system. Using the reciprocity theorem, analytic expressions were derived for the radiation pattern of a microwave horn in front of an infinite plasma slab. These predictions did not agree with the experimental values. By using a theoretical model which treats the plasma as a uniform infinite slab and which considers diffraction around the edge of the experimental plasma container, most of the important features of the measurements could be explained. This illustrated importance of diffraction effects due to the finite size of the plasma on the experimental measurements. In order to simulate the influence of a plasma sheath on the radiation pattern of a microwave antenna in the laboratory, a finite plasma contained in a dielectric bottle and a "real" microwave measurements system must always be used. The result is that some refraction, reflection, absorption and diffraction effects are present. It was thus necessary to ascertain these effects in detail in order to either eliminate or minimize their influence and to be able to make a detailed quantitative interpretation of the experimental results.

Consequently, a comprehensive series of investigations designed to test the validity of various theoretical treatments of plasma properties

and to assess the accuracy of various microwave systems for determining the properties of plasmas which are finite in extent using free-space microwave techniques was undertaken.

Theoretical results were obtained for prediction of plasma effects such as plasma boundaries, refractive defocussing, non-uniformity of plasma and diffraction due to finite size of the plasma. Measurements on various experimental geometries demonstrated the influence of the dielectric boundaries of the plasma container, the effects of multiple reflections within the measurement system and the precautions which must be exercised both in the measurement and interpretation of the results. Measurements of plasma properties using a number of different microwave arrangements were assessed and the limitations of the various systems shown. Finally, free-space microwave determination of the properties of a plasma generated in helium and in argon were made.

Having thus gained considerable insight into the effect of the limitations of the finite size of the plasma, it is now possible to design and conduct more quantitative experiments on the properties of antennas in ionized media. A natural extension of the aforementioned study of the effect of an isotropic plasma sheath on the characteristics of a microwave antenna is to perform similar measurements in the presence of a plasma immersed in a static magnetic field and hence ascertain if the sheath can be made transparent through the use of magnetic fields. In order to perform such investigations a magnetic field facility is necessary. Such a magnetic field apparatus has been set-up and tested and preliminary considerations of the investigation of antenna properties in the presence of anisotropic plasma sheaths has been made.

The research programme conducted under this contract can thus be divided into the following phases:

1. Investigation of Antenna Properties in the Presence of Isotropic Ionized Media.
2. Microwave Measurements of Finite Plasmas.
3. Preliminary Considerations and Facilities for Investigation of Antenna Properties in the Presence of Anisotropic Ionized Media.

The first two phases have been described in detail in scientific reports. Consequently, only a brief account of these investigations will be given here. This report also contains preliminary consideration of antenna properties in the presence of anisotropic media and a description of a magnetic field facility set-up for such investigations.

As a result of the investigations conducted under Contract AF 19(604)-7334 the following scientific reports and papers were written:

Scientific Reports

G.G. Cloutier, M.P. Bachynski, K.A. Graf — "Antenna Properties in the Presence of Ionized Media" AFCRL-62-191, March (1962).

M.P. Bachynski, G.G. Cloutier, K.A. Graf — "Microwave Measurements of Finite Plasmas" AFCRL-63-161, May (1963).

Papers Published

G.G. Cloutier, M.P. Bachynski — "Antenna Radiation Patterns in the Presence of a Plasma Sheath", Proc. Symp. on The Plasma Sheath, Plenum Press.

G.G. Cloutier, M.P. Bachynski — "Antenna Characteristics in the Presence of a Plasma Sheath", Proc. Symp. on E-M Theory and Antennas, Pergamon Press, pp. 537-548 (1963).

M.P. Bachynski, K.A. Graf — "Electromagnetic Properties of Finite Plasmas" RCA Review XXV, March (1964) - (to be published).

The following papers were presented on work conducted under AF 19(604)-7334

G.G. Cloutier, M.P. Bachynski — "Antenna Radiation Patterns in the Presence of a Plasma Sheath", 2nd Symp. on The Plasma Sheath, Boston, April 10-12 (1962).

G.G. Cloutier, M.P. Bachynski — "Antenna Characteristics in the Presence of a Plasma Sheath", Symp. on E-M Theory and Antennas, Copenhagen, June 25-30 (1962).

M.P. Bachynski, G.G. Cloutier — "Free-Space Microwave Measurements of Plasma Properties" PTGAP International Symp., Boulder, July 9-11 (1963).

II ANTENNA PROPERTIES IN THE PRESENCE OF ISOTROPIC IONIZED MEDIA

Experiments have been conducted which were designed to examine the influence of an isotropic plasma sheath located in front of the aperture of an x-band (9.7Gc) horn antenna on the far-field radiation pattern and impedance of that antenna. The experimental techniques, radiation pattern and impedance measurement of the antenna in the presence of plasma and theoretical investigations and interpretations are described below.

(a) Experimental Techniques

Containment and Generation of the Plasma: To approximate a slab of plasma, the plasma was confined in a cylindrical glass container terminated at both ends by parallel low loss dielectric (polystyrene) plates. The size of the container was limited by the requirements for a uniform discharge throughout the entire volume and by the amount of power required to generate a sufficiently intense plasma (for the x-band microwave region) in this large volume. The final size of the container (see Fig. 1) was 8 inches in diameter and 4-3/4 inches long corresponding to a thickness of the order of 3.5 wavelengths at x-band.

In order to apply power to the gas in the container, two flat electrodes made of non-magnetic stainless steel were located within the container at a distance of 6-1/4 inches apart. Outlet and inlet connections for evacuating the plasma container and admitting the gas into it were also provided. The plasma is generated by applying a 60c/s voltage through a 10:1 step-up transformer to the electrodes. Typical operating conditions are a voltage of 900 volts r.m.s. across the discharge and a current of one ampere both suitable monitored by an ammeter and voltmeter located in the circuit. Due to the relatively high power generation in the plasma ($\sim$ 1 kilowatt), it was necessary to operate the discharge in short bursts of not more than one second to prevent overheating the container. Synchronization of the measurements with the firing of the plasma was accomplished from a main control switch.

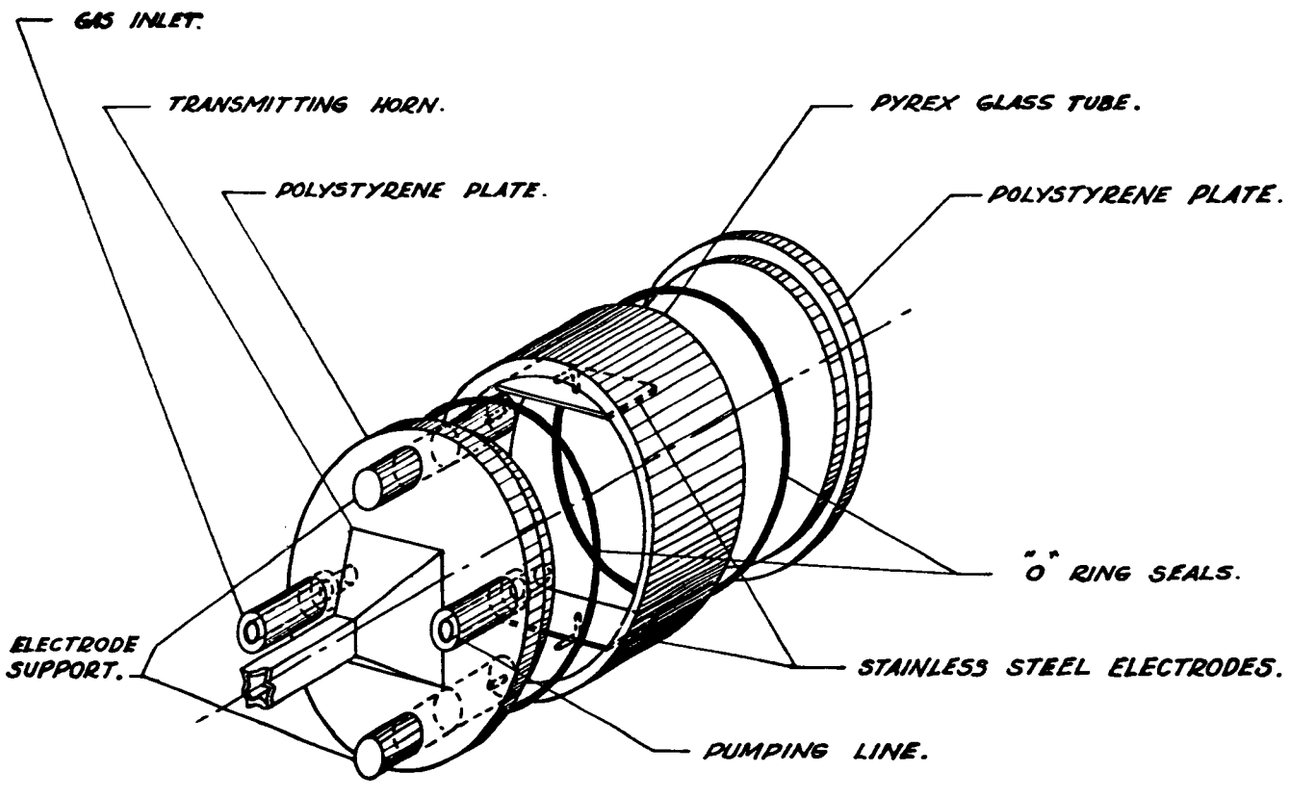

Fig. 1: Exploded view of the plasma container.

Helium gas was employed for the discharge and introduced into the plasma container through a fine control needle valve in series with a pressure regulator and a high pressure helium reservoir. In order to prevent accumulation of impurities in the plasma container and to insure reproducibility of the plasma conditions, a continuous gas feed system was used in which a small helium flow rate maintained the gas pressure in the plasma container at a constant value. The arrangement of the plasma container, the discharge electrical supply unit and the gas handling system are shown in Fig. 2.

Microwave Arrangement and Techniques: The microwave transmitting horn (15db gain) is also shown in Fig. 2, together with the plasma container positioned on a rotary turntable. The receiver horn and auxiliary microwave system is located in the far-field of the transmitter. The turntable is motor driven and the angle of rotation is determined by a synchro-generator. The entire microwave arrangement is located within an anechoic room in such a way as to eliminate reflection from the walls.

The microwave measurements are carried out using the "multiple probe" technique developed by Osborne[1]. The multiprobe system allows simultaneous measurements of phase and amplitude to be made over a wide dynamic range and at a very rapid sampling rate. The resulting display on an oscilloscope trace is a polar plot of amplitude and phase, i.e. the magnitude of the radius vector corresponds to the signal amplitude and the polar angle to the phase of the microwave signal. The system can be used for measurement of either the transmitted or reflected signal.

In this experiment a system was developed to display on an oscilloscope the changes of phase and amplitude of the microwave signal transmitted through or reflected by the plasma as the plasma characteristics changed during one-quarter of a cycle of the 60 cycle gas discharge. By applying to the oscilloscope a series of sharp brightening pulses at a repetition rate of 10 Kc/s, the measurements were displayed as a series of bright spots as shown in Fig. 3. In this manner 40 points or 40 values of the plasma properties could be sampled in one-quarter

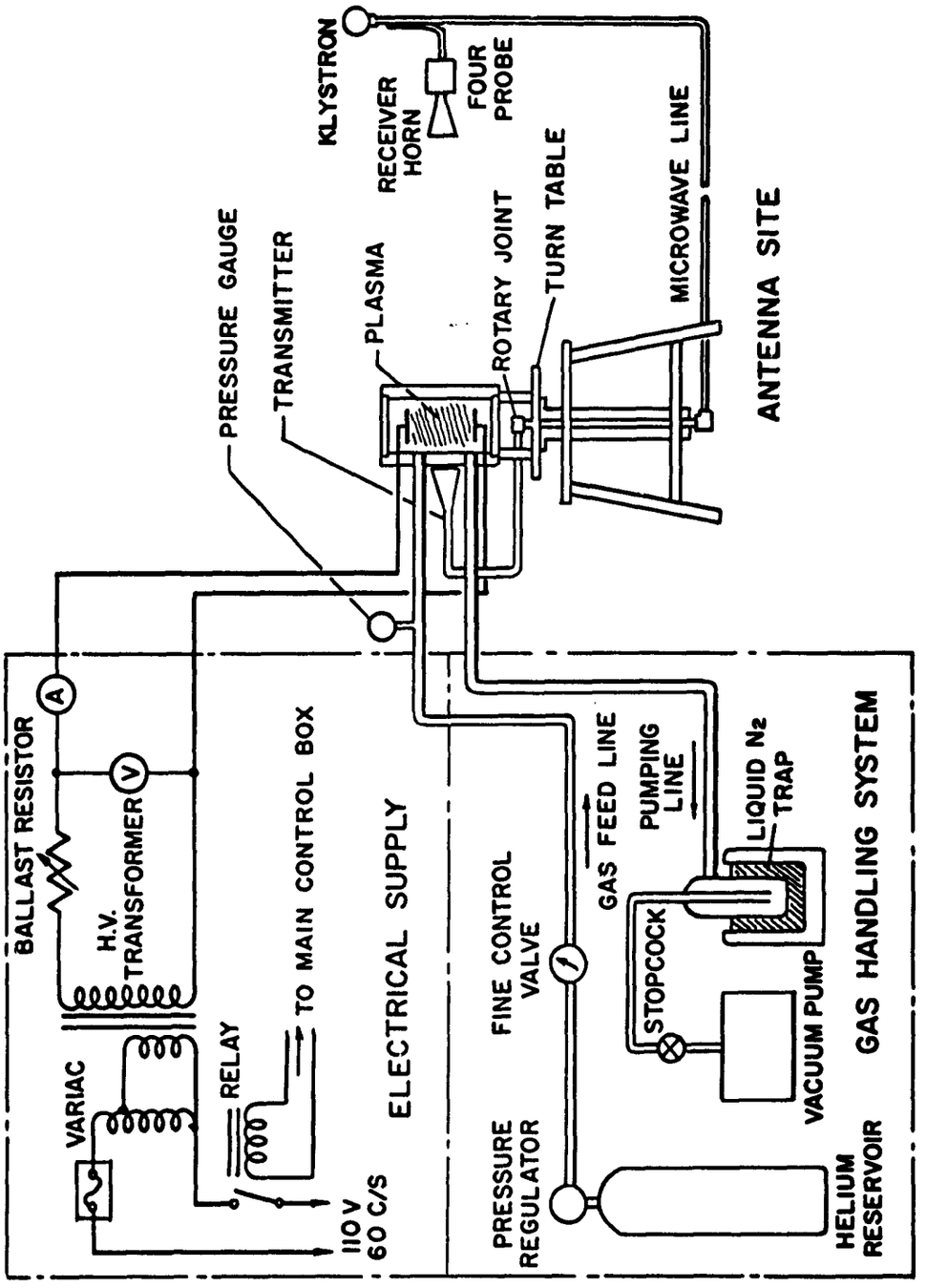

Fig. 2: Schematic diagram of the experimental set-up.

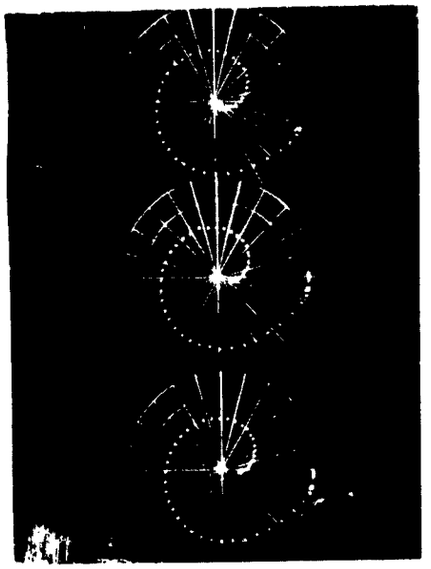

Fig. 3: Typical measurements of transmission of electromagnetic waves through a time-varying plasma using the multiple probe technique at a frequency of 9.7Gc. The radius vector of the polar display corresponds to amplitude while the polar angle is a direct measure of the phase of the microwave signals.

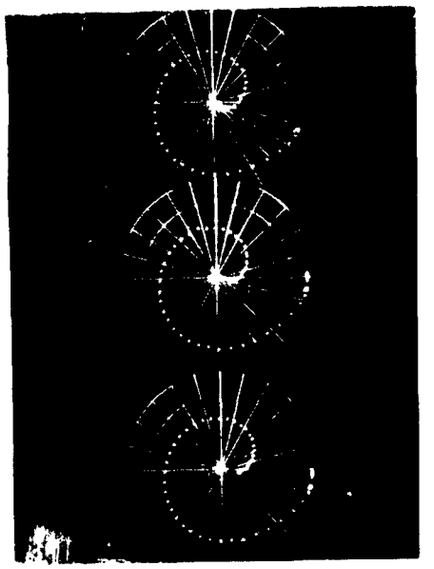

Fig. 3: Typical measurements of transmission of electromagnetic waves through a time-varying plasma using the multiple probe technique at a frequency of 9.7Gc. The radius vector of the polar display corresponds to amplitude while the polar angle is a direct measure of the phase of the microwave signals.

cycle of the discharge. Figure 3 illustrates a typical display of microwave transmission measurement across the bottle. The points appearing near the edge of the screen correspond to the zero voltage condition across the discharge and it is seen that as the discharge intensity is increased, a large attenuation and phase shift is observed for a x-band (9.7Gc) signal passing through the plasma. Note the continuous unambiguous display of phase change in excess of an angle of 360°. This is another of the advantages of the multiple probe technique and display. In addition, scale expansion for greater accuracy at the high attenuation levels can also readily be done.

The optimum conditions under which a uniform plasma in helium of sufficient electron density to markedly affect x-band signal frequencies could be produced was experimentally determined to occur at pressures ranging from 0.30 to 1.0 torr. At low pressure, the electron density is insufficient, while at higher pressures the discharge becomes non-uniform constricting itself to the region between the electrodes. For the measurements presented here, the helium pressure was maintained at 0.85 torr which assuming a uniform plasma slab corresponds to a plasma frequency of about 0.8 of the signal frequency at x-band at the peak of the discharge cycle.

(b) Antenna Pattern and Impedance Measurements in the Presence of Plasma

Far-Field Antenna Patterns: The far-field antenna radiation patterns in the presence of a plasma were measured in the following way. Since the discharge could only be run for a short interval of time due to the large amount of power dissipated in the plasma container, a record of the phase and amplitude of the received signal for a fixed scanning angle was obtained over a quarter cycle of the discharge by means of the multiple probe sampling system. Consequently, it was only necessary to run the discharge a fraction of a second for the measurements at a given scanning angle. The same procedure was then repeated

at two degree intervals of scanning angle. The far-field radiation patterns for a given plasma intensity could then be obtained by plotting the attenuation of a given dot on the multiple probe display as function of the scanning angle. The phase variation with scanning angle for a specific plasma could similarly be obtained from a plot of the phase angle variation for a given dot. The dots on the displays are synchronized with the gas discharge and can thus be used as time markers corresponding to different plasma properties. The antenna radiation patterns for other plasma intensities are, of course, constructed from the positions of other dots on the multiple probe displays.

For the above procedure to be valid, the electronic microwave sampling system must be kept stable during a complete set of measurements and the discharge must be accurately reproducible for each angle of the scanning range. The tests and procedures to achieve this are described in detail by Cloutier and Bachynski[8].

Typical measurements of the far-field radiation pattern (both amplitude and phase) ofa microwave horn in the presence of a sheath of plasma are shown in Fig. 4. The variations shown in Fig. 4 were obtained at x-band (9.7Gc) with the electric vector of the transmitting horn set in the horizontal direction. (A similar result is obtained with the other polarization).

The general characteristics of the x-band radiation patterns of the horn antenna in the presence of a plasma are the following. A pronounced minimum is observed at normal incidence and this minimum becomes predominant with increasing plasma density. The side lobes of the antenna pattern tend to increase relative to the main lobe power level and at large scanning angles ($30\text{-}40^{\circ}$) may be greater than their no plasma value. The phase front emanating from the plasma covered antenna tend to become more planar with increasing electron density. Due to the limited size of the plasma container it is evident that the effects at large scanning angles are seriously affected by diffraction around the edges of the container. At greater electron densities ($\omega_p/\omega > 0.75$ where ω_p = plasma frequency, ω = signal frequency), the received signal

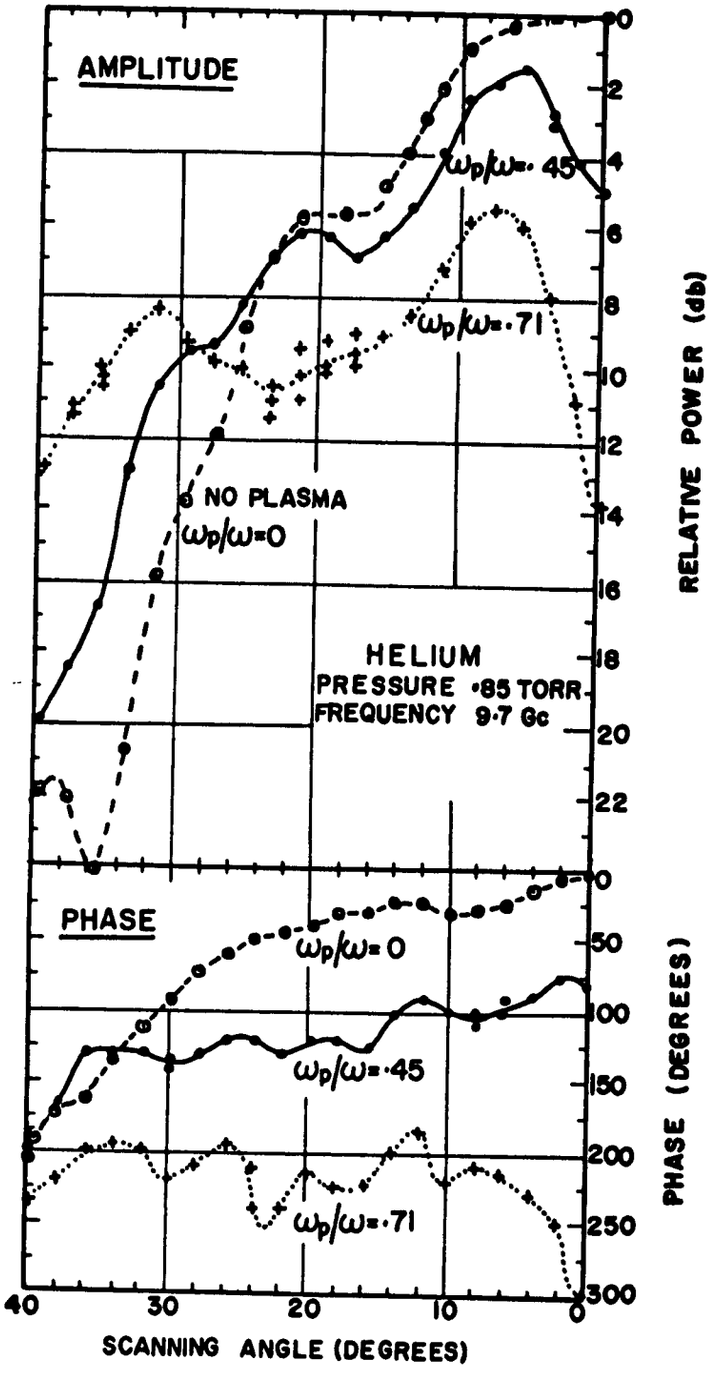

Fig. 4: Measured far-field radiation pattern (intensity and phase) in the presence of a helium plasma at x-band (9.7Gc).

is generally more than 15 decibels below the signal received at normal incidence in the absence of the plasma. These patterns are not shown in Fig. 4, but their power levels lie well below those illustrated.

Auxiliary measurements of phase shift of a microwave signal transmitted directly across the plasma were used to evaluate the electron concentration and hence the plasma frequency. The evaluation of the electron concentration was based on the theory for a uniform slab of plasma of thickness equal to that of the interior of the plasma container. This gave average electron concentration of 10^{12} electrons/cm^3 at the peak intensity of the gas discharge. Since microwave measurements of attenuation are much more sensitive to the geometrical arrangement of the experiment, it is consequently much more difficult to obtain accurate conclusions regarding the collision frequency.

Antenna Impedance: The signal incident on the plasma and reflected back into the transmitting horn creates a mismatch at the transmitter. This effect of the plasma on the impedance of the transmitting horn was also examined using the multiple-probe system. The multiple-probe system gives a very convenient direct Smith chart display of the antenna impedance.

Typical variations of the antenna impedance with plasma properties at x-band frequencies are shown in Fig. 5. The multiple probe display has been expanded to correspond to a preset nominal voltage standing wave ratio (VSWR) at the outer ring of the record. The centre point of the display corresponds to a VSWR of one and the transmitting horn has been matched to the plasma container when there is no plasma. The variation of the antenna impedance is then given by the spiral trace starting from the origin and tracing out the antenna impedance over one-quarter cycle of the gas discharge (from the no plasma intensity).

At x-band, even for plasma densities approaching the "cut-off" condition, the VSWR introduced by the plasma does not exceed 1.70. Comparing the VSWR measurements with transmission measurements (Fig. 3) it can be seen that, as expected, the highest mismatch corresponds to conditions of least transmission or greatest attenuation. It thus appears

is generally more than 15 decibels below the signal received at normal incidence in the absence of the plasma. These patterns are not shown in Fig. 4, but their power levels lie well below those illustrated.

Auxiliary measurements of phase shift of a microwave signal transmitted directly across the plasma were used to evaluate the electron concentration and hence the plasma frequency. The evaluation of the electron concentration was based on the theory for a uniform slab of plasma of thickness equal to that of the interior of the plasma container. This gave average electron concentration of 10^{12} electrons/cm^3 at the peak intensity of the gas discharge. Since microwave measurements of attenuation are much more sensitive to the geometrical arrangement of the experiment, it is consequently much more difficult to obtain accurate conclusions regarding the collision frequency.

Antenna Impedance: The signal incident on the plasma and reflected back into the transmitting horn creates a mismatch at the transmitter. This effect of the plasma on the impedance of the transmitting horn was also examined using the multiple-probe system. The multiple-probe system gives a very convenient direct Smith chart display of the antenna impedance.

Typical variations of the antenna impedance with plasma properties at x-band frequencies are shown in Fig. 5. The multiple probe display has been expanded to correspond to a preset nominal voltage standing wave ratio (VSWR) at the outer ring of the record. The centre point of the display corresponds to a VSWR of one and the transmitting horn has been matched to the plasma container when there is no plasma. The variation of the antenna impedance is then given by the spiral trace starting from the origin and tracing out the antenna impedance over one-quarter cycle of the gas discharge (from the no plasma intensity).

At x-band, even for plasma densities approaching the "cut-off" condition, the VSWR introduced by the plasma does not exceed 1.70. Comparing the VSWR measurements with transmission measurements (Fig. 3) it can be seen that, as expected, the highest mismatch corresponds to conditions of least transmission or greatest attenuation. It thus appears

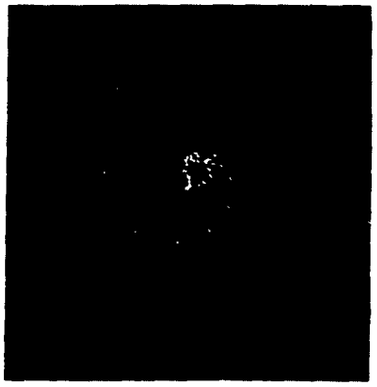

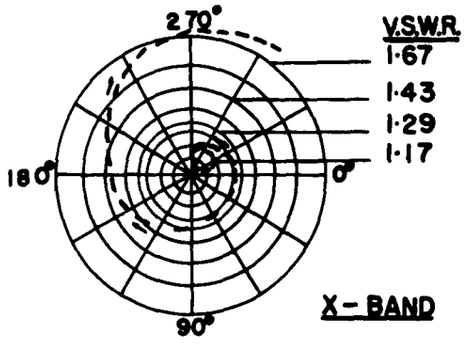

Fig. 5: Measured antenna impedance in the presence of plasma sheaths of different properties at x-band (9.7Gc).

that even at high electron densities most of the microwave energy penetrates into the plasma where at the peak plasma intensities a great fraction of the incident energy is absorbed and/or scattered by the plasma. The results are consistent with calculation based on a lossy slab of plasma[3].

(c) Radiation Pattern of a Microwave Horn in Presence of an Infinite Plasma Slab

Application of Reciprocity Theorem - Using Lorentz's reciprocity theorem it can be shown[3] that the field $\vec{E}_1(2)$, due to a source T_1, observed at point T_2 in the far-field may be expressed by

$$\vec{E}_1(2) = \vec{a} \int_{s_1} (\vec{H}_1 \times \vec{E}_2 - \vec{H}_2 \times \vec{E}_1) \cdot \vec{n}_1 \, ds \qquad (1)$$

where $\vec{a}$ is a vector along $\vec{E}_1(2)$,

$\vec{n}_1$ is a unit vector normal to the surface s_1

and E_2 and H_2 are the fields due to a dipole source at T_2.

From Equation (1) it is seen that the field due to the source T_1 may be evaluated at T_2 from a knowledge of the fields due to T_1 and T_2 on the surface s_1. It can be shown that by properly choosing the surface s_1 it is possible to greatly simplify the problem of evaluating the radiation pattern of an antenna in the presence of a plasma sheath. The experimental arrangement may be represented by the schematic diagram of Fig. 6.

The surface of integration s_1 is chosen as an infinite plane lying between the aperture of the transmitting horn T_1 and the surface of the plasma slab facing the transmitter. In our experiment the receiving horn T_2 is located in the far-field of the plasma slab. Therefore a wave launched from T_2 can be regarded to a good approximation as a plane wave incident on the plasma slab. The field on s_1, due to the point source at T_2 can thus be written as

$$\begin{aligned} E_2(\phi) &= T(\phi)\, E_{2o}(\phi) \\ H_2(\phi) &= T(\phi)\, H_{2o}(\phi) \end{aligned} \qquad (2)$$

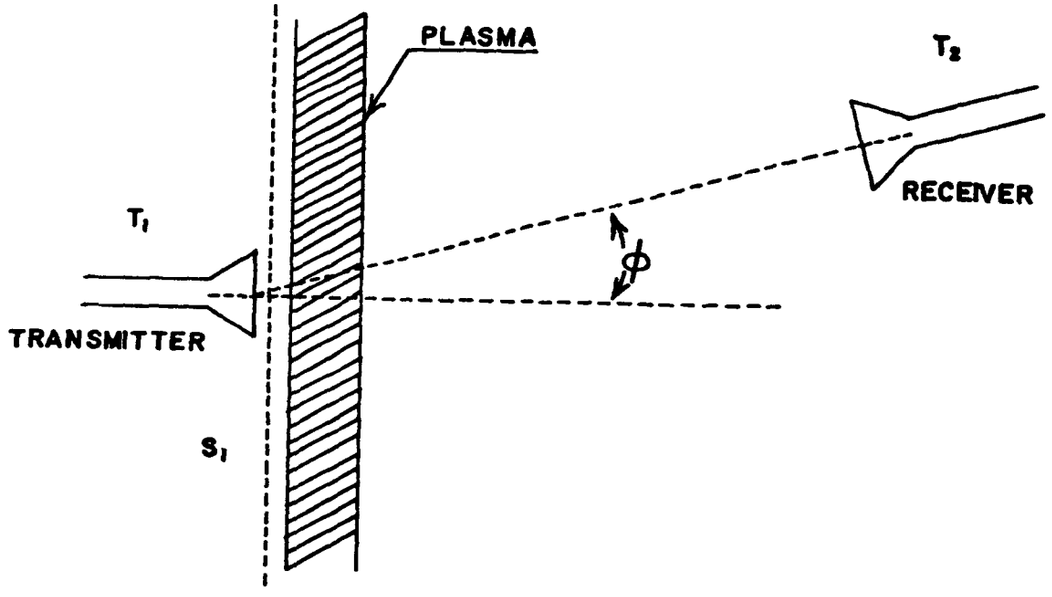

Fig. 6: Schematic diagram describing the parameters used in derivation of the radiation pattern of a microwave horn in the presence of a uniform plasma slab.

where $T(\phi)$ is the amplitude transmission coefficient of a plane wave incident on the plasma slab at an angle ϕ. E_{2o}, H_{2o} is the amplitude of the field incident on the plasma slab. The field on s_1 due to the transmitting horn T_1 is given by the phase and amplitude distribution of the field in the aperture of the horn. Since $T(\phi)$ is independent of position on s_1, Eq. (1) becomes

$$\vec{E}_1(2) = T(\phi)\vec{a}\int_{s_1}(\vec{H}_{2o}\times\vec{E}_1 - \vec{H}_1\times\vec{E}_{2o})\cdot\vec{n}\,ds \tag{3}$$

Furthermore since E_{1o}, H_{1o} can be described by a plane wave the integral over s_1 essentially represents the far-field radiation pattern of the transmitting horn T_1. Therefore the radiation pattern of the horn in the presence of a plasma slab can be expressed by

$$\vec{E}_1(2) = T(\phi)\,\vec{U}_1(\phi) \tag{4}$$

where $U_1(\phi)$ is the far-field radiation pattern of the horn T_1. Equation (4) is extremely useful since it shows that the radiation pattern can be computed simply from the knowledge of the transmission coefficient of the plasma slab and the far-field radiation pattern of the transmitting horn. The above derivation is justified as long as the absorptivity of the plasma to microwaves is not too large i.e. within the limits of the geometrical optics approximations.

The transmission and reflection coefficients of an infinite slab of plasma d bounded by free space when a plane electromagnetic wave is incident on the plasma at an angle θ are given by[3]:

$$TT^* = \Big\{(Z_r^2+Z_i^2)(\sinh^2 Pd + \sin^2 Qd) + 2Z_r\cosh Pd\sinh Pd + \sinh^2 Pd + \cosh^2 Pd + 2Z_i \sin Qd\cos Qd\Big\}^{-1} \tag{5}$$

$$RR^* = TT^*(L^2+M^2)(\sinh^2 Pd + \sin^2 Qd) \tag{6}$$

where:

TT^*, RR^* are the power transmission and reflection coefficients respectively

$$D = (P + jQ)d$$

$$P = \left[\tfrac{1}{2}\sqrt{(K_r - \sin^2\theta)^2 + K_i^2} - \tfrac{1}{2}(K_r - \sin^2\theta)\right]^{\frac{1}{2}}$$

$$Q = \left[\tfrac{1}{2}\sqrt{(K_r - \sin^2\theta)^2 + K_i^2} + \tfrac{1}{2}(K_r - \sin^2\theta)\right]^{\frac{1}{2}}$$

$$K_r = 1 - \left(\frac{\omega_p}{\omega}\right)^2 \frac{1}{1 + (\nu/\omega)^2}$$

$$K_i = \left(\frac{\omega_p}{\omega}\right)^2 \frac{\nu/\omega}{1 + (\nu/\omega)^2}$$

ω, ω_p, ν are respectively the radio frequency, plasma frequency and effective collision frequency,
and for a <u>horizontally polarized incident field</u> (E perpendicular to plane of incidence)

$$Z_r = \frac{Q}{2k}\left[\frac{k^2\cos^2\theta + Q^2 + P^2}{\cos\theta\ (Q^2 + P^2)}\right]$$

$$Z_i = -\frac{P}{2k}\left[\frac{k^2\cos^2\theta - Q^2 - P^2}{\cos\theta\ (Q^2 + P^2)}\right]$$

$$L = -(Q/P)Z_i$$

$$M = (P/Q)Z_r$$

while for a <u>vertically polarized incident field</u> ($\vec{E}$ in plane of incidence)

$$Z_r = \tfrac{1}{2}\left(\frac{P}{k}K_i + \frac{Q}{k}K_r\right)\left[\frac{1}{\cos\theta(K_r^2 + K_i^2)} + \frac{k^2\cos\theta}{P^2 + Q^2}\right]$$

$$Z_i = \tfrac{1}{2}\left(\frac{P}{k}K_r - \frac{Q}{k}K_i\right)\left[\frac{1}{\cos\theta(K_r^2 + K_i^2)} - \frac{k^2\cos\theta}{P^2 + Q^2}\right]$$

$$L = \left(\frac{QK_r + PK_i}{QK_i - PK_r}\right)Z_i$$

$$M = \left(\frac{PK_r - QK_i}{PK_i + QK_r}\right)Z_r$$

Based on the above derivation of the transmission coefficient for a plane wave incident on a plasma slab, computations were made for a plasma characterized by $(\omega_p/\omega) = 0.75$ and $(\nu/\omega) = 0.1$. The thickness of the plasma slab was set at three wavelengths ($\lambda = 3$cm).

The computed values of the power transmission coefficient TT^* are plotted in Fig. 7 on a decibel scale as function of the angle of incidence on the plasma slab. The radiation pattern of the microwave horn in the presence of the plasma slab was then obtained (using Eqn. 4) by adding graphically the power transmission coefficient in decibels to the measured radiation pattern (in dbs) of the microwave horn. The resulting curve is also shown in Fig. 7. It is seen that the attenuation caused by the presence of the infinite slab of plasma at normal incidence is 7 decibels and that no increase in the power received is predicted as the scanning angle is increased as is observed in the experimental measurements.

Application of Diffraction Theory: A direct theoretical investigation of the experimental arrangement is prohibitively complicated and hence a suitable simple model which can lend itself to theoretical analysis and which adequately describes the experimental arrangement must be sought. Since the major complexity of the experiment is introduced by the finite size of the plasma container a series of measurements were conducted on the influence of the container on the radiation pattern of the horn. In this way it was established that the effect of the entire container could be effectively approximated by the outside dielectric plate of the plasma container alone, as shown in Fig. 8. Furthermore using diffraction theory[4] and taking into account the directivity of the microwave horn antenna, the effects predicted analytically agree well with experiment. Consequently, the theoretical model adopted for comparison with the experimental determinations of the effect of a plasma on the radiation characteristics of a microwave horn was that of a horn radiator located directly behind an infinite uniform slab of plasma with a dielectric plate on the opposite side of the plasma representing the plasma container.

With this theoretical model it is possible to apply diffraction theory taking into account the presence of the plasma. The derivation of

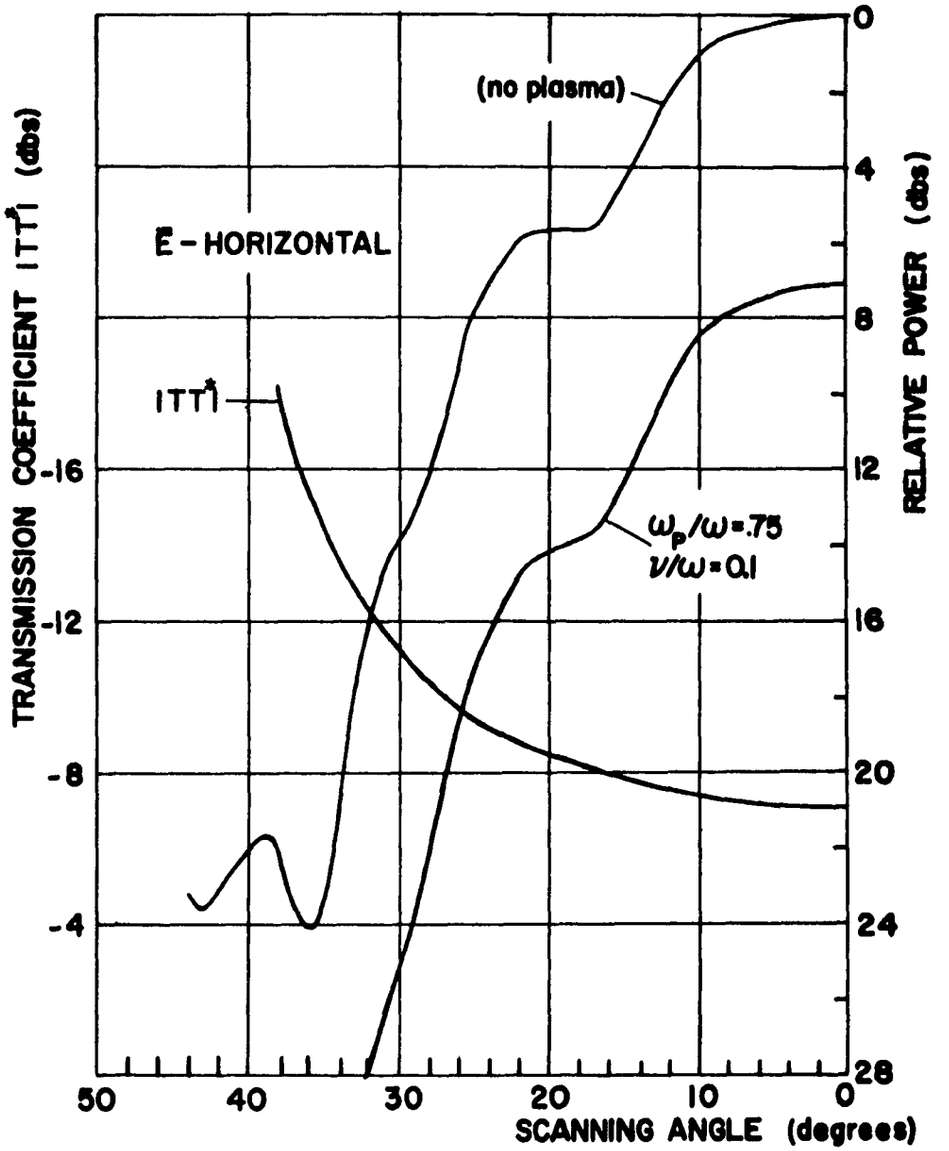

Fig. 7: The power transmission coefficient for a uniform plasma slab and the radiation pattern of the microwave horn in the presence of this plasma slab.

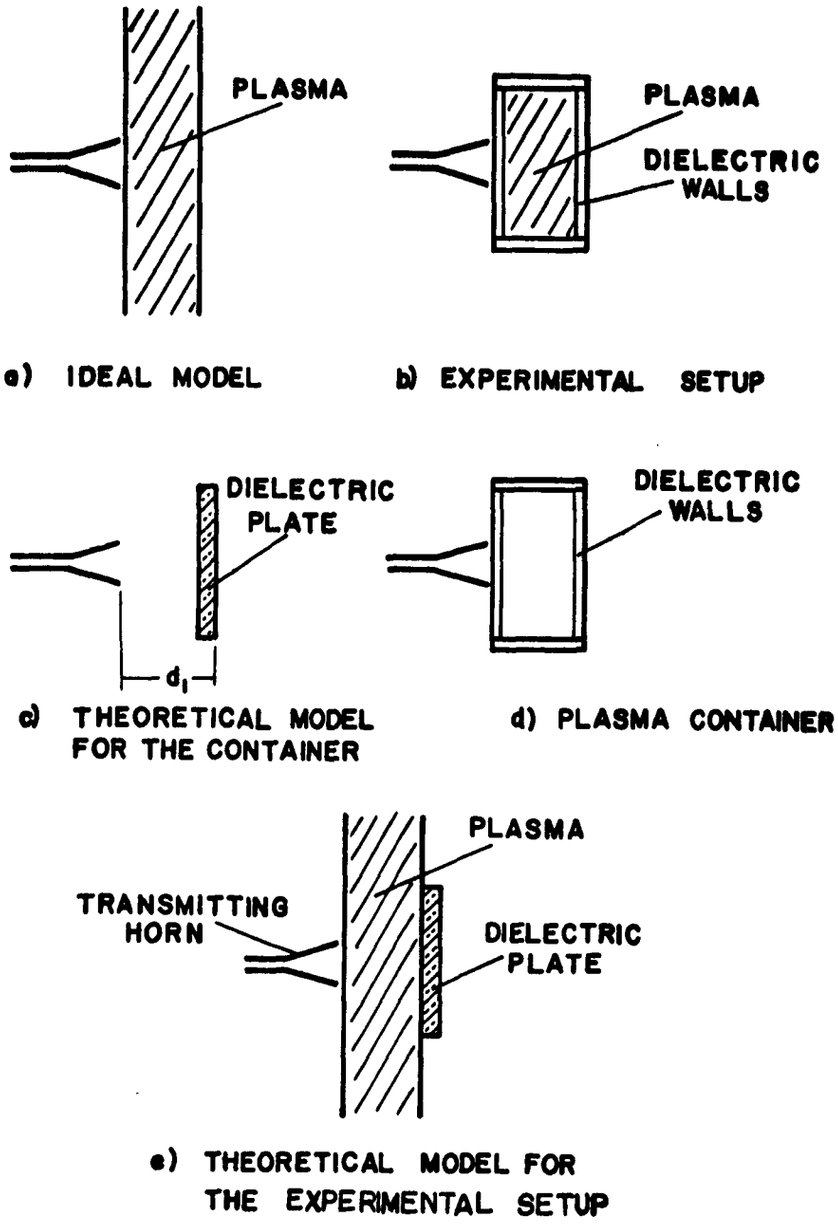

Fig. 8: Schematic diagrams of the various models used in the interpretation of the measurements.

this solution can now be carried out in a manner analagous to the derivation for diffraction by a dielectric disc conducted previously. The field intensity in the far-field region when a plasma slab is located between the source and the dielectric plate as given by the scalar Kirchhoff diffraction theory can be written[2]

$$I(q) = [ka)^2 - q^2][(I_1 + I_2)^2 + (I_3 + I_4)^2] \tag{7}$$

where $q = ka \sin\theta$

$k = 2\pi/\lambda$, λ is the free-space wavelength

a = radius of the dielectric plate

θ = the diffraction or scanning angle measured from the normal to the plate.

$$I_1 = \int_0^1 \frac{e^{-kay_1\sqrt{p^2+r^2}}\, e^{-\beta r^2}\, \cos(ka\alpha_1\sqrt{p^2+r^2})\, J_0(qr)}{\alpha_1\sqrt{p^2+r^2}} r dr \tag{8a}$$

$$I_2 = \int_1^{r_0} \frac{e^{-kay_2\sqrt{p^2+r^2}}\, e^{-\beta r^2}\, \cos(ka\alpha_2\sqrt{p^2+r^2}) J_0(qr)}{\alpha_2\sqrt{p^2+r^2}} r dr \tag{8b}$$

$$I_3 = \int_0^1 \frac{e^{-kay_1\sqrt{p^2+r^2}}\, e^{-\beta r^2}\, \sin(ka\alpha_1\sqrt{p^2+r^2}) J_0(qr)}{\alpha_1\sqrt{p^2+r^2}} r dr \tag{8c}$$

$$I_4 = \int_1^{r_0} \frac{e^{-kay_2\sqrt{p^2+r^2}}\, e^{-\beta r^2}\, \sin(ka\alpha_2\sqrt{p^2+r^2}) J_0(qr)}{\alpha_2\sqrt{p^2+r^2}} r dr \tag{8d}$$

and

$$\alpha_1 = n_{or} + (n + n_{or})\frac{d}{d_1} \qquad K_r = 1 - \left(\frac{\omega_p}{\omega}\right)^2 \frac{1}{1 + (\nu/\omega)^2}$$

$$\alpha_2 = n_{or} = \left(\frac{|K| + K_r}{2}\right)^{\frac{1}{2}} \qquad K_i = \left(\frac{\omega_p}{\omega}\right)^2 \frac{\nu/\omega}{1 + (\nu/\omega)^2}$$

$$\gamma_1 = n_{oi}\left(1 - \frac{d}{d_1}\right) \qquad |K| = [K_r^2 + K_i^2]^{\frac{1}{2}}$$

$$\gamma_2 = n_{oi} = \left(\frac{|K| - K_r}{2}\right)^{\frac{1}{2}}$$

ν = effective electron collision frequency

d = thickness of dielectric plate

n = dielectric constant of the plate

$p = d_1/a$ is the normalized distance between the source and the dielectric plate

d_1 = distance from source to dielectric plate, which is the thickness of the plasma

J_0 is the Bessel function of the first kind

$r = \rho/a$ is a normalized radius vector

ρ = radius vector in polar co-ordinates

$e^{-\beta\rho^2}$ is the illumination function approximating the directivity of the horn pattern. β is selected to fit the main lobe of the radiation pattern

r_o is the upper limit of integration.

The analytic solution (7) is sufficiently involved to require computation on an electronic computer. Figure 9 shows such theoretical curves obtained for the following parameters:

a = 10 cm	λ = 3.1 cm
d = 1.9 cm	β = 1.33 cm
n = 1.58 cm	r_o = 2 cm
d_1 = 14 cm	

These values correspond to the experimental conditions for x-band

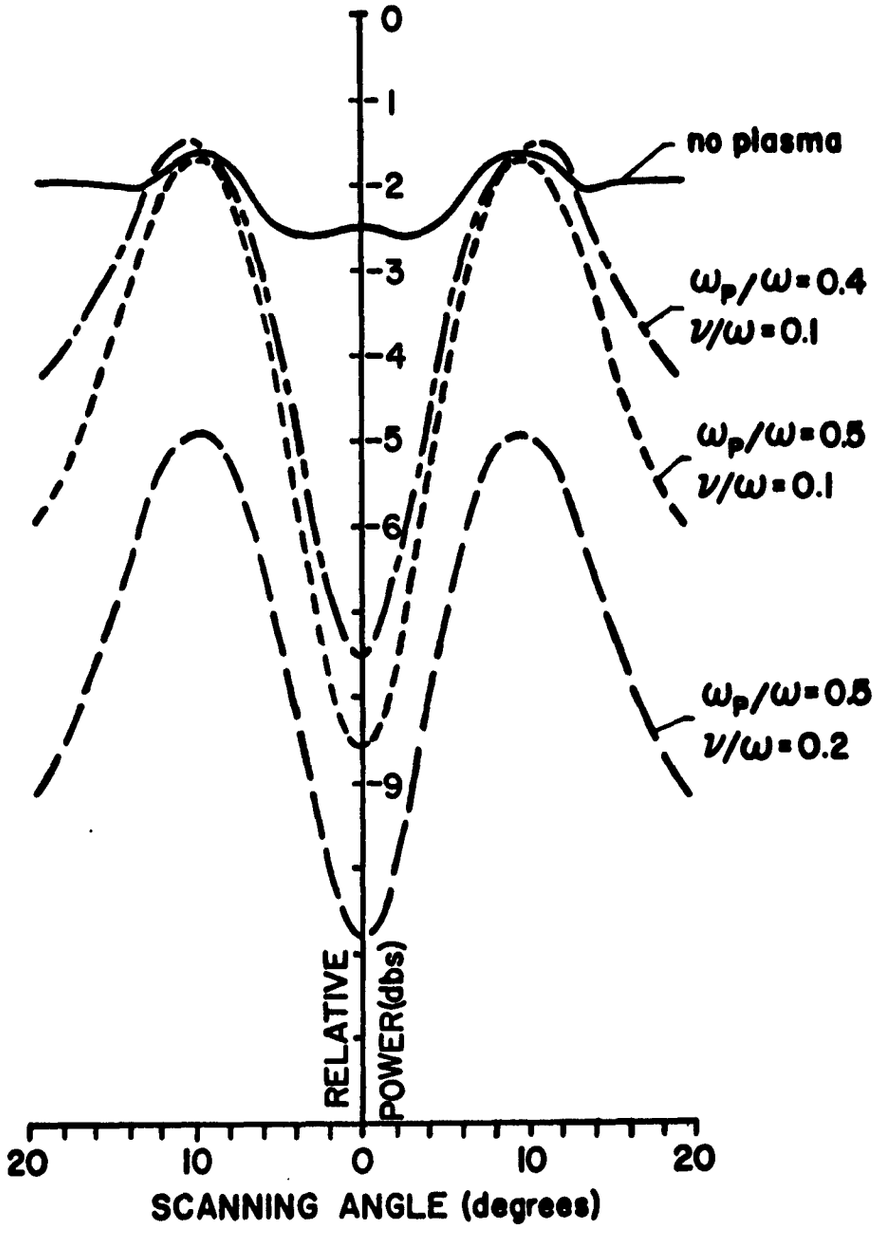

Fig. 9: Theoretical far-field radiation patterns for a microwave horn in the presence of an infinite plasma slab and including diffraction effects due to the edge of the plasma container.

measurements except that the actual plasma thickness in the experiment was 3.5λ. Due to the directivity of the source, the upper limit of integration could be taken as $r_0 = 2$. The computed patterns display only the main lobe of the radiation pattern since the approximations in the theory are no longer valid for scanning angles larger than 20 degrees.

In agreement with the experimental observations (Fig. 4) the power received at normal incidence decreases rapidly as the plasma intensity increases, resulting in a deep minimum in the radiation pattern at normal incidence. The effect of increasing collision frequency is also shown and results in an effective lowering of the overall power level of the far-field radiation pattern. The predicted power level is, however, greater than that measured experimentally. This may be due to the fact that reflection at the plasma boundaries, refraction at the first dielectric plate and nonuniformity in the plasma are not considered in the analysis.

It thus seems essential, before going on to investigate the effect of more complex plasma sheaths(such as a plasma which is anisotropic due to the presence of a static magnetic field) on antenna behaviour, to ascertain in detail the influence of these diffraction, reflection and refraction effects. Once these phenomena are known and better understood, then their influence can be either eliminated or minimized and better quantitative interpretation of the effect of the plasma sheath itself on antenna behaviour can be made. Such a series of investigations is described in the next chapter.

III MICROWAVE MEASUREMENTS OF FINITE PLASMAS

In practice laboratory plasmas are finite in extent; they may be contained by material walls, the boundaries of the plasma may not be well defined and the plasma may be non-uniform in both space and time. Similarly the practical measurement system may not produce a plane incident wave, the source and the receiver both have finite radiation patterns, the plasma may be located in the near field of the source and multiple interactions may occur between any of the source, the plasma

container, the plasma and the receiver. The result is refraction, reflection, absorption and diffraction phenomena which are not easy to define and interpret but the understanding of which is essential before accurate quantitative determination of plasma properties is possible.

Although a number of microwave free-space measurements of plasma have been reported[5-10] and some of the above limitations have been mentioned, there does not appear to have been a systematic attempt to assess the predictions of various simple theoretical models of the plasma, develop theories to account for the influence of the aforementioned effects and to test the accuracy of various microwave arrangements for determining the properties of plasmas which are finite in extent.

As part of the research under Contract AF 19(604)-7334 theoretical predictions have been developed and typical numerical values calculated for plasma effects such as plasma boundaries, refractive defocussing by the plasma, non-uniformity of the plasma. Experiments on various microwave arrangements have been conducted to show the influence of the dielectric boundaries of the plasma container, the effect of multiple reflections within the measurement system and the precautions which must be exercised both in the measurements and in the interpretation of the results. Measurements of plasma properties with different experimental arrangements have been tested and the limitations of the various systems ascertained. In addition, free-space measurements of the properties of a slab or sheath of plasma generated in helium and argon using the "optimum" microwave arrangement have been made. This work is summarized in the following sections.

(a) Theory of Microwave Properties of Finite Plasmas

Effect of Boundaries on Transmission and Reflection of Waves by a Plasma: Many calculations on the effect of a plasma on an incident plane electromagnetic wave are based on a theoretical model in which the influence of the boundaries of the plasma are completely ignored. The

electromagnetic wave is considered to traverse a region of plasma equal in extent to a given physical dimension but the effect of reflection from the interface between the plasma and freespace and multiple reflections within the plasma are neglected (see Fig. 10a). This "unbounded plasma" model thus predicts the attenuation and phase shift that the plasma would introduce to a plane homogeneous electromagnetic wave traversing a given distance in an infinite, uniform, isotropic plasma.

A more realistic model (Fig. 10b) considers a plane, homogeneous wave normally incident on a uniform, isotropic "plasma slab" bounded by free space. In this model both reflections from the interfaces and multiple reflections within the plasma are taken into account.

In a laboratory plasma, the plasma is very often contained by material walls. A theoretical model to take into account the effect of the material container is a slab of plasma bounded by two flat dielectric plates (as shown in Fig. 10c).

Calculations of the attenuation and phase-shifts introduced by a plasma to an incident electromagnetic wave based on these three models have been made and compared for various plasma parameters. The predictions of the different models give an indication of the range of validity of each model and the accuracy of measurement of plasma properties to be expected when free-space microwave techniques are used.

(i) Unbounded Plasma Model - In a uniform, neutral plasma of electron density n and effective collision frequency ν, the dielectric constant can be written for a harmonic time varying field ($e^{j\omega t}$) as[7]:

$$K = K_r - jK_i = 1 - \left(\frac{\omega_p}{\omega}\right)^2 \left(\frac{1}{1+(\nu/\omega)^2}\right) - j\left(\frac{\omega_p}{\omega}\right)^2 \left(\frac{\nu/\omega}{1+(\nu/\omega)^2}\right) \qquad (9)$$

$$= 1 - \frac{N}{1+S^2} - j\frac{NS}{1+S^2}$$

where:

ω_p is the plasma frequency = $(ne^2/m\varepsilon_o)^{\frac{1}{2}}$

e,m are respectively the electronic charge and mass

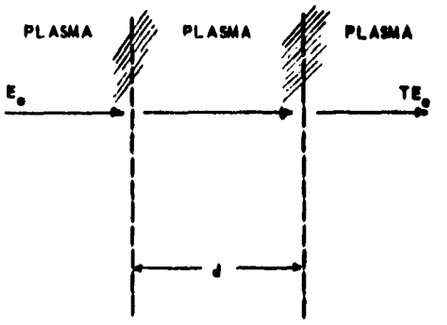

(a) Unbounded Plasma

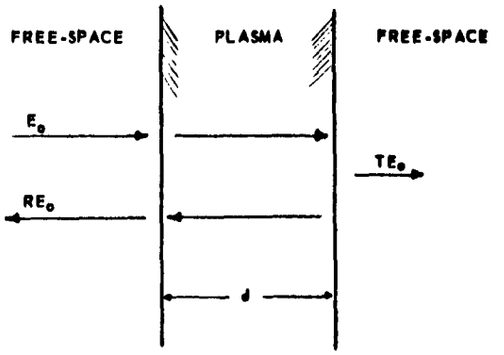

(b) Plasma Slab

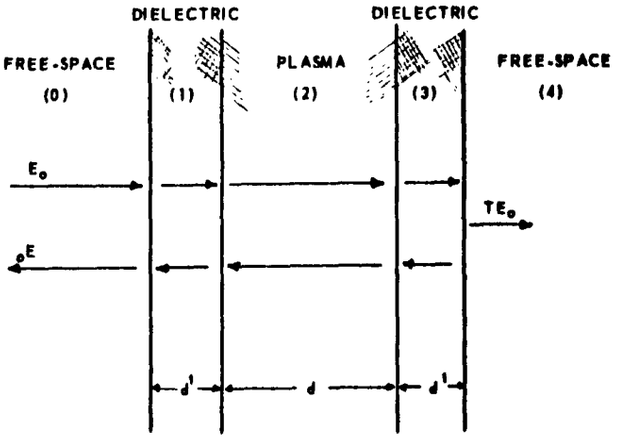

(c) Plasma Slab Bounded by Dielectric Plates

Fig. 10 Theoretical models for determining the transmission and reflection of electromagnetic waves by a plasma
(a) unbounded plasma,
(b) plasma slab bounded by free-space,
(c) plasma slab contained within dielectric plates in free space.

ε_o is the permittivity of free space

ω is the radian radio frequency

N,S are normalized electron density and collision frequency parameters given by: $N = (\omega_p/\omega)^2$; $S = \nu/\omega$

For a plane homogeneous electromagnetic wave the propagation constant (γ), attenuation constant (α) and phase constant (β) can be written as:

$$\gamma = \alpha + j\beta \tag{10a}$$

$$\alpha = k\left(\frac{|K| - K_r}{2}\right)^{\frac{1}{2}} \tag{10b}$$

$$\beta = k\left(\frac{|K| + K_r}{2}\right)^{\frac{1}{2}} \tag{10c}$$

where:

$$|K| = (K_r^2 + K_i^2)^{\frac{1}{2}}$$

and $k = 2\pi/\lambda$ is the free space wave number.

For a wave propagating a distance d in the plasma, the transmission coefficient T, and the reflection coefficient R are given by:

$$T = 1 - e^{-\alpha d} \tag{11a}$$

$$R = 0 \tag{11b}$$

The attenuation of the wave after propagating a distance d in the plasma is given by:

$$\alpha d = 2\pi\left(\frac{\alpha}{k}\right)\left(\frac{d}{\lambda}\right) \tag{12a}$$

The phase shift which occurs when β/k changes from unity (no plasma) to some value defined by the plasma is:

$$\phi = 2\pi\left(\frac{d}{\lambda}\right)\left[1 - \left(\frac{\beta}{k}\right)\right] \tag{12b}$$

(ii) "Plasma Slab" Model: The theory for an "unbounded plasma" is very simple to apply. It is usually considered quite accurate if the refractive index of the plasma is close to unity, in which case reflections from the plasma - freespace interfaces will be insignificant. To check the validity of such assumptions, calculations were performed to determine the attenuation and phase-shift of a plasma slab sharply bounded by free space. Writing down the boundary conditions at each interface and solving the electromagnetic equations gives the transmission coefficient for normal incidence[3,11] as:

$$T = \frac{E_T}{E_0} = [\cosh(\alpha d + j\beta d) + (Z_r - jZ_i)\sinh(\alpha d + j\beta d)]^{-1} \qquad (13a)$$

The reflection coefficient (applied to the fields) is similarly obtained and found to be

$$R = T\left[Z_i\left(\frac{\beta/k}{\alpha/k}\right) + j\,Z_r\left(\frac{\alpha/k}{\beta/k}\right)\right]\sinh(\alpha + j\beta)d \qquad (13b)$$

where:

$$Z_r = \tfrac{1}{2}\left(\frac{\beta}{k}\right)\left(\frac{|K| + 1}{|K|}\right) \quad ; \quad Z_i = \tfrac{1}{2}\left(\frac{\alpha}{k}\right)\left(\frac{|K| - 1}{|K|}\right)$$

The incident energy which is not reflected or transmitted by the plasma slab is absorbed; the absorbed power A_ω is given by:

$$A_\omega = 1 - RR^* - TT^* \qquad (14)$$

where the R^*, T^* refer to the complex conjugates of R and T respectively.

(iii) Plasma Slab Bounded by Dielectric Plates: Laboratory measurements on plasmas are usually significantly affected by the container in which the plasma is confined. Even when the index of refraction of the plasma is close to unity, the combined effect of reflection from the container and the plasma may be significant. To study the magnitude of this effect, calculations were made for a model consisting of a plasma slab bounded by two dielectric plates. The geometry was as shown in Fig. 10c.

At normal incidence, the waves in the plasma and the dielectric will be plane waves. Nine "composite" waves representing all possible reflections are of interest. One can write all the boundary conditions of the electric field and the magnetic field across the various interfaces. Solving the resulting equations for the transmission and reflection coefficients of the slab of plasma bounded by dielectric plates in free-space gives[3]:

$$T = \left\{ \left[\cosh^2 \gamma'd' + \sinh^2 \gamma'd' + \left(\frac{Z_1}{Z_0} + \frac{Z_0}{Z_1}\right) \frac{\sinh 2\gamma'd'}{2} \right] \cosh \gamma d \right.$$

$$+ \tfrac{1}{2} \left\{ \left(\frac{Z_1}{Z_2} + \frac{Z_2}{Z_1}\right) \sinh 2\gamma'd' + \left(\frac{Z_2}{Z_0} + \frac{Z_0}{Z_2}\right) \cosh^2 \gamma'd' \right.$$

$$\left. \left. + \left(\frac{Z_1^2}{Z_0 Z_2} + \frac{Z_0 Z_2}{Z_1^2}\right) \sinh^2 \gamma'd' \right\} \sinh \gamma d \right\}^{-1} \qquad (15a)$$

$$R = T \left\{ \left(\frac{Z_1}{Z_0} - \frac{Z_0}{Z_1}\right) \sinh \gamma'd' \cosh \gamma'd' \cosh \gamma d \right.$$

$$\left. + \tfrac{1}{2} \left[\left(\frac{Z_2}{Z_0} - \frac{Z_0}{Z_2}\right) \cosh^2 \gamma'd' + \left(\frac{Z_1^2}{Z_0 Z_2} - \frac{Z_0 Z_2}{Z_1^2}\right) \sinh^2 \gamma'd' \right] \sinh \gamma d \right\} \qquad (15b)$$

where:

γ, γ' are the propagation constants of the plasma and the dielectric plates respectively,

d, d' are respectively the thickness of the plasma and a dielectric plate,

Z_0, Z_1, Z_2 are the impedances of free space, dielectric and plasma respectively.

If the dielectric plates are considered lossless, the propagation constant of the dielectric γ' will be purely imaginary.

$$\gamma' = j\beta' = jk \left(\frac{\beta'}{k}\right) = j\mu \frac{2\pi}{\lambda}$$

where μ is the index of refraction of the dielectric plates.

The impedances of the dielectric and plasma can be written in terms of the freespace impedance as:

$$Z_1 = \frac{Z_0}{\sqrt{K_1}} = \frac{Z_0}{\mu} \quad ; \qquad Z_2 = \frac{Z_0}{\sqrt{K}} = Z_0 \left(\frac{jk}{\alpha + j\beta} \right)$$

where:

K_1 is the dielectric coefficient of the dielectric.

(iv) Comparison of the Three Models: The plots of the attenuation and phase shift dependence on electron density for the three models show that the phase-shift is perturbed less by the interface conditions than the attenuation for low values of electron density. Since, very generally, phase shift is associated primarily with electron density and attenuation with the electron collision frequency, the effect of the interfaces makes the collision frequency more in doubt than the electron density.

A polar plot of the amplitude and phase of a transmitted signal, calculated for the three models, is shown for comparison in Fig. 11. The curve drawn in each case is for collision frequencies (ν/ω) of 0.03 and 0.1. Because of interface effects, and the thickness of plasma and dielectric plates which were used in the calculations, the deviation for the three curves is more pronounced at some electron densities than at others. As an example of the effect of the boundaries, note that for a phase shift of 360°, the electron density (n/n_0) measured by all three methods is 0.8.

The "unbounded" theory shows less than 3db attenuation; when the dielectric plates and the interfaces are taken into account more than 6db attenuation is obtained. This is a significant difference. Conversely, it can be deduced that an attenuation of 6db would give a collision frequency of 0.03 by the "dielectric plate" calculations, and a collision frequency of about 0.06 by the "unbounded" theory. As the collision frequency increases the differences between the various models becomes less and less significant.

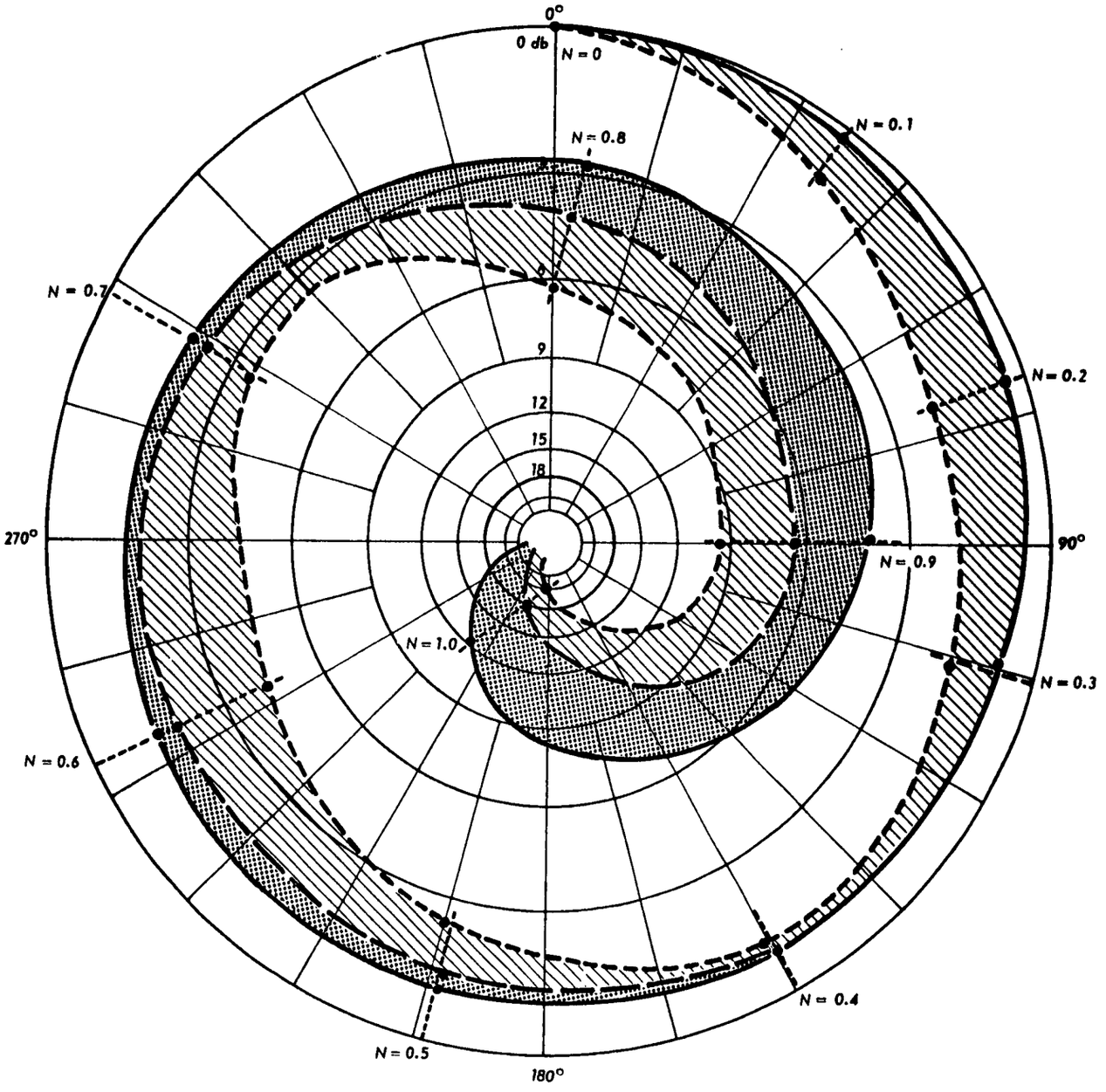

Fig. 11a: Comparison of attenuation and phase shift as predicted by the three theoretical models for the plasma for $\nu/\omega = 0.03$.

Solid Curve is for "Unbounded Plasma"
Dashed Curve is for "Bounded Plasma"
Dotted Curve is for "Plasma Bounded by Dielectric Plates"

$\mu = 1.58$; $d'/\lambda = 0.567$; $d/\lambda = 1.84$

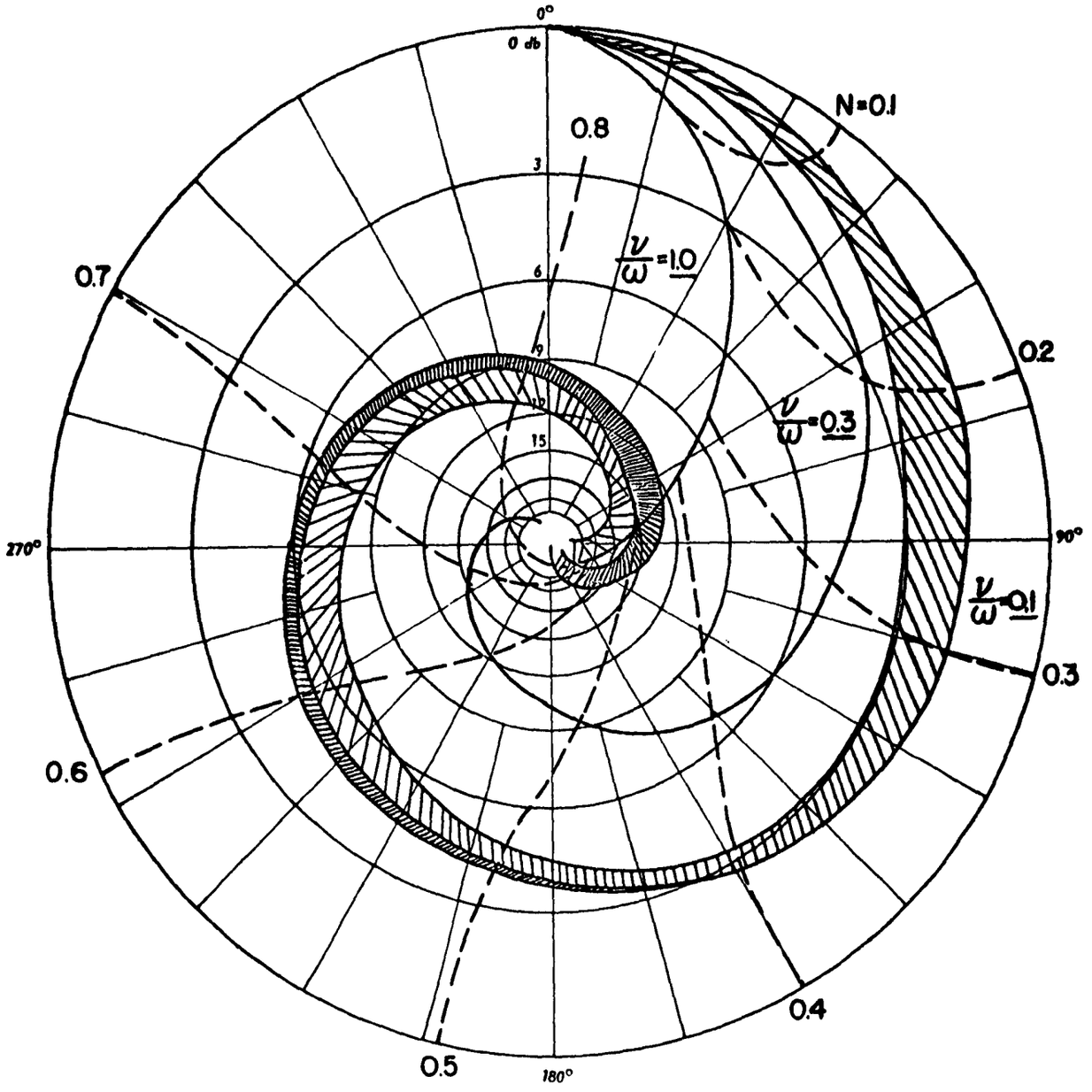

Fig. 11b: Comparison of attenuation and phase shift as predicted by the three theoretical models for the plasma for $\nu/\omega = 0.10$. The distinction between the models becomes less significant with increasing collision frequency. For $\nu/\omega = 0.3$ and 1.0 all models predict about the same result.

It is also interesting to note that the difference between the unbounded theory and the plasma slab model are not significant for low electron densities ($N < 0.4$); however, the effects of the dielectric plates on the plasma slab at these low electron densities are important due to the "matching" effects on the incident field.

Refractive Defocussing by Uniform Plasma Slabs and Cylinders: Microwave systems used for the free-space measurement of plasma properties can be broadly classified as to the type of incident wave front. The arrangements most often employed are of the type that result in either an incident plane wave (by the use of auxiliary lenses), a spherical incident wave (unfocussed point source) or a highly focussed beam (using lenses or other focussing devices) to give a high degree of spatial resolution.

Since the refractive index of the plasma ($\mu = K^{\frac{1}{2}}$) will, in general, not be equal to the refractive index of free-space ($\mu_0 = 1$), then refraction will occur at each boundary between plasma and free-space. Using the concepts of geometric optics, the electromagnetic energy can be considered as travelling along ray paths or rays which are normal to the planes of constant phase of the wavefront. (We shall neglect in the sequel the situation which can arise[1,2] whereby the rays do not coincide with the direction of energy travel - i.e. the direction of the Poynting vector is not normal to the phase front i.e. inhomogeneous plane waves.) The net result of the refraction is that the incident beam of energy is spread out or defocussed by the plasma. (This is due to the fact that for the plasma $\mu < 1$; for a dielectric with refractive index greater than unity ($\mu > 1$) a focussing of the beam results.) The plasma can thus be considered as a lens of refractive index less than unity. The net result of this refractive defocussing is that the energy density of the radiation in the region where it can be measured by a microwave receiving system has been decreased not only by the amount of energy absorbed by the plasma but also by the amount by which it has been spread out. Consequently, in order to obtain a measure of the energy absorbed by the plasma (and hence get a measure of collision frequency) some

estimate of the refractive defocussing is essential.

Subject to the limitations of geometric optics (dimensions large compared to wavelength, losses in plasma small, etc.) it is possible to derive expressions for the refractive defocussing by uniform plasma slabs and plasma cylinders. These are discussed in the sequel.

(i) Plane Wave Incident: For a plane wave incident normally on a slab of plasma no refractive defocussing occurs as shown in Fig. 12a.

A plane wave incident on a uniform, cylindrical plasma will be refracted. With reference to Fig. 12a let the extreme ray of an incident beam of radiation of radius a be intercepted by a plane of half-width A located a distance R from the centre of the cylinder of plasma of radius r. The angles of incidence and refraction are respectively θ_i and θ_n, while the other parameters are defined in the diagram. Using Snell's Law and geometric considerations, it is easy to show that in the small angle limit:

$$\frac{a}{A} = \frac{r}{r + 2(\frac{1}{\mu} - 1)R}$$

When the refractive index of the plasma is unity ($\mu = 1$), then $a = a_o$ or

$$\frac{a_o}{A} = 1$$

For an extreme ray of radius A, the effective radius of the beam of incident radiation which is intercepted is a. The effect of the plasma is to reduce the radius of the incident beam which is intercepted from a_o to a. A measure of the refractive defocussing effect in one dimension is then:

$$\eta = \frac{a}{a_o} = \frac{r}{r + 2(\frac{1}{\mu} - 1)R} = \frac{1}{1 + 2(\frac{1}{\mu} - 1)\frac{R}{r}} \qquad (16)$$

We shall call η the "refractive defocussing coefficient" or in most cases

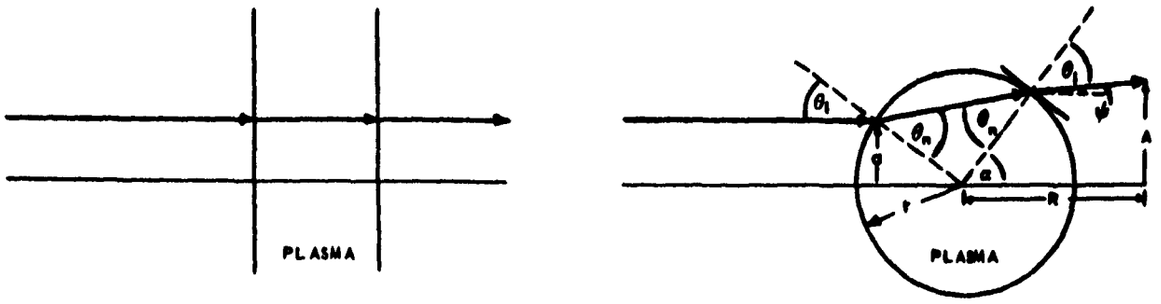

(a) Plane wave incident

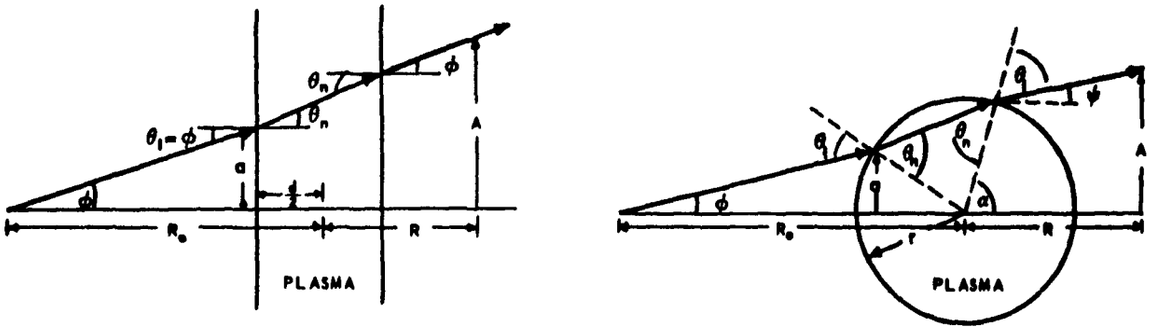

(b) Spherical Wave incident

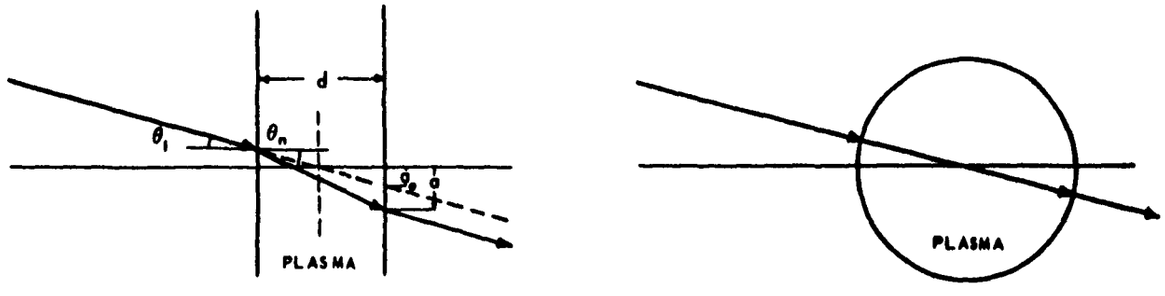

(c) Focused beam

Fig. 12 Refractive defocusing introduced by a uniform plasma for
(a) plane wave incident,
(b) spherical wave incident,
(c) focused beam incident.

the "refractive defocussing".

Note that if $\mu > 1$, then $\eta > 1$, i.e. we get focussing.

For a plane wave incident, the defocussing coefficient η is a measure of the beam of energy intercepted by a receiver of aperture dimension A, located at R in the presence of the cylinder of plasma relative to that intercepted when there is no plasma cylinder. Notice that for a plane incident wave the spreading or defocussing of energy occurs only in the plane normal to the cylinder axis and no defocussing effect is present along the axis of the cylinder.

(ii) Spherical Wave Incident (Point Source): A spherical wave incident upon a uniform slab or cylinder of plasma will result in refractive defocussing of the incident beam as shown in Fig. 12b.

To determine the refractive defocussing for a spherical wave incident upon a uniform slab of plasma we can proceed as before. The result is

$$\frac{a}{A} = \frac{R_o - \frac{d}{2}}{R_o + R - d\left\{1 - \frac{\cos\phi}{\sqrt{\mu^2 - \sin^2\phi}}\right\}}$$

and

$$\eta = \frac{a}{a_o} = \frac{1}{1 - \frac{d}{R + R_o}\left(1 - \frac{\cos\phi}{\sqrt{\mu^2 - \sin^2\phi}}\right)} \tag{17a}$$

In the small angle approximation, $\cos\phi \to 1$, $\sin\phi \to 0$ and:

$$\eta = \frac{1}{1 + \left(\frac{1}{\mu} - 1\right)\frac{d}{R + R_o}} \tag{17b}$$

For a spherical wave emenating from a point source, the total energy received depends on the cross-sectional area of the beam normal to the direction of propagation - i.e. it is proportional to a^2. Hence

the reduction in received power due to refractive defocussing is given by η^2. A typical variation of η^2 with electron density is shown in Fig. 13.

For a spherical wave incident on a uniform cylinder of plasma, following the procedure as before (see Fig. 12b) the relevant equations become:

$$\frac{a}{A} = \frac{r(R_o - r)}{r(R + R_o) + 2\left(\frac{1}{\mu} - 1\right) R\, R_o}$$

and

$$\eta = \frac{a}{a_o} = \frac{1}{1 + 2\left(\frac{1}{\mu} - 1\right)\frac{RR_o}{r(R_o + R)}} \qquad (18)$$

A similar result to Eqn. (18) has been obtained previously by Heald[12,13]. Notice that this is the refractive defocussing (power) for a line source located parallel to the axis of the cylinder of plasma, i.e. a cylindrical incident wave. For a point source, the reduction in power due to refraction defocussing will be given by the product of Eqns. (17b) and (18) since the defocussing will be two dimensional.

(iii) Focussed Beam: A focussed beam incident on a slab of plasma and focussed at the centre of the slab will be defocussed as shown in Fig. 12c. From Snell's Law and geometric considerations we arrive at:

$$\eta = \frac{a_o}{a} = \left(\frac{2}{\mu}\cos\theta_i - 1\right)^{-1} \sim \frac{\mu}{2 - \mu} \qquad (19)$$

The reduction in power for a focussed beam incident on a slab of plasma will be proportional to η^2 since η is the refractive defocussing along a radius of the incident beam and the total incident power is proportional to the area of (radius)^2 of the incident beam.

An incident beam focussed at the centre of a uniform cylinder of plasma will not suffer refractive defocussing in the plane normal to the axis of the cylinder (see Fig. 12c). There will, however, be

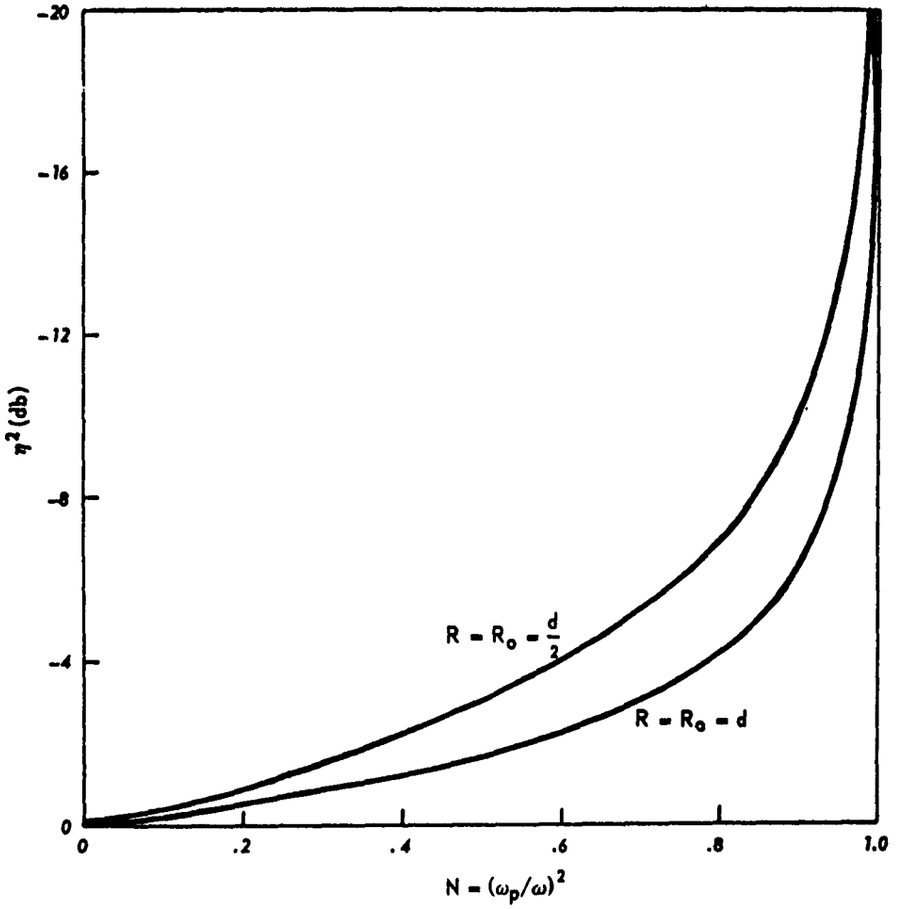

Figure 13: Reduction in received power due to refractive defocusing by a uniform slab of plasma when a spherical wave is incident on the plasma

refractive defocussing in the direction along the axis of the cylinder since in the axial direction the cylinder will present a plane rather than cylindrical surface. This refractive defocussing is given by Eqn.(19).

Effects of Non-Uniformity of Plasma

(i) Plasma Properties Varying in Direction of Propagation

No Boundaries: Consider a plane wave incident normally on a slab of plasma of thickness d. Let the electron density be a function of position in the slab in the direction of propagation only. Since the plane wave is incident normally on the slab of plasma no refractive defocussing effects will occur even if the plasma properties vary in the direction of propagation.

Initially, neglect the effect of the plasma boundaries so that the reflected wave and multiple internal reflections within the plasma can be ignored. (We shall return to these later.) This is a reasonable assumption for a dilute plasma or a very lossy plasma.

Considering only the wave transmitted through the plasma then, the phase change $\Delta\phi$ and attenuation A_α introduced by the plasma are:

$$\Delta\phi = k\int_0^d \left(\frac{\beta(z)}{k} - 1\right) dz \quad ; \quad A_\alpha = k\int_0^d \frac{\alpha(z)}{k}\, dz \tag{20}$$

where:

$\beta(z)$, $\alpha(z)$ are the phase and attenuation coefficients respectively and $k = 2\pi/\lambda$ the wave number in free space.

It is advantageous to normalize the phase change and attenuation with regard to the thickness of the slab. Setting $s = z/d$ yields:

$$\Delta\Phi = \frac{\Delta\phi}{kd} = \int_0^1 \left(\frac{\beta(s)}{k} - 1\right) ds \quad ; \quad \Lambda = \frac{A_\alpha}{kd} = \int_0^1 \frac{\alpha(s)}{k}\, ds \tag{21}$$

The effect on a plane wave introduced by the plasma slab is then:

$$e^{-kd(\Lambda - j\,\Delta\Phi)}$$

When the losses in the plasma are small $K_r >> K_i$ (this is the only type of plasma for which present free-space microwave techniques are applicable) we can write:

$$\frac{\beta(s)}{k} = K_r^{\frac{1}{2}} = \sqrt{1 - N(s)} \tag{22}$$

where:

$$N(s) = \frac{\omega_p^2(s)}{\omega^2} = \frac{e^2\, n(s)}{m\, \epsilon_0 \omega^2}$$

For a dilute lossless plasma $N(s) << 1$ so that

$$\frac{\beta(s)}{k} - 1 \simeq -\frac{N(s)}{2} \qquad \text{and} \qquad \Delta\Phi = -\tfrac{1}{2} \int_0^1 N(s)\, ds \tag{23}$$

Thus for a dilute plasma the change in phase depends only on the total electron density along the path and not on the electron density distribution. In the sequel we shall <u>not</u> make the dilute plasma approximation in considering the effect of the form of the electron distribution on the phase of the transmitted electromagnetic wave but will retain the restriction that $K_r >> K_i$.

The effect of the electron density profile on the phase of an electromagnetic wave transmitted through a plasma has been considered by Wharton[15] and by Motley and Heald[16]. We shall adopt the slightly more general results due to Johnston[17].

Consider the electron density profile in the slab of plasma to be given by a "barn roof" type of distribution of the form:

$$\begin{aligned} N &= \frac{A}{1-A} N_m s && 0 < s < (1-A) \\ N &= N_m \left[A + \frac{(1-A)}{A} \left(s - \left\{ 1-A \right\} \right) \right] && (1-A) < s < 1 \end{aligned} \tag{24}$$

where:

N_m is the maximum normalized electron density

$A(\leq 1)$ is the height of the "shoulder" and is also the ratio of the average electron density to the maximum electron density - i.e. the average electron density in the slab is $A\,N_m$.

The normalized phase change introduced by a slab of plasma of this form of electron distribution is then:

$$\Delta\Phi = \int_0^{1-A} \left[1 - N_m \frac{A}{1-A}\, s\right]^{\frac{1}{2}} ds + \int_{1-A}^{1} \left[1 - N_m \left\{A + \frac{1-A}{A}\left(s - \left\{1-A\right\}\right)\right\}\right]^{\frac{1}{2}} ds - 1$$

$$= \frac{2}{3N_m}\left\{\frac{1-A}{A} + \left(\frac{A}{1-A} - \frac{1-A}{A}\right)\left(1 - AN_m\right)^{3/2} - \frac{A}{1-A}\left(1-N_m\right)^{3/2}\right\} - 1 \qquad (25)$$

For a uniform slab, $A = 1$, $N = N_m$ and we go back to the original integral (Eqn. 21) to obtain

$$(\Delta\Phi)_{A=1} = (1 - N_m)^{\frac{1}{2}} - 1 \qquad (26)$$

A plot of $\Delta\Phi$ vs. N_m for different density profiles (different values of A) is shown in Fig. 14a. If we now normalize the results to correspond to slabs of equal total electron content (equal values of AN_m) the result is shown in Fig. 14b. The striking feature to note is that the phase is quite <u>insensitive</u> to the electron density profile even for densities corresponding very near to the plasma frequency <u>but</u> depends almost exclusively on the total electron content. It is thus <u>impossible</u> with phase measurements performed at a <u>fixed</u> frequency to ascertain with any degree of accuracy the electron density profile. Only measurements performed at a number of different radio frequencies on the same plasma can hope to give an indication of the electron density distribution. This corresponds to keeping A fixed (same plasma conditions) and varying N_m (by changing the radio frequency).

An indication of the dependance of the attenuation on the

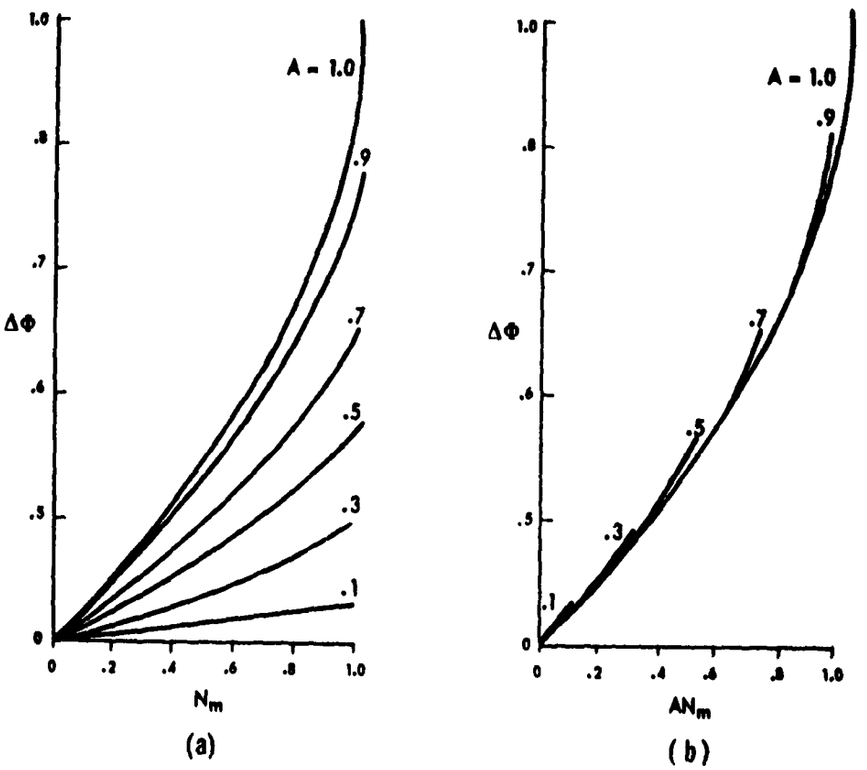

Fig. 14 (a) Variation of phase change introduced by a plasma with normalized electron density for different spatial distributions of electron density, (After Johnston[16]).

(b) Variation of phase change introduced by a plasma with average normalized electron density for different spatial distributions of electron density, (After Johnston[16]).

the electron density profile is of value for analysing experimental data. To a first approximation, the effective collision frequency is independent of the electron density and will be considered as a constant throughout the slab in the ensuing discussion. In a plasma where $K_r >> K_i$, the attenuation coefficient becomes:

$$\frac{\alpha(s)}{k} \simeq \frac{K_i}{2K_r^{\frac{1}{2}}} = \frac{\nu}{\omega} \frac{N(s)}{\sqrt{1-N(s)}} \tag{27}$$

For the "barn roof" distribution of electron densities given by Eqn. (24), the normalized attenuation coefficient is:

$$A = \frac{\nu}{\omega} \int_0^1 \frac{N(s)\, ds}{(1-N(s))^{\frac{1}{2}}}$$

$$A = \frac{\nu}{\omega} \left[\int_0^{1-A} \frac{\frac{A}{1-A} N_m s \, ds}{\left[1 - \frac{A}{1-A} N_m s\right]^{\frac{1}{2}}} + \int_{1-A}^{1} \frac{N_m \left[A + \frac{1-A}{A}\left(s - \left\{1-A\right\}\right)\right]}{\left[1 - N_m \left\{A + \frac{1-A}{A}\left(s - \left\{1-A\right\}\right)\right\}\right]^{\frac{1}{2}}} ds \right] \tag{28}$$

These are the standard integrals which yield:

$$A = \frac{\nu}{\omega} \frac{4}{3N_m} \left[\frac{1-A}{A} - \left(\frac{1-A}{A} - \frac{A}{1-A}\right)\left(1 + \frac{AN_m}{2}\right)\left(1 - AN_m\right)^{\frac{1}{2}} - \frac{A}{1-A}\left(1 + \frac{N_m}{2}\right)\left(1 - N_m\right)^{\frac{1}{2}} \right] \tag{29}$$

For a uniform slab ($A = 1$, $N = N_m$) we go back to the initial expression (Eqn. (21)) to obtain:

$$(A)_{A=1} = \frac{\nu}{\omega} \frac{N_m}{(1-N_m)^{\frac{1}{2}}}$$

A plot of $A/\nu/\omega$ vs N_m for different density profiles is shown in Fig. 15a. Again normalizing the results to total electron content of the slab, (Fig. 15b) reveals that the effect of the density distribution is not

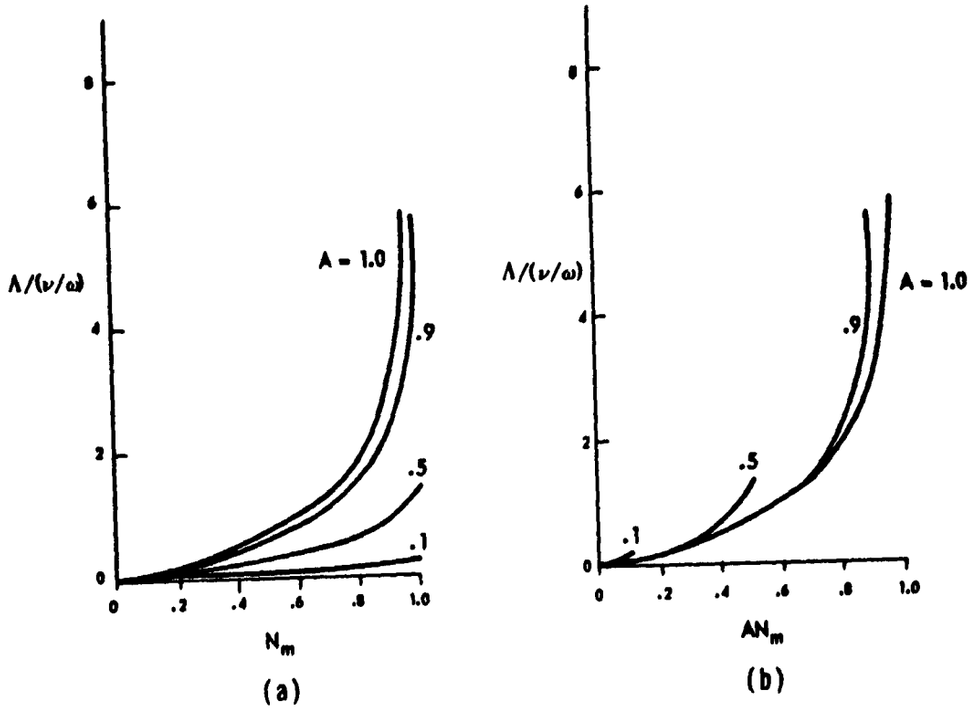

Fig. 15 (a) Variation of normalized attenuation introduced by a plasma with normalized electron density for different spatial distributions of electron density

(b) Variation of normalized attenuation introduced by a plasma with average normalized electron density for different spatial distribution of electron density.

significant until $N_m > 0.8$, i.e. the electron density must be at least 80% of the cut-off density before the attenuation becomes sensitive to the electron density profile. It is thus apparent that single frequency measurements of either or both phase and attenuation will give little information on the electron density distribution throughout the plasma. Simultaneous probing at multiple frequencies offers some hope in this direction.

Effect of Boundaries: The effect of the electron density varying in the direction of propagation (z-direction) on the fields reflected and transmitted by a plasma slab have been considered by a number of people (see for example Budden[18], and Nicoll and Basu[19]) with probably the best set of numerical results being recently obtained by Albini and Jahn[20,21], for a "trapezoidal" electron distribution - i.e. a uniform slab of plasma bounded by symmetric linear ramps of electron density. Such a "trapezoidal" electron distribution (in the notation of Albini and Jahn) is shown in Fig. 16. Note that changing Z_o/λ is equivalent to changing the electron density profile whereas changing Z_t/λ simply changes the thickness of the slab. The total electron density over a cross-section of the slab is $N_m(Z_t - Z_o)$, while the average electron density is $N_m(1 - (Z_o/Z_t))$. Taking the numerical results of Albini and Jahn and plotting them against $(Z_t - Z_o)/\lambda$ for different values of the "ramp" distance Z_o/λ results in the curves shown in Fig.17. Note that $(Z_t - Z_o)/\lambda$ is the normalized width of a uniform plasma slab of electron density equal to the maximum density of the trapezoidal distribution and containing the same number of electrons as the slab of width Z_t and having a "trapezoidal" distribution of electrons along its width.

Figure 17a shows the variation in amplitude of the reflected and transmitted signals with slab thickness for different "ramp" distances (Z_o/λ) for a lossless plasma of dielectric coefficient $K = 0.25$. As expected, the more gradual the "ramp", the better is the "match" of the plasma and hence the more the signal which is transmitted through the slab and the less the signal reflected from the plasma. The important point to notice is that the positions of the maxima and minima of both

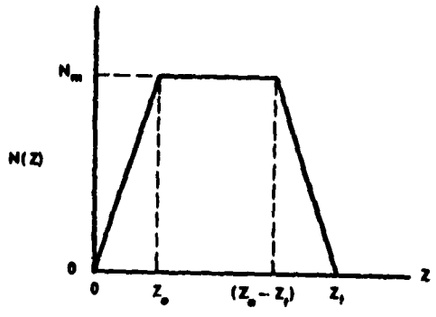

Fig. 16: Trapezoidal distribution of electron density in a plasma slab as used by Albini and Jahn (ref. 20, 21) in computing effect of spatial electron distribution on transmission and reflection of electromagnetic waves.

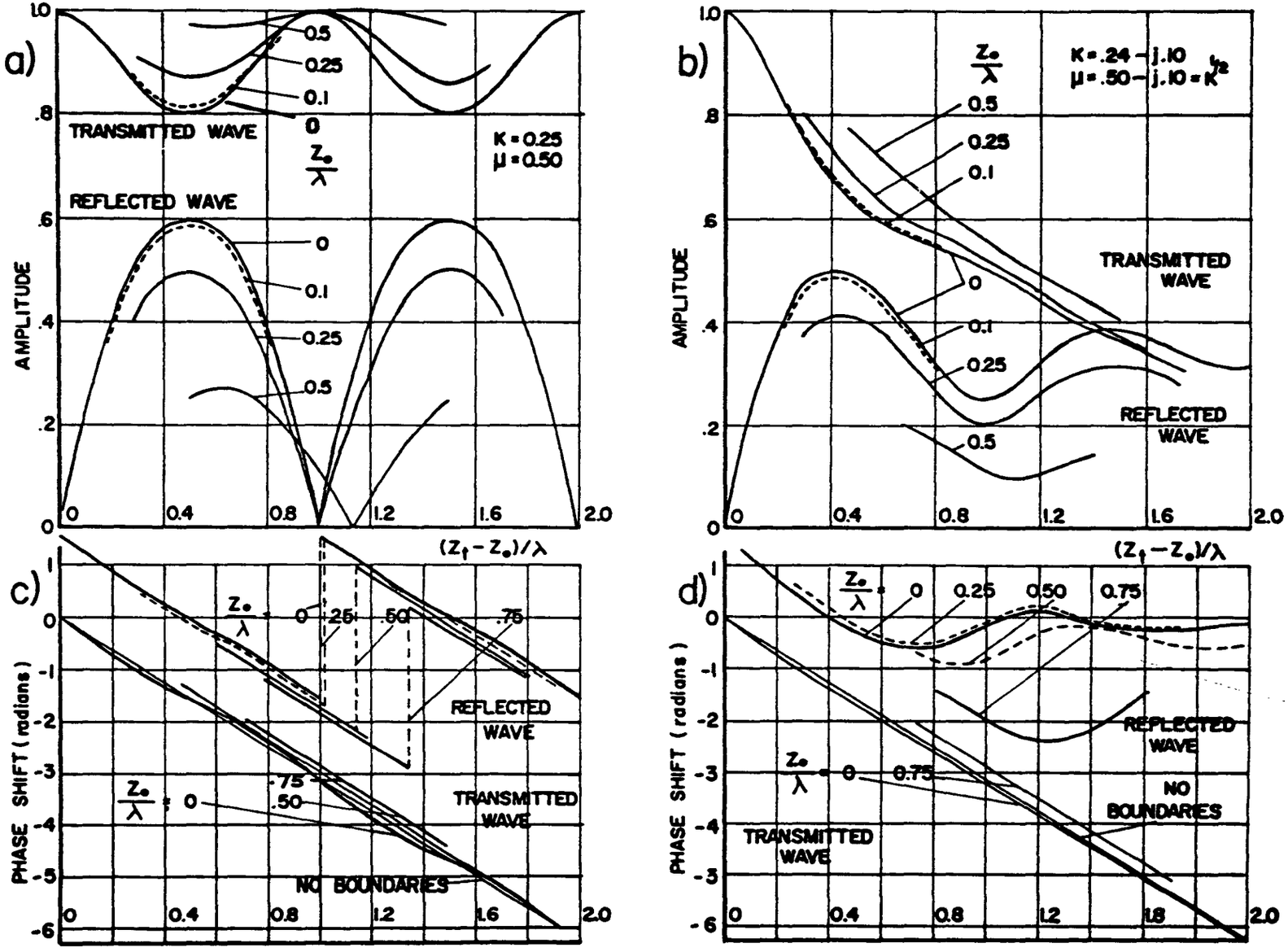

Fig. 17: Effect of spatial distribution of electron density, based on Albini and Jahn[19,20] on amplitude and phase shift of transmitted wave.

the reflected and transmitted signals depend on the <u>total</u> electron density or the physical length of a uniform plasma slab, and not on the actual physical dimensions of the slab. This is the case until the "ramp" dimensions become quite significant ($Z_o/\lambda \geq 0.50$).

The effect of losses on the behaviour of the amplitude of the transmitted and reflected waves is shown in Fig. 17b for a plasma of dielectric coefficient $K = 0.24 - j \cdot 10$. In the presence of losses the signals become less sensitive to the shape of the boundaries. In particular the transmitted signal does not depend significantly on the shape of the electron density profile.

As before the minima and maxima which have become drastically damped occur at the same position for "ramp" distances up to 0.5λ when the slab dimensions are normalized to those of a uniform slab.

The phase of the transmitted and reflected waves[21] can also be put in a normalized form which shows their dependence on the total electron content and relative insensitivity to the shape of the electron density profile. Albini and Jahn plot the total phase shift of the transmitted wave Φ_T upon passing through a plasma slab of thickness Z_t and include the free space path as well. To put this result into the form of the phase change introduced by the plasma $\Delta\Phi$ it is necessary to subtract from Φ_T the plasma change in a path length Z_t in free-space. Thus,

$$\Delta\phi_t = 2\pi \frac{Z_t}{\lambda} - |\phi_T|$$

In Fig. 17c and 17d are shown plots of the phase shift of the transmitted wave introduced by the plasma normalized to total electron density. The phase shift is very nearly the same as calculated for the unbounded plasma. The effect of boundaries is to make the phase undulate slightly about the no boundary value. The influence of losses does not introduce any significant modifications. The density profile changes the phase very slightly - by an amount which cannot be used by the present day precision of plasma microwave measurements to give any reliable information on the density profile of the plasma.

For the phase of the reflected signal consider the reflections to occur from the slab as if the boundary was located at the midpoint between where the plasma starts and where the maximum electron density has been reached. This is again replacing the slab by an equivalent (in total electrons) uniform slab of the maximum density. We, therefore, take the phase of the reflected wave Φ_R as calculated by Albini and Jahn[21] and add $2\pi/\lambda\ Z_o$ to their result (since the effective boundary of the slab is considered to be at $Z_o/2$ and the wave has to travel this distance twice). Thus:

$$\Delta\phi_r = \Phi_R + \frac{2\pi}{\lambda} Z_o \quad .$$

Plots of $\Delta\phi_r$ vs $(Z_t - Z_o)/\lambda$ (i.e. slab width) are shown in Fig. 17c and 17d. Only at values of $Z_o/\lambda > 0.5$ does the character of the reflected phase depart notably from that of a uniform slab whose electron density is the same as the maximum of the "trapezoidal" electron distribution and which contains the same total number of electrons as the "trapezoidal" slab.

(ii) Plasma Properties Varying Normal to Direction of Propagation: Consider a plane wave normally incident upon a plasma slab. The properties of the slab are constant throughout the thickness of the slab, but depend on the distance from the centre of the plasma slab. That is the electron density n(r) varies in the direction normal to the direction of propagation. At the incident boundary of the slab (z = 0), the phase front of the incident plane wave coincides with the front face of the slab. At the second boundary of the slab (z = d) the phase of the wave emanating at a height r above the centre line of the slab is:

$$\Delta\phi = kd\ [1 - \sqrt{1 - N(r)}]$$

The phase difference between the wave coming through the slab at height r to the phase of the wave coming out at the centre of the slab (r = 0) is

$$\Delta\phi(r) - \Delta\phi(0) = kd\ [-\sqrt{1 - N}(r) + \sqrt{1 - N_o}] \qquad (30)$$

where:

$N_0 = \frac{n_0 e^2}{m\varepsilon_0\omega^2}$ and n_0, the electron density along the width of the slab position r = 0

$N(r) = n(r) \frac{e^2}{m\varepsilon_0\omega^2}$

Eqn. (30) is thus the equation of the phase front (surface of constant phase) of the wave emenating from the plasma. In physical space the important parameter is the optical path length. The surface of the constant path length is given by:

$$\Phi(r) = \frac{\Delta\phi(r) - \Delta\phi(0)}{k} = d[-\sqrt{1-N(r)} + \sqrt{1-N_0}] \tag{31}$$

This is the shape in free space of the planes of constant phase given in terms of physical dimensions.

Considering that the phase fronts are orthogonal to the direction of energy travel, the ray incident upon the slab of plasma at height r is refracted so that it emerges at some angle $\phi(r)$ given by:

$$\tan\phi(r) = -\frac{d\Phi(r)}{dr} = -\frac{d}{2}\frac{dN(r)/dr}{\sqrt{1-N(r)}} \tag{32}$$

If the beam of incident radiation of radius a is intercepted by a plane of half-width A located a distance R from the second surface of the slab then the refractive defocussing (η) intorudced by the non-uniform electron density variation of the slab can be determined from:

$$\tan\phi(a) = \frac{A-a}{R} = -\frac{d}{2}\frac{(dN(r)/dr)_{r=a}}{\sqrt{1-N(a)}} \tag{33}$$

or

$$\eta = \frac{a}{A} = 1 + \frac{d \cdot R}{2A}\frac{dN(r)/dr}{\sqrt{1-N(a)}} \tag{34}$$

A variety of different variations of the electron density with direction normal to the direction of propagation and the corresponding

refractive defocussing coefficient are possible. A convenient distribution for laboratory experimental purposes is the parabolic distribution, $N(r) = N_0(1 - \Gamma(r/r_0)^2)$ where r_0 is the radius of the plasma and Γ represents the amount by which the electron density has decreased at the edge of the experimental plasma relative to the electron density at the centre (N_0). Despite the fact that the resulting equation for $\eta(a)$ is transcendental it can be very readily solved.

Numerical results for a parabolic distribution of electron densities as determinedfrom Eqn. (34) are shown in Fig. 18. As can be seen if the plasma is non-uniform then very strong attenuation effects can be obtained due to these refractive effects.

The geometrical optics type of refractive defocussing as we have considered cannot take into account the phase difference between the various rays (from different radii) as they reach the receiving antenna. In order to do this, resort must be made to diffraction theory.

Electromagnetic Wave Propagation Through Laboratory Plasmas as a Diffraction Problem: Most laboratory scale plasmas are only a few wavelengths in extent and hence when the properties of the plasma are to be measured using electromagnetic waves, diffraction will play a major role in determining the electromagnetic energy that emanates from the plasma and its distribution in space.

When considering diffraction phenomena, the Kirchhoff scalar diffraction formula, although not rigorous in its formulation, has enjoyed considerable success when applied to actual physical problems. Using the scalar diffraction formula, the field u at point p may be written:

$$u(p) = -\frac{1}{4\pi}\int_S \int \left\{ \frac{e^{-jks}}{s} \frac{\partial \psi}{\partial n} - \psi \frac{\partial}{\partial n}\left(\frac{e^{-jks}}{s}\right) \right\} dS \qquad (35)$$

where: s is the distance of the field point p to the surface of integration

ψ is the value of incident field (amplitude and phase) at the element of integration

n is the normal derivative in the plane of integration

S is the surface of integration.

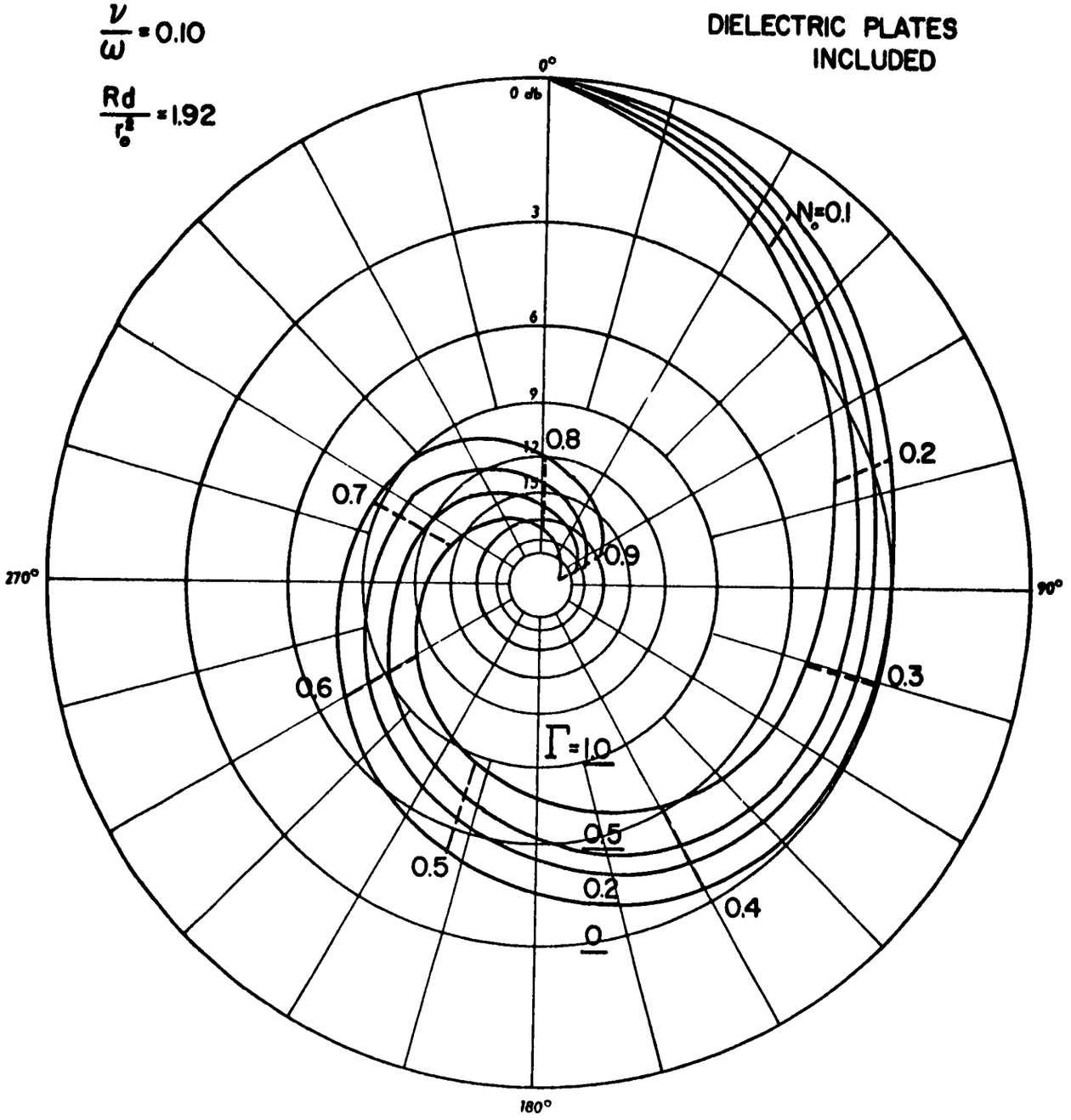

Fig. 18: Phase and attenuation of a plane incident wave transmitted through a slab of plasma including the effect of dielectric plates and of lateral defocusing in one-dimension for a parabolic distribution of electron density in direction normal to direction of propagation, ($\Lambda = \rho_o$).

(i) Application to Point Source Illuminating Finite Plasma Slab:

To consider the diffraction phenomena introduced by a finite plasma, let a source of electromagnetic energy be situated at point S (see Fig. 19a) a distance (R-d) from a uniform slab of plasma of thickness d. The exit pupil of the system is an aperture of radius r located at the exit position of the plasma slab. [In practice[38], it is found that the exit pupil of a finite plasma container determines the major diffraction effects so that the above model is a good approximation to a cylindrical slab of plasma of radius r and thickness d.] This exit pupil is taken as the surface of integration. The problem is then to determine the incident field over the exit pupil and perform the integration according to Eqn.(35) in order to evaluate the field at the point p. The result can be written:

$$u(p) = \frac{jk\,a^2}{2\pi RR'} e^{-jk\left(R + R' + \left\{\frac{\beta}{k} - 1\right\}d\right)} e^{-\alpha d} \int_0^1 \int_0^{2\pi} U_o(l) e^{-\alpha f a^2 l^2} e^{-jk\left(g + \frac{\beta}{k} f + \frac{1}{2R'}\right)a^2 l^2} \cdot e^{jk\frac{\rho a}{R'} l \cos(\phi - \phi)}\, l\, dl\, d\phi \qquad (36)$$

where:

$R' = [(R_o + x)^2 + \rho^2]^{\frac{1}{2}}$

U_o = free-space radiation pattern of the source representing both the strength and directivity of the radiation.

$$f = \left[2d\left\{1 + \frac{\beta}{k}\left(\frac{R}{d} - 1\right)\right\}^2\right]^{-1}$$

$$g = \left[2(R-d)\left(1 + \frac{d}{(R-d)\,\beta/k}\right)^2\right]^{-1}$$

and the other parameters are defined in Fig. 19a.

Making the substitution:

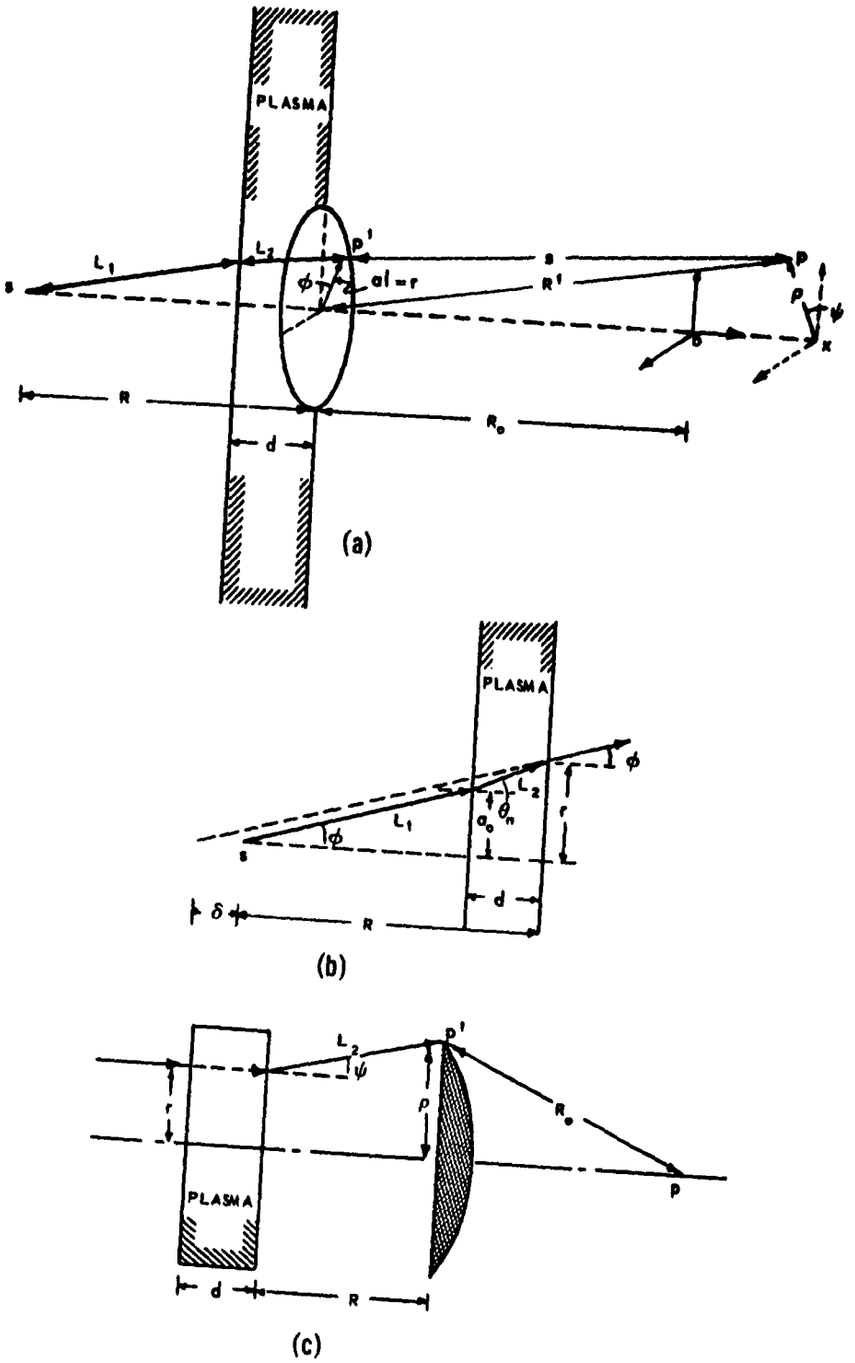

Fig. 19: (a) Geometry for derivation of diffraction due to a plasma slab located in front of a circular aperture in a metal screen.
(b) Optical distance travelled by radiation from source to exit pupil of diffracting system.
(c) Optical distance travelled by radiation through plasma and from exit pupil to field point p.

$$P = k\left(g + \frac{\beta}{k} f + \frac{1}{2R'}\right) a^2$$

$$Q = \frac{ka}{R'} \rho$$

$$\Theta = k(R + R' + (\beta/k - 1)d)$$

the integration with respect to ϕ is readily executed to give:

$$u(p) = j\frac{(2\pi a^2)}{\lambda RR'} e^{-j\Theta} e^{-\alpha d} \int_0^1 U_0(l) e^{-\alpha f a^2 l^2} J_0(Ql)\, l\, dl \tag{37}$$

where J_0 is the zero order Bessel function of the first kind.

For the field along the principal axis of the system $Q = 0$ so that:

$$u(p) = \frac{j(2\pi a^2)}{\lambda RR'} e^{-j\Theta} e^{-\alpha d} \int_0^1 U_0(l)\, e^{-(\alpha f a^2) l^2}\, e^{-jPl^2}\, l\, dl \tag{38}$$

Consider the field along the principal axis for a lossless plasma ($\alpha = 0$) which is uniformily illuminated from a point source located at S (i.e. $U_0(l) = u_0 = \text{constant}$). In this case:

$$\frac{u(p)}{u_0} = j\,\frac{(2\pi a^2)}{\lambda RR'}\, e^{-j\Theta} \int_0^1 e^{-jPl^2}\, l\, dl$$

$$= j\,\frac{(2\pi a^2)}{\lambda RR'}\, e^{-j\Theta} \cdot \frac{e^{-jP/2}}{2}\left[\frac{\sin(P/2)}{P/2}\right] \tag{39}$$

The intensity along the principal axis is thus:

$$I(p) = \frac{k^2 a^4}{4(RR')^2}\left[\frac{\sin(P/2)}{(P/2)}\right]^2 \tag{40}$$

This is just the field along the principal axis of a circular aperture. To study the influence of the plasma we must consider the parameter P. After some algebra we can write:

$$\left(\frac{P}{2}\right) = \frac{ka^2}{4}\left(\frac{1}{R'} + \frac{1}{R + d\left(\frac{1}{\beta/k} - 1\right)}\right) \sim \frac{ka^2}{4}\left(\frac{1}{R'} + \frac{1}{R} - \frac{d}{R^2}\left(\frac{1}{\beta/k} - 1\right)\right)$$

The effect of the plasma is thus to decrease the value of (P/2) since the term $\beta/k \;/\; [d + (R - d)\,\beta/k]$ decreases as β/k decreases. The effect of the plasma is to shift the axial radiation pattern of the system.

When the plasma is lossy ($\alpha \neq 0$) and if the directivity of the incident radiation can be approximated in the form:

$$U_0(l) = u_0\, e^{-\beta_0 l^2}$$

then Eqn. (38) can be written:

$$\frac{u(p)}{u_0} = \frac{j(2\pi a^2)}{\lambda RR'}\, e^{-j\theta} \int_0^1 e^{-j[P - j\{\alpha f^2 + \beta_0\}]l^2}\, l\, dl$$

$$= \frac{j(2\pi a^2)}{\lambda RR'}\, e^{-j\theta}\, \frac{e}{2}^{-j[P - j\{\alpha f a^2 + \beta_0\}]/2} \left[\frac{\sin\left[\frac{P - j(\alpha f a^2 + \beta_0)}{2}\right]}{\left[\frac{P - j(\alpha f a^2 + \beta_0)}{2}\right]}\right] \quad (41)$$

The intensity along the principal axis is then:

$$I(p) = \frac{k^2 a^4}{4(RR')^2} \left(\frac{e^{-(\beta_0 + \alpha f a^2)}}{\frac{P^2 + (\beta_0 + \alpha f a^2)^2}{4}}\right) \left[\frac{1}{2}\left\{\cosh(\beta_0 + \alpha f a^2) - \cos P\right\}\right] \quad (42)$$

The effect of the losses in the plasma on the intensity is the same as the effect of using a directive antenna.

(ii) Application to Plane Wave Illumination of Plasma Whose Properties Change in Radial Direction: Consider a plane wave incident on a slab of plasma as shown in Fig. 19c. The plasma is considered to be non-uniform with the electron density N(r) depending upon distance r from the centre of the plasma. A ray incident upon the plasma at r emerges from the plasma at angle ϕ. Assume a perfect lens is located a distance R from the second surface of the slab. The energy at the focus

of the lens is then readily determined if we know the field distribution incident upon the lens. We then find[22] from a plane incident wave and a parabolic variation of the radial electron distribution

$$(u)p = \frac{jk}{2}\rho_o^2 \frac{e^{-jk(R_o+R)}}{R_o} e^{-j(Pkd+W)}\left[\frac{\sin W}{W}\right] \qquad (43)$$

where:

$$W = \frac{k}{2}(RS+Qd)\eta^2(\rho_o^2/r_o^2)$$

$$S = \left(\frac{d}{r_o}\Gamma N_o\right)^2(1+N_o+N_o^2)$$

$$P = \left[1-\frac{N_o'}{2}\left(1+j\frac{\nu}{\omega}\right)\left\{1+\frac{N_o'}{4}(1+j\nu/\omega)\right\}\right]$$

$$Q = \frac{N_o'}{2}\Gamma\left(1+j\frac{\nu}{\omega}\right)\left[1+\frac{N_o'}{2}(1+j\nu/\omega)\right]$$

$$N_o' = N_o/(1+\nu^2/\omega^2)$$

$$\eta = r/\rho$$

r_o = radius of plasma

ρ_o = radius of lens

Note that P and W are complex so that the expression is not as simple as it seems. When the plasma and the lens are the same size: $\rho_o = r_o$ and the values of η calculated in the previous section are applicable. (Otherwise η is calculated from Eqn. 34 with A set equal to ρ_o).

In the limiting case of:

(a) uniform plasma: $\Gamma = 0$, so that $S = 0$, $Q = 0$ and $W = 0$.

$$u(p) = \frac{jk}{2}\rho_o^2 \frac{e^{-jk(R_o+R)}}{R_o} e^{-jkd\left\{\left[1-\frac{N_o'}{2}\left(1+\frac{N_o'}{4}\right)\right]-\frac{\nu}{\omega}\frac{N_o'}{2}\left(1+\frac{N_o'}{2}\right)\right\}kd} \qquad (44)$$

(b) lens against plasma: $R = 0$, $\eta = 1$, $W = \frac{k}{2} Qd$

$$u(p) = \frac{jk}{2} \rho_o^2 \frac{e^{-jkR_o}}{R_o} e^{-jk(P+Q/2)d} \left[\frac{\sin\left\{(kd/2)\, Q\right\}}{\left\{\frac{kd}{2} Q\right\}} \right]$$

Numerical results for a parabolic distribution of electrons are shown in Fig. 20 which illustrates the effect of the non-uniformity in electron density, the effect of the distance of the lens from the plasma and the effect of collision frequency. One can, for example, perform measurements at different positions from the plasma in order to determine the degree of non-uniformity of the plasma. Note that the non-uniformity in the electron density of the plasma and the geometry of the arrangement (Rd/r_o^2) have a far-greater influence on the electromagnetic wave passing through the plasma than does the collision frequency.

(b) Experimental Study of Microwave Systems: Many microwave measurements of plasma properties by free-space propagation techniques have been carried out without a detailed knowledge of the possible influence of various effects such as refraction, reflection and diffraction on the actual measurements of a signal transmitted through the plasma. One of the aims of the microwave measurements presented in this section is to show how important these effects may be in some given experimental configurations. It is also intended to demonstrate experimentally how these effects can be minimized and what is the optimum experimental arrangement for a given plasma container and microwave transmitting and receiving antennas.

An extensive series of measurements have been carried out on three basic experimental arrangements in order to establish the microwave characteristics of the measuring systems in the absence of a plasma. The three microwave systems which have been the subject of investigation are represented in Fig. 21. In Fig. 21a the cylindrical dielectric container terminated by flat polystyrene plates is illuminated by a microwave horn; the receiving antenna is also a microwave horn. This

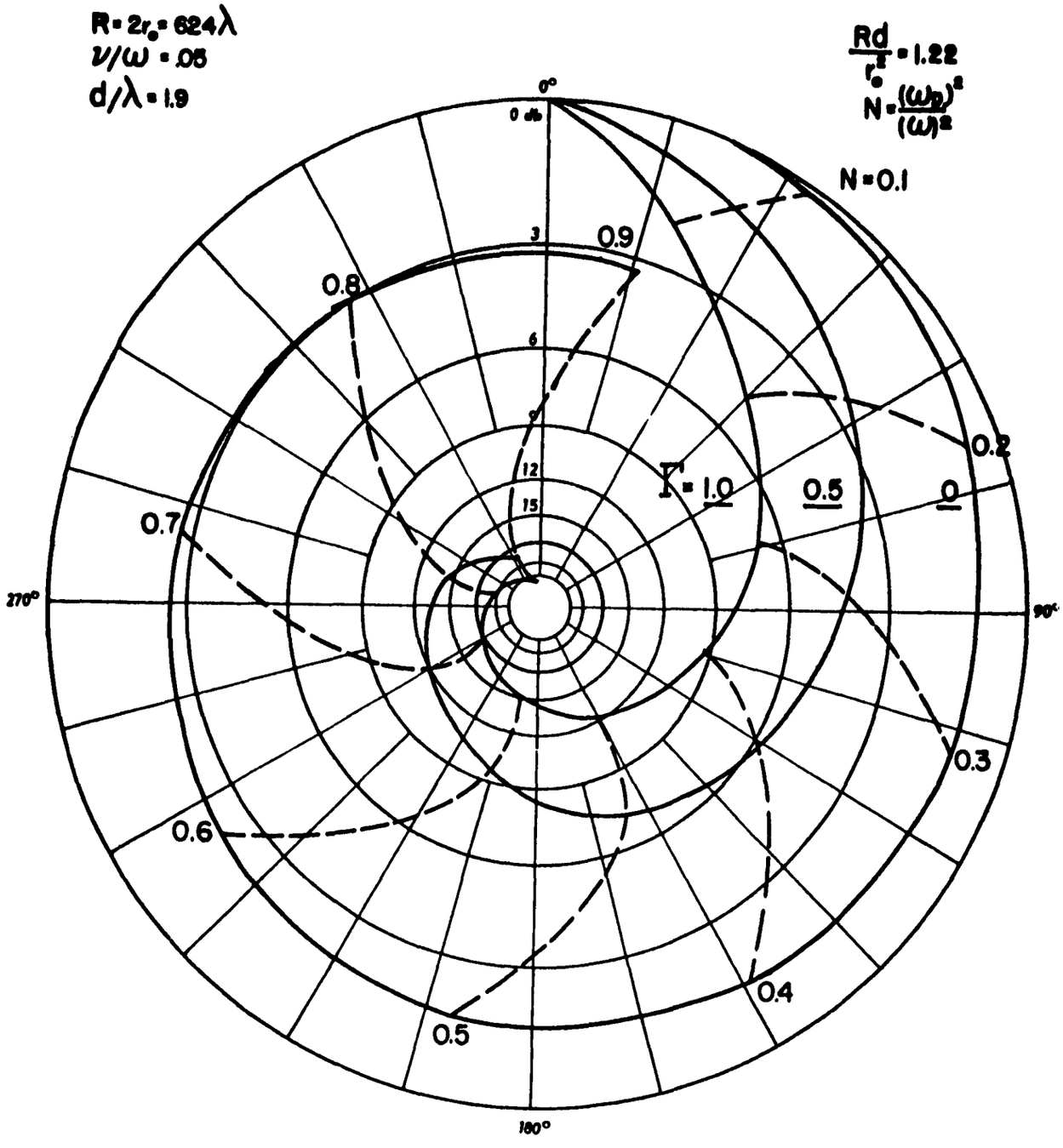

Fig. 20a: Phase and intensity of an incident plane wave transmitted through a slab of plasma and diffracted by a circular metal screen forming the exit pupil of the microwave optics system showing the effect of non-uniformity in electron density in the direction normal to the direction of propagation (A parabolic distribution of electron density in the lateral direction and $A = r_0 = \rho_0$ is assumed).

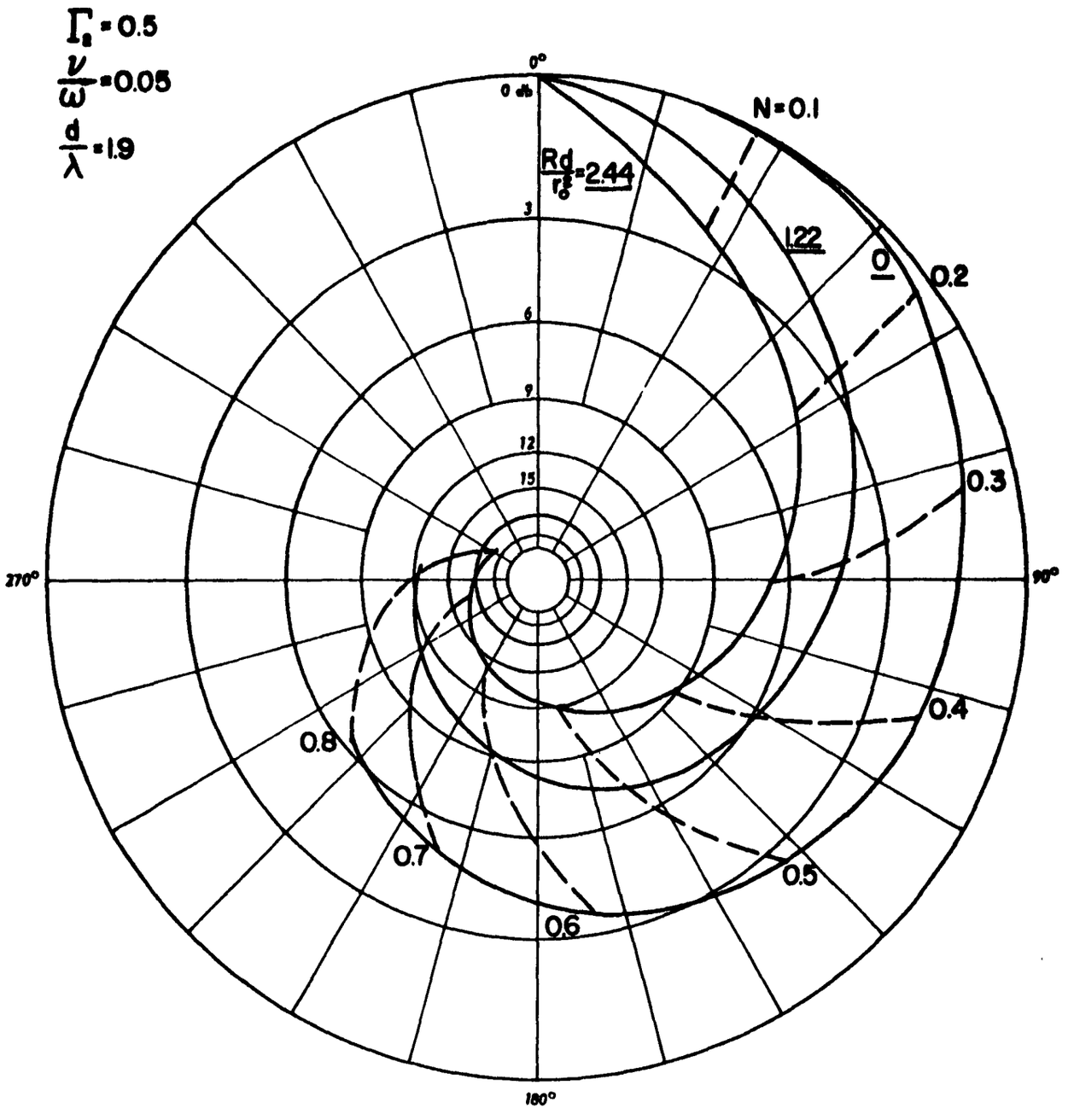

Fig. 20b: Phase and intensity of an incident plane wave transmitted through a slab of plasma and diffracted by a circular metal screen forming the exit pupil of the microwave optics system showing the effect of the distance of the receiving lens from the exit pupil, ($A = r_o = \rho_o$).

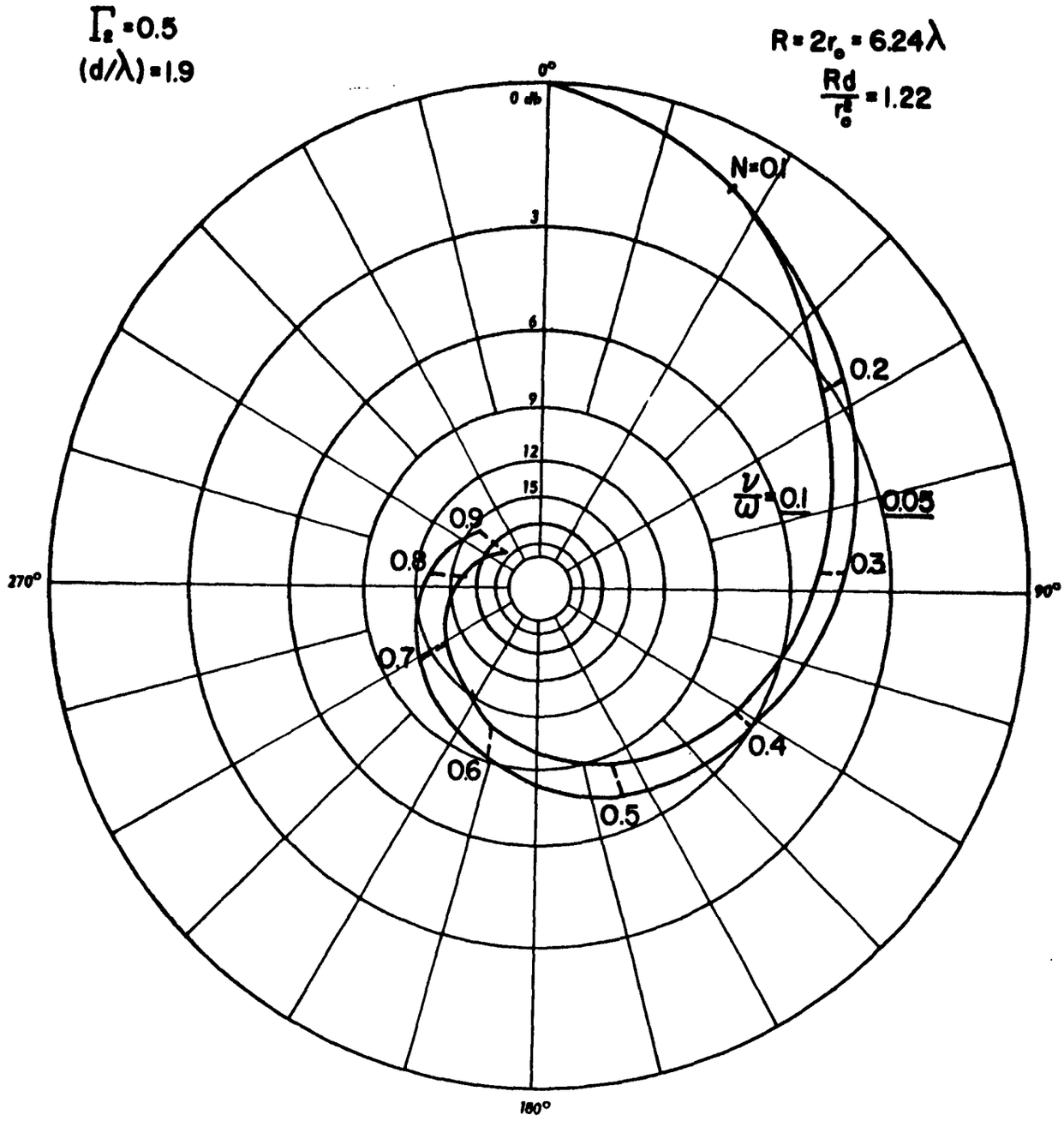

Fig. 20c: Phase and intensity of an incident plane wave transmitted through a slab of plasma and diffracted by a circular metal screen forming the exit pupil of the microwave optics system showing the effect of various values of collision frequency, ($A = \rho_0 = r_0$).

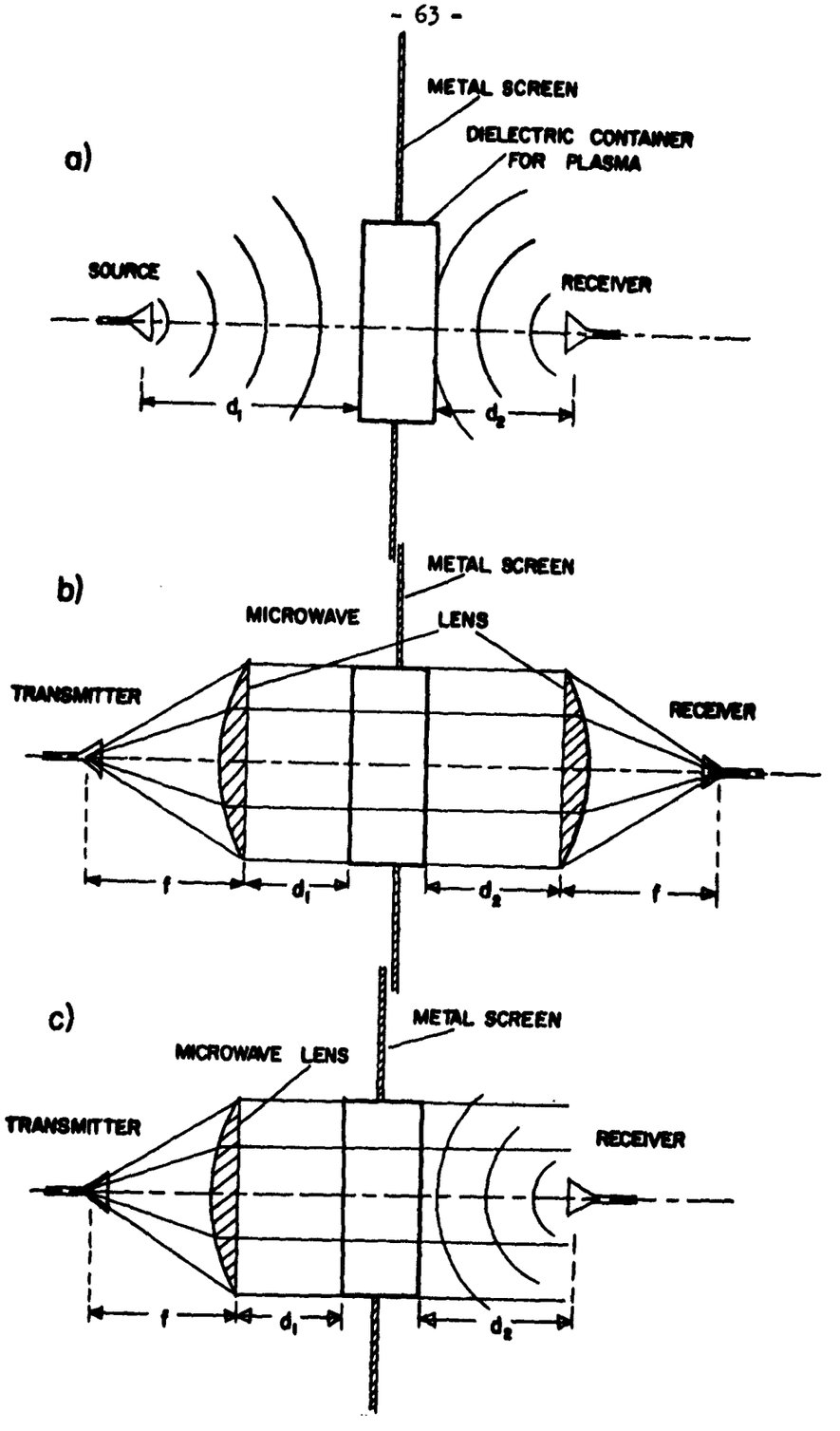

Fig. 21: Basic microwave systems for studying plasma by free-space propagation.

arrangement can be described by a point source illuminating the dielectric plates between which a plasma slab is generated. A spherical phase front is incident upon the dielectric container. Such an experimental arrangement has the advantage of simplicity, but the theoretical interpretation is somewhat difficult since both the transmitting and receiving antennas are concerned with spherical waves.

The use of microwave lenses is the most practical way of lauching and receiving a plane wave in a usual laboratory arrangement. At microwave frequencies practical lenses can only be a few wavelengths in size and, therefore, diffraction effects become important. Such an arrangement is shown in Fig. 21b. In both cases the transmitting and receiving feeds are located at the focus of the transmitting and receiving lenses. From the optical point of view the plasma slab is then illuminated by a plane wave. However, due to the limited size of the lenses and the plasma container, diffraction effects will take place which must be taken into account when comparing theory with measurement.

A third possible arrangement is that shown in Fig. 21c. In this case a lens may be used to launch a plane wave incident on the plasma and a microwave horn is used to detect the transmitted signal. The alternate arrangement which consists in launching a spherical wave with a microwave horn and receiving with a highly directive system such as a lens is also possible and is equivalent to that shown in Fig. 21c, (provided the plasma satisfies the condition of reciprocity).

Microwave System Consisting of Transmitting and Receiving Horn Antennas: A series of measurements have been performed using the configuration shown in Fig. 21a and the following effects studied:

(i) Stray Scattering

Stray scattering is defined as the energy emerging from the transmitting antenna, which reaches the receiver after reflection from objects surrounding the plasma container. Stray scattering can be reduced or eliminated by placing a metal screen around the plasma container and by surrounding the antennas and the plasma container with microwave absorbing

material. In this way any energy not directed toward the plasma container is prevented from reaching the receiving antenna. The degree of stray scattering depends naturally on the directivity of the transmitting and receiving antennas. It was found that the use of a metal screen, when open waveguide antennas are used, greatly reduces the large fluctuations in the received signal observed in the absence of the metal screen. The stray scattering is less important when using a more directive 15db-horn. However, even in this case considerable reduction of the undulations due to the received rf energy are observed when a metal screen is used.

The use of a metal screen around the plasma container gives rise to a stronger diffraction effect due to the sharp discontinuity in the refractive index at the periphery of the cylindrical container. This is not really a disadvantage since even without the metal screen a certain amount of diffraction takes place which, when mixed with the stray scattering, cannot in general be treated theoretically. The theoretical treatment of the diffraction by an aperture in a metal screen is well known and for the case of a circular aperture this problem can be solved.

For all the measurements discussed in the sequel, a metal screen 2 feet by 2 feet has been used around the cylindrical container and some microwave absorbing material has been placed around the microwave propagation system. With this arrangement stray scattering is essentially eliminated and it is possible to examine the influence of other factors on the microwave measurements. The other factors which have been studied are the presence of the plasma container, various types of microwave feeds, and various positions of the transmitting and receiving antennas.

(ii) Influence of Plasma Container on Microwave Measurements

Tests have been carried out to determine the influence of the plasma (dielectric) container on the microwave measurements. For a given position of the transmitting horn on the axis of the cylindrical bottle the receiving horn was displaced along the axis of propagation and the field intensity was plotted as function of the position of the receiver. The cylindrical container was then removed and the same procedure was repeated.

Measurements were also obtained by leaving in position the cylindrical section of the container and removing the two flat polystyrene plates. The set of data so obtained are shown in Fig. 22. During these measurements the transmitting 15db horn was located against the flat face of the dielectric container and kept in the same position when the container was removed. It is interesting to note that, although larger undulations due to multiple reflections are observed when the plasma container is present, the general shape of the curve remains essentially unchanged whether the dielectric bottle is present or not. The curve obtained when only the cylindrical section of the container is in place indicates that the undulations observed are mostly due to the flat faces of the plasma container.

(iii) Multiple Reflections

In order to facilitate the interpretation of the undulations observed in the field intensity one can use the simple model of an electromagnetic wave propagating through the system and being reflected at various surfaces.

This model has been useful in explaining the series of experimental curves shown in Figs. 23a and 23b which illustrate these multiple reflection effects. In Fig. 23a, the power received by a 15db gain horn is plotted as function of the position (d_2) of the receiver for three positions (d_1) of the transmitting horn. The transmitting horn was displaced away in steps of one quarter wavelength. The regular undulations with a period $\lambda/2$ observed as the receiver is moved away from the dielectric container are just those predicted by such a model.

The results shown in Fig. 23b illustrate the case when the thickness (t) of the dielectric slab instead of the transmitter position (d_1) is changed. For these measurements the cylindrical container was replaced by dielectric plates of various thicknesses. It is seen that as expected the magnitude of the undulations passes through maxima and minima when the thickness of the dielectric plate is increased by a quarter wavelength. The small inset diagram in Fig. 23b illustrates more specifically this effect since it presents the amplitude of the

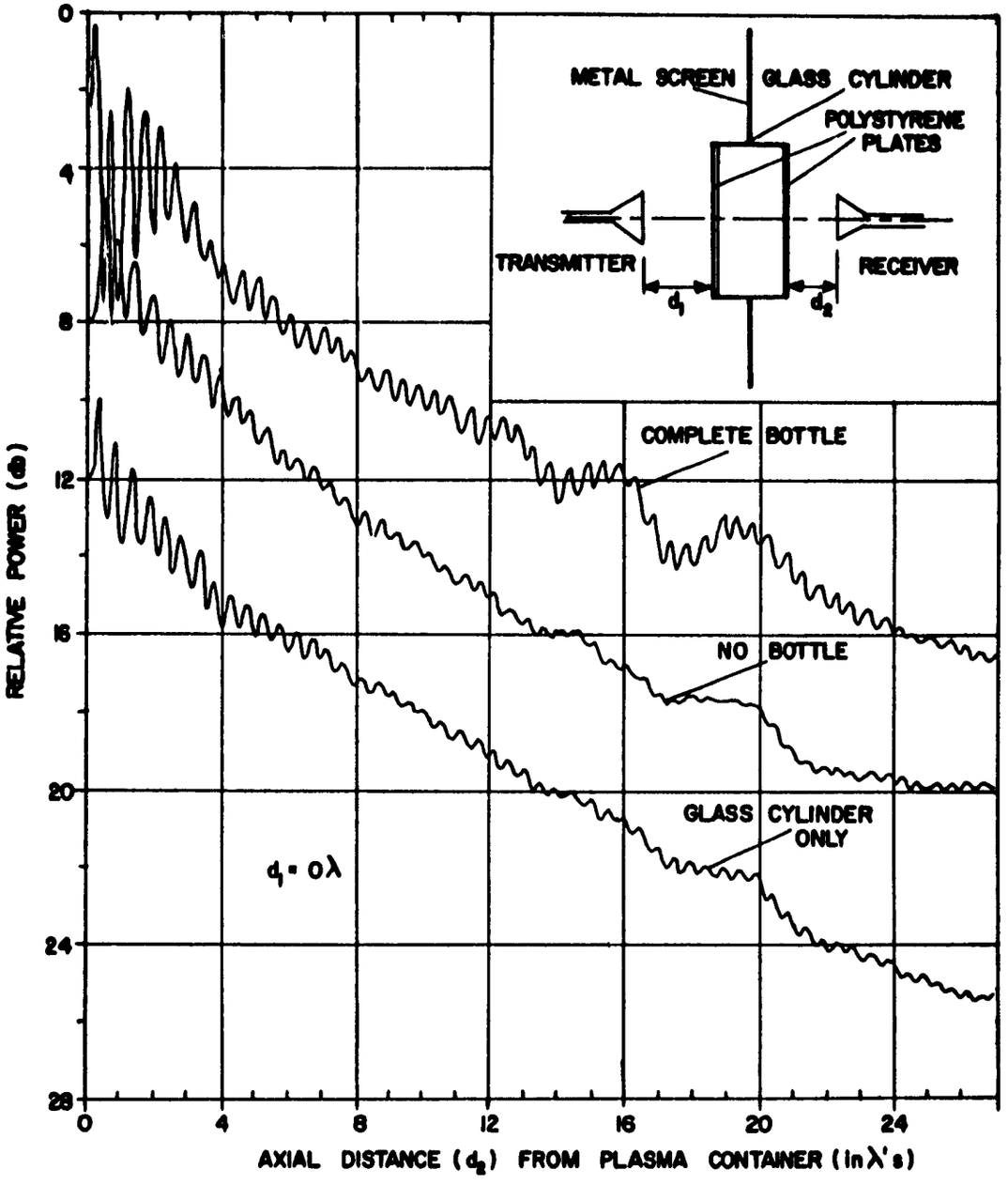

Fig. 22: Influence of the plasma container on the microwave measurements.

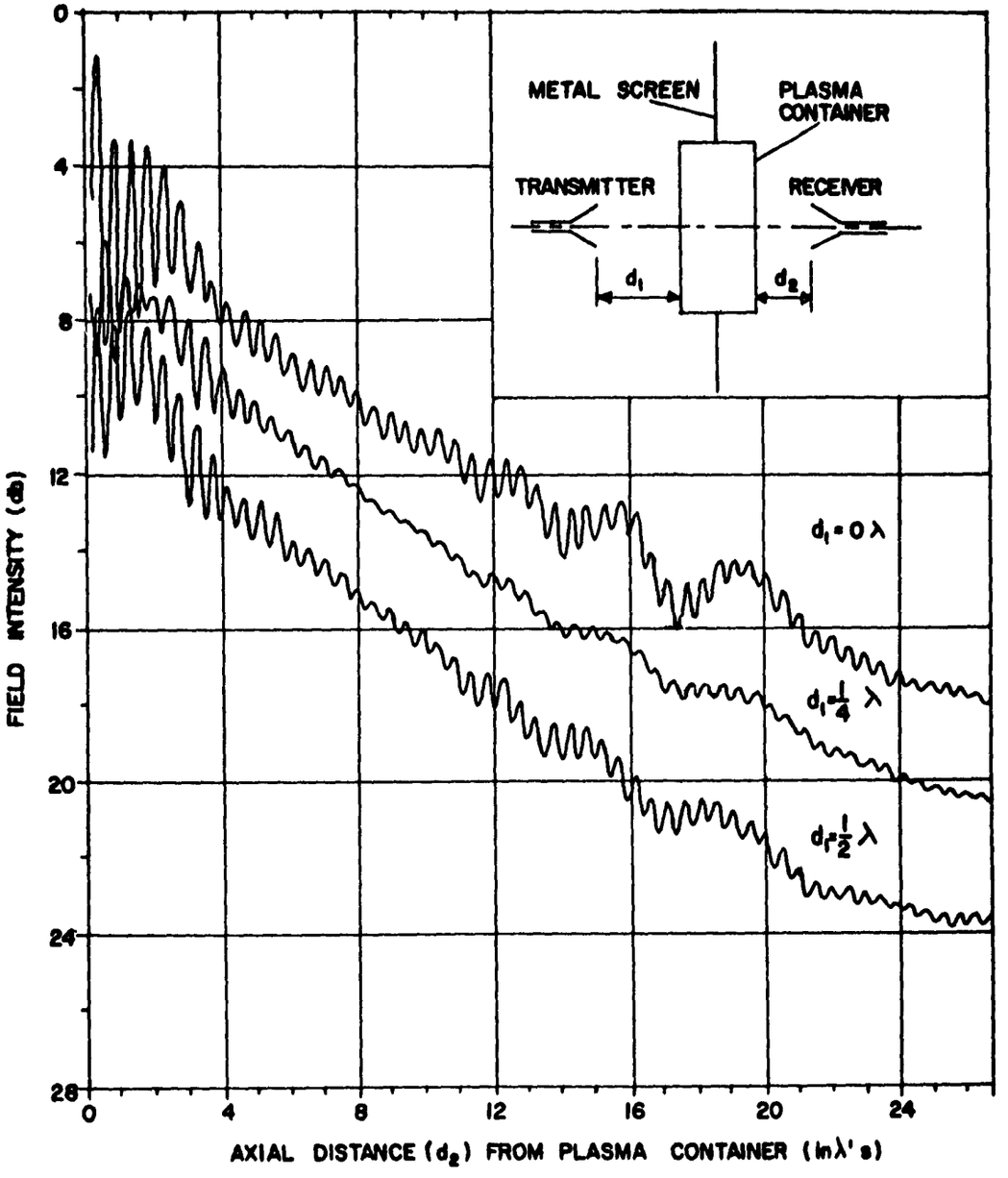

Fig. 23a Relative power received as function of the receiver position (d_2) for various distances (d_1) between the transmitter and the plasma container.

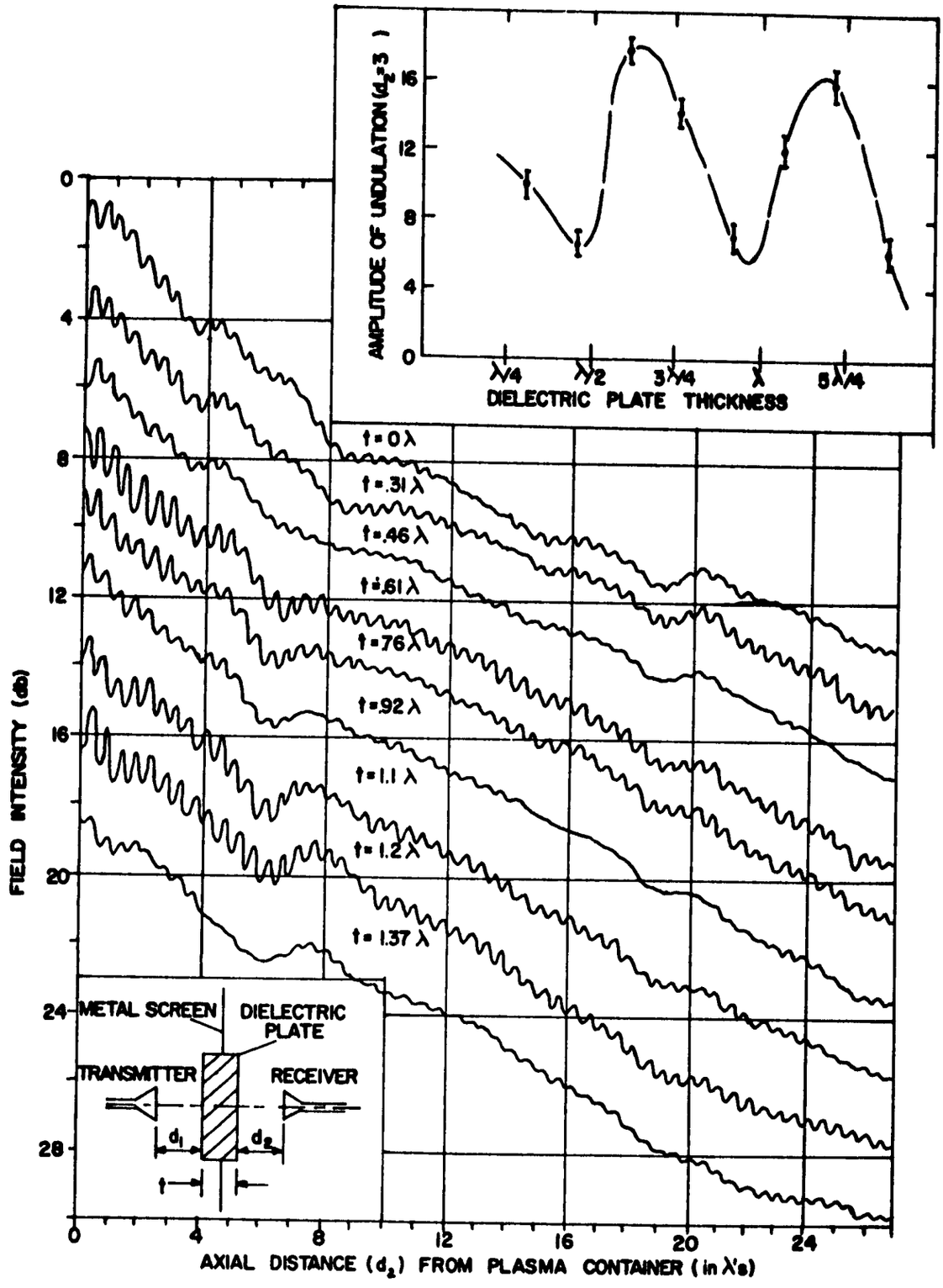

Fig. 23b Series of measurements of power received as function of receiver position illustrating the matching of the transmitting system by changing the thickness of the dielectric slab.

undulations as a function of the thickness of the dielectric plate.

(iv) Diffraction Effects

As mentioned earlier because of the limited dimensions of the screen aperture (size of plasma container) diffraction effects will be strong. Therefore, particular care should be given in setting up the experiment so that changes in the transmitted signal (amplitude and phase) in the presence of a plasma are not too greatly affected by diffraction effects.

An illustration of how critical is the position of the transmitting and receiving antennas on the energy diffracted in the receiving plane is shown in the experimental measurements of Fig. 24 obtained using 15db horns to transmit and receive the signal. Even more pronounced effects are seen if less directive antenna are used.

The diffraction effects can be predicted by using the Kirchoff's formulation of the problem as discussed previously.

From the curves shown in Fig. 24, it appears that for any position of the transmitting antenna, the optimum position of the receiver would be at least 10 wavelengths from the dielectric container where the power appears less sensitive to the position of the receiver.

Microwave System Containing Transmitting and Receiving Lenses: One of the disadvantages of using microwave horns to illuminate the plasma under investigation is the fact that one has to deal with spherical waves and as shown previously these waves are strongly affected by refractive defocussing through a plasma slab. In order to reduce the defocussing effects and to work with an experimental arrangement which is closer to the theoretical model of a plasma slab, an experimental study has been carried out to investigate the microwave characteristics of a transmitting system (see Fig. 21b) using microwave lenses. In this case it is possible to simulate the conditions of plane wave propagation and thus facilitate the interpretation of microwave measurements in the presence of a plasma.

The following discussion will describe two types of measurements:

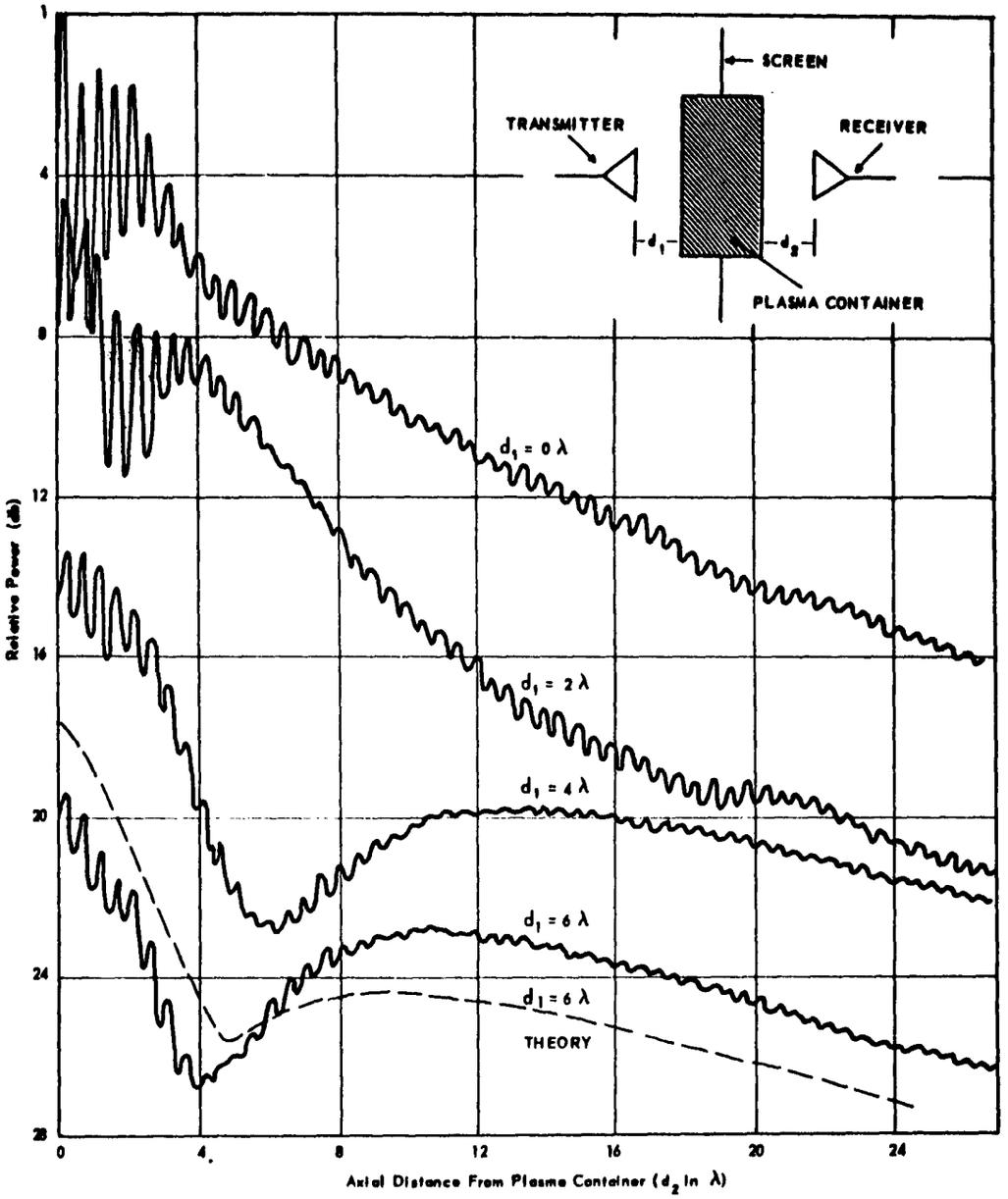

Fig. 24 Microwave power received as function of distance from the plasma container when 15db gain horns are used as source and receiver. Each measurement represents a different position of the transmitter with respect to the plasma container.

(i) Field Intensity Around the Focus of the Receiving Lens: For these experiments the transmitting system was formed by a 15db horn located at the focus of an 8-inch diameter microwave lens. Another lens identical to the transmitting lens was located on the receiving end. Both lenses were located on the axis of the plasma container and at a distance of 8-inches from it. The receiving feed was moved along the axis of propagation of the system and the field intensity was measured as function of the position of the receiving feed.

In Fig. 25 are shown two sets of measurements obtained when using a 15db gain horn and an open waveguide as the receiving feed. For each feed type a measurement was obtained with and without the plasma container in the plane (metal screen) separating the transmitting and receiving systems. It is seen that the dielectric container does not appeciably affect the field intensity variation around the focus of the receiving lens except for the multiple reflections which produce the regular undulations and which will be discussed later on. Therefore, as far as the interpretation of these results one can neglect the presence of the plasma container.

(ii) Field Intensity as Function of Position of Receiving Lens System: In the previous discussion of the theoretical model of a plane wave transmitted through a plasma slab it was found that an increase in electron density, when the electron collision frequency is small, produces effectively a reduction of the optical path length across the plasma slab. In the experiments described here the change in the optical path length is produced by displacing the receiving lens system along the optic axis. These measurements essentially simulate the effects produced by a plasma (except for electron collision frequency) and permit establishing a priori the optimum experimental arrangement for investigating a plasma slab located in a circular aperture of a metal screen. This, of course, implies that the plates of the dielectric container are matched to free-space. In the present experiment the optical thickness of the plates is one wavelength and these reflections should not take place at the walls of the container.

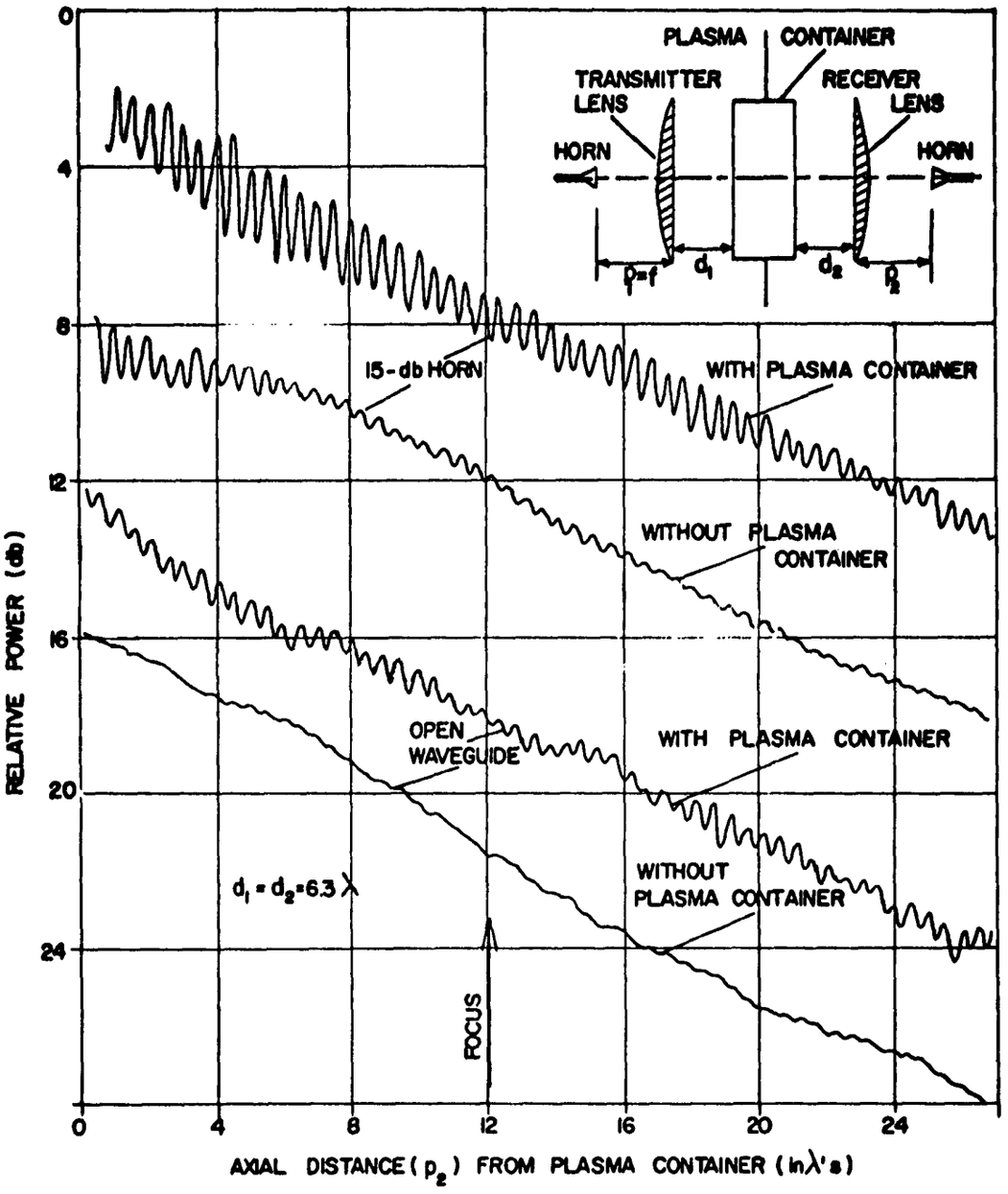

Fig. 25 Axial field intensity around the focus of the receiving lens with and without the plasma container. The two top curves were obtained using the 15-db gain horn as the receiver, the lower curves were obtained using an open waveguide.

In the discussion of the microwave measurements obtained with horn-feeds illuminating the plasma container and measuring the field intensity of the transmitted signal, it was found that two important effects, namely multiple reflections and diffraction had to be considered. In a similar way these effects are found to be the most important ones when using microwave lenses.

Multiple Reflections

When using microwave lenses, multiple reflections may be more serious than without lenses, since one deals essentially with plane waves and since additional reflecting surfaces are added to the microwave transmission system by the presence of the dielectric lenses. In Fig. 26 are shown a series of measurements of field intensity as function of the position of the receiving lens system for fixed distances (P_2) between the receiving horn and the receiving lens. It is noted that the amplitude of the undulations passes from a maximum value to a minimum value by changing the position (P_2) between the receiving horn and the receiving lens. Also the amplitude of the undulations passes from a maximum value to a minimum value by changing the position (P_2) of the receiver with respect to the lens by a quarter-wavelength.

The interpretation of these results can be demonstrated as before by examining the various components of the incident plane wave reaching the receiver after reflections at different planes in the system.

The presence of lenses in the microwave system introduces an additional source of reflection for the sampling signal. It is possible to reduce the reflections at the lens surfaces by adding quarter-wave matching plates to the lenses. Two such matching plates were made of polystyrene following the design proposed by Morita and Cohn[83]. These plates were placed against the flat face of the semi-convex lenses. The reflection on the curved surface of the lens facing the feed are negligible since the energy emerging is then not reflected back into the feed. The effectiveness of the matching plates is illustrated by the curves of Fig. 27 where the field intensity as function of

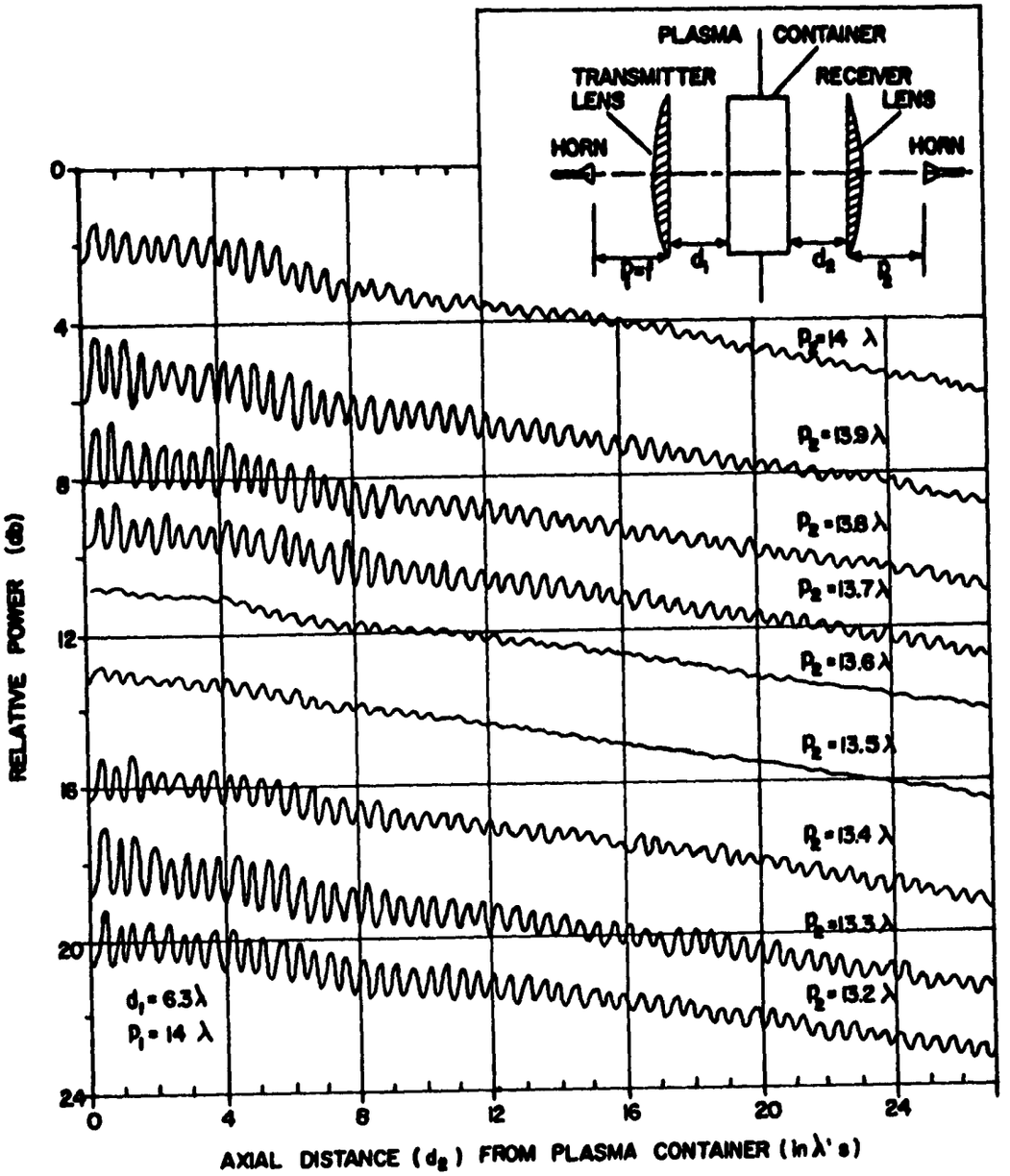

Fig. 26 Field intensity as function of the axial position of the receiving lens system for various positions of the receiving feed with respect to the receiving lens.

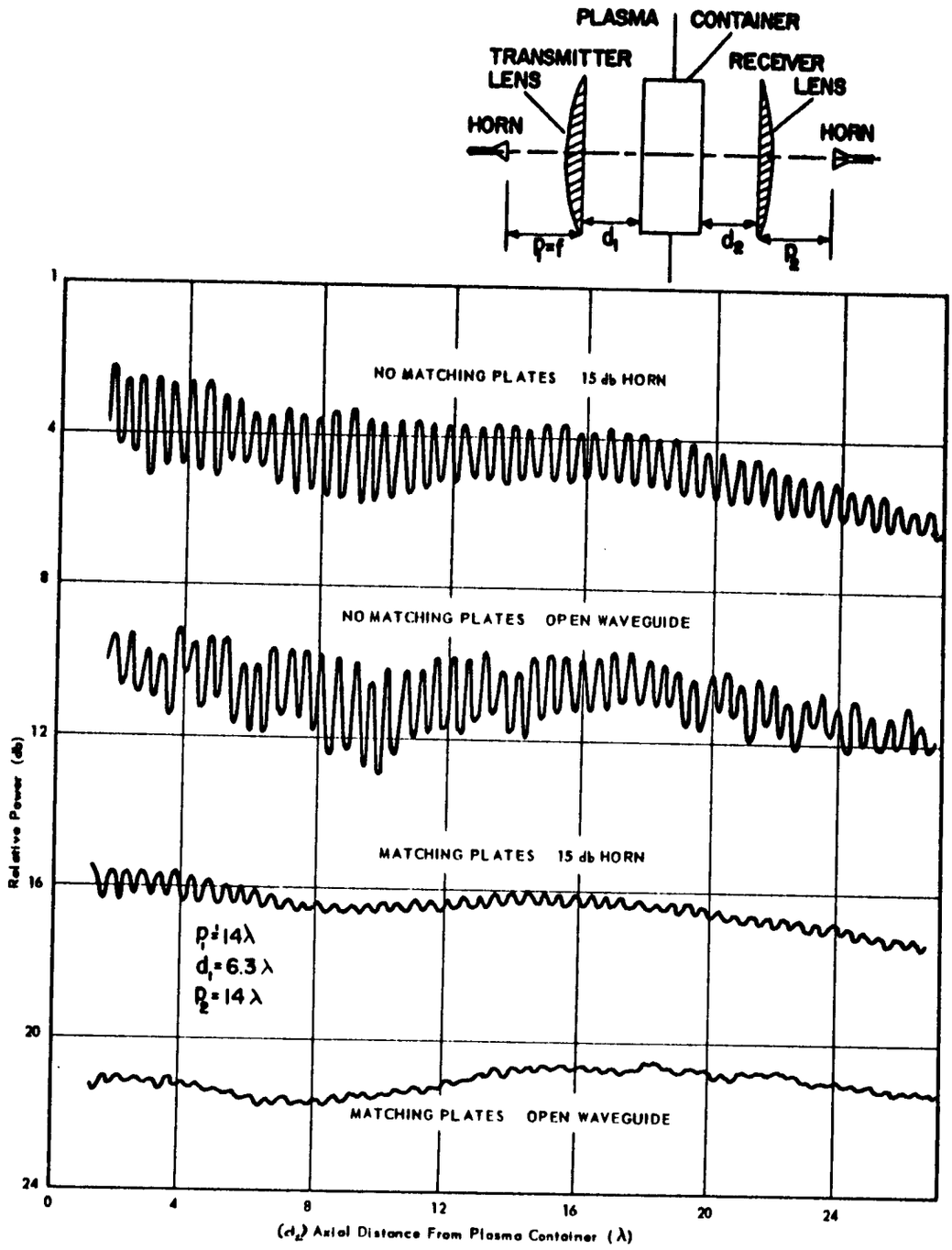

Fig. 27 Field intensity as function of position of the receiving lens system with and without matching plates on the microwave lenses.

the position of the receiving lens system is shown for the lenses with and without the matching plates. The cases where a 15db gain horn and an open waveguide are used for the feeds are illustrated.

Diffraction Effects

When using microwave lenses with the feeds at the focus the microwave energy is essentially directed as a parallel beam. Hence, diffraction effects caused by the metal screen surrounding the plasma container should be less important than when using microwave horns to illuminate the container. In fact, when microwave horns are used to illuminate the lenses then, because of the directivity of the horns, energy diffracted at the edge of the lenses and the container should be considerably reduced. Since in this case, one can consider that the energy is propagating as a parallel beam, it is expected that no change in the field intensity should be observed as the receiving lens system is moved along the optic axis. This point is illustrated in Fig. 28 where the field intensity is plotted as function of the axial position of the receiving system for the three types of feed horns used in these experiments. It is noted that the power remains essentially constant over a distance of 24 wavelengths. The measurements shown in Fig. 28 represent the optimum conditions for studying the characteristics of the plasma generated in the dielectric container. From these curves it can be noted that any drop in power as a plasma is formed in the plasma can be attributed to power absorption in the plasma and/or to defocussing of microwave energy due to inhomogeneities in the plasma itself. It is assumed here that no reflection takes place between the dielectric plates of the plasma container.

Microwave System Consisting of Transmitting Lens and Receiving Horn: A third possible arrangement for a microwave system is that consisting of a lens lauching the wave and a microwave horn acting as the receiver. The alternate arrangement of a transmitting horn and a receiving lens represents an equivalent situation.

Some measurements have been carried out to examine the field intensity as measured by a receiving horn when the plasma container was illuminated by a plane wave launched with a microwave lens. The variation

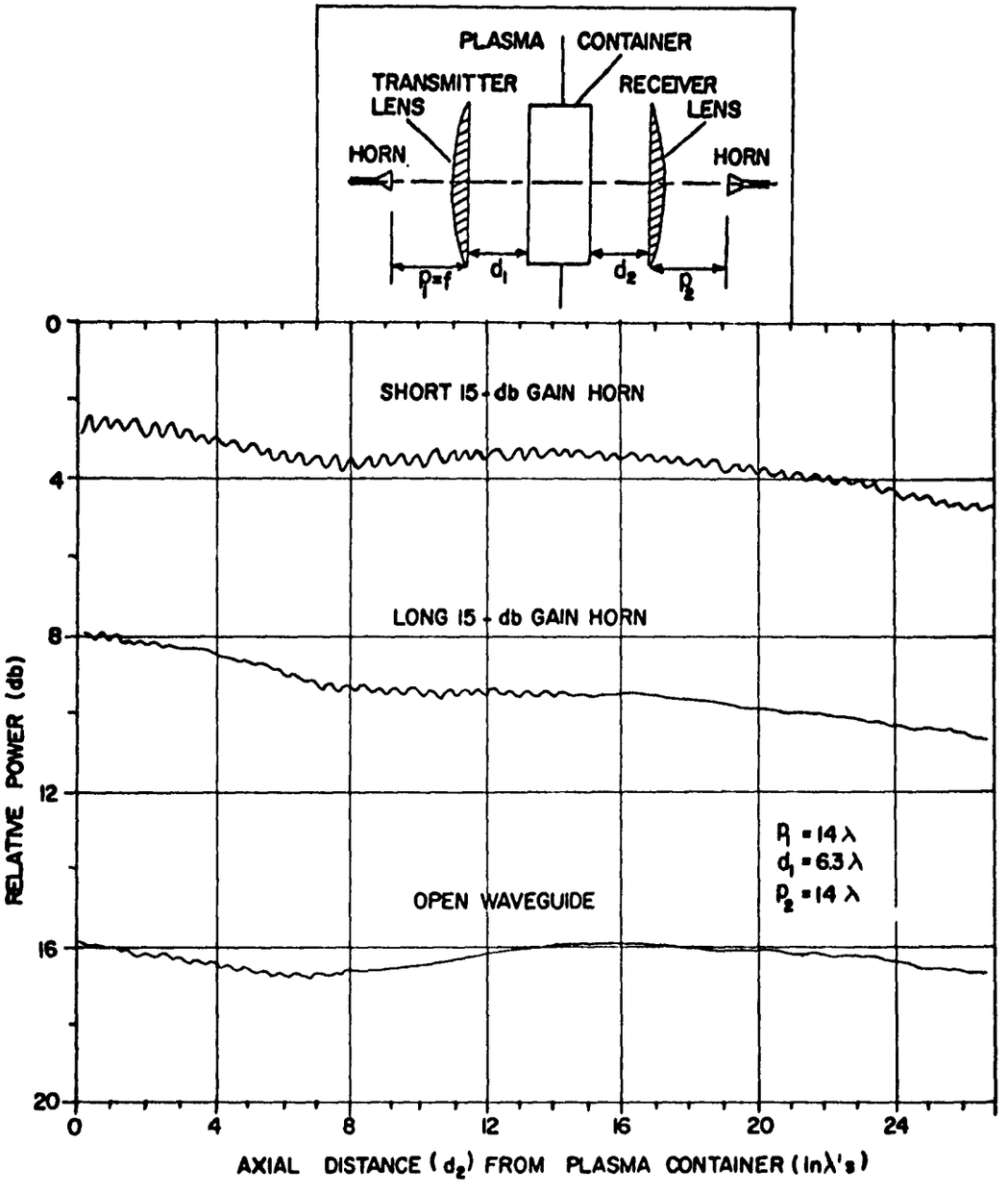

Fig. 28 Field intensity as function of the axial position of the receiving lens system for three different types of microwave feeds at the focus of the receiving lens.

of the power received as function of the position of the receiving horn are shown in Fig. 29 for three types of receivers: a short 15db horn, a long tapered 15db horn and an open waveguide. The regular undulations due to multiple reflections through the system are seen to decrease in amplitude when using an open waveguide or a well matched horn instead of the short 15db horn. The undulations can be reduced by using the technique described above. The variation of the field intensity along the axis can be predicted using diffraction theory.

The power variation observed with a horn as the receiver and microwave lens as the transmitter are very similar to those obtained above when two horns were used as transmitter and receiver. In fact, the situation discussed here is a limiting case of the two horn arrangement when the transmitting horn is far removed from the diffracting aperture ($R = \infty$). In the arrangement discussed here the refractive defocussing when the plasma is present should be small since a plane wave is essentially propagating through the plasma.

(c) Free Space Microwave Measurements of Plasma Properties

The measurements performed were made to supplement the earlier work on the effect of ionized media and hence an effort was made to keep the experimental conditions for the plasma similar. The experimental arrangement and technique has already been discussed in Chapter II.

Free Space Microwave Measurements of Plasma Using Various Microwave Arrangements: In Section IIIb, a detailed investigation was made of the influence of stray scattering, multiple reflections, near field effects and diffraction effects on measurements made (in the absence of a plasma) with various microwave systems. A number of techniques for avoiding or minimizing these effects in order to be able to make more meaningful measurements of plasma properties were outlined. These investigations point to the following arrangements as being most satisfactory for microwave measurements:

1. Horn Transmitter and Receiver Microwave System

A - Transmitting antenna distance to plasma container (d_1) $\approx 0\lambda$
Receiving antenna distance to plasma container (d_2) $\approx 5\lambda$

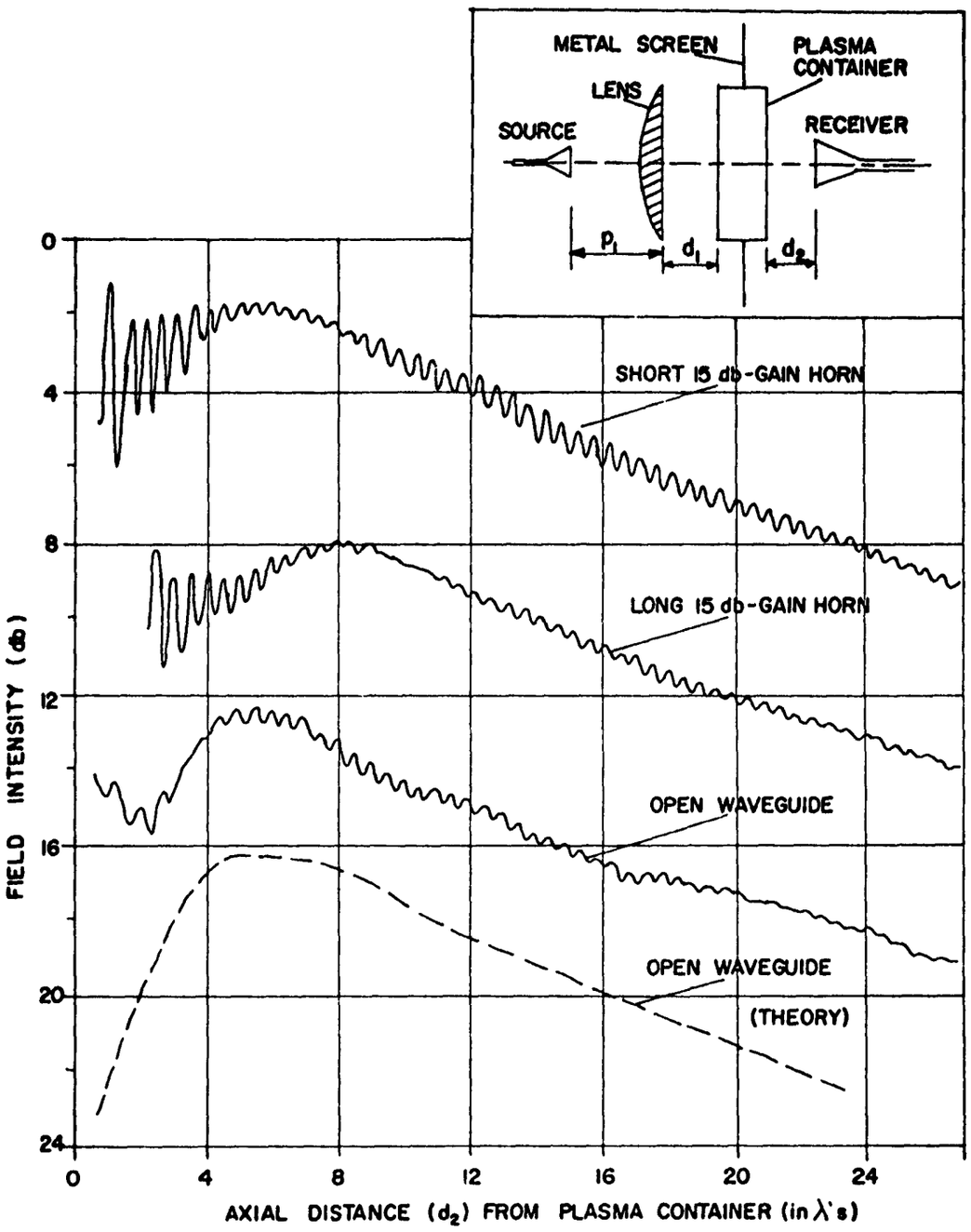

Fig. 29 Field intensity as function of the axial position of the receiver for different types of receiving antennas.

OR

B - Transmitting antenna distance to plasma container (d_1) = 5λ
Receiving antenna distance to plasma container (d_2) = 17λ

In each case a metal diffracting screen surrounding the plasma container, plasma container faces with optical thickness as near to $n\lambda/2$ as possible and suitable shielding from stray reflections is necessary.

2. Microwave Lenses on Transmitting and Receiving Antennas

Lens distance (on transmitter side) from plasma container (d_1) = 6.3λ
Lens distance (on receiver side) from plasma container (d_2) = 6.3λ
Distance transmitter (receiver) to microwave lens = 14.7λ

Matching plates on the flat surfaces of the lenses, diffracting screen, plasma container faces $n\lambda/2$ optically thick and shield (as above) required as well.

3. Microwave Lens on Transmitting Side and Horn Receiver

Lens distance (on transmitter side) from plasma container (d_1) = 6.3λ
Transmitter distance from microwave lens (P_1) = 14.7λ

Same precautions as previous case.

These "optimum" arrangements were then used to study the transmission and reflection of e-m waves by a slab of plasma. A comparison of the results obtained with each system in the presence of the plasma was made in order to ascertain the best arrangement for determining the properties of the plasma. The results obtained are discussed in the sequel.

Transmission measurements performed when the transmitting horn is against the plasma container and the receiving horn 5λ from the container are shown in Fig. 30. Large "cusps" appear in the traces indicating significant multiple reflections in the presence of the plasma. There is a significant difference between the measurements performed when the incident electric vector is parallel to the electrodes compared to the

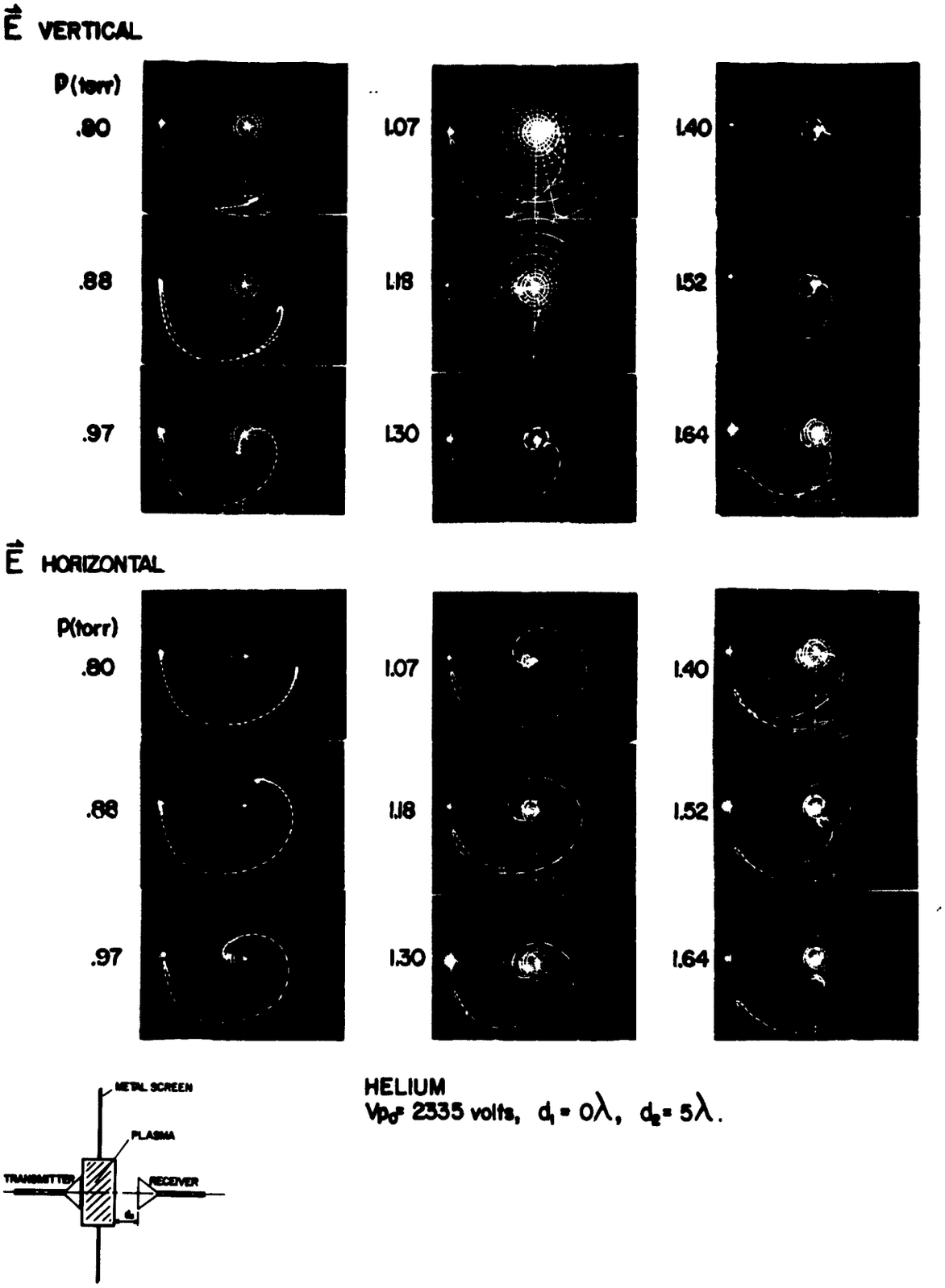

Fig. 30 Series of microwave transmission measurements made on a slab of plasma generated in Helium using a microwave system consisting of transmitting and receiving horn antennas located near the plasma container.

case when the incident electric vector is normal to the electrodes. More will be said of these measurements (hereafter called arrangement A) when they are compared to the results obtained with the other arrangements.

Transmission measurements made with the transmitting horn 5λ from the plasma container and the receiving horn 17λ from the plasma container (arrangement B) are shown in Fig. 31a. Less phase shift and greater attenuation than for the measurements of arrangement A are apparent. This would be expected in the basis of refractive defocussing by a slab of plasma when a spherical wave is incident on the plasma. Again a large dependance exists on the orientation of the incident electric field relative to the electrodes. This is attributed to reflections taking place from the electrodes, the phase of which are different (by 180°) for the two polarizations of the incident field.

When lenses are used both on the transmitting and receiving portions of the system, then as shown in Fig. 31b, there is no dependence on the incident field orientation or polarization; both series of measurements giving essentially the same result. In addition, the appearance of "cusps" is markedly reduced and these appear only when the plasma is quite dense (corresponding to multiple reflections originating from the plasma). The flat walls of the plasma container are approximately one wavelength in optical thickness and, therefore, are matched to free-space. However, when a plasma is present, multiple reflections can occur from the plasma boundaries. These reflections depend on the plasma conditions and increase in amplitude as the plasma density approaches the cut-off condition.

We thus see that different results are obtained for the same plasma, the measurements being strongly influence by the experimental measurement system. For a horn (or point) source, refractive defocussing effects appear which cause a reduction in the measured amplitude of the fields. Strong reflections from the sources result in "cusps" in the measured traces (particularly when the source and receiver are near the plasma) which significantly alter the measurements. Finally, reflections from the electrodes have a major effect on an incident spherical

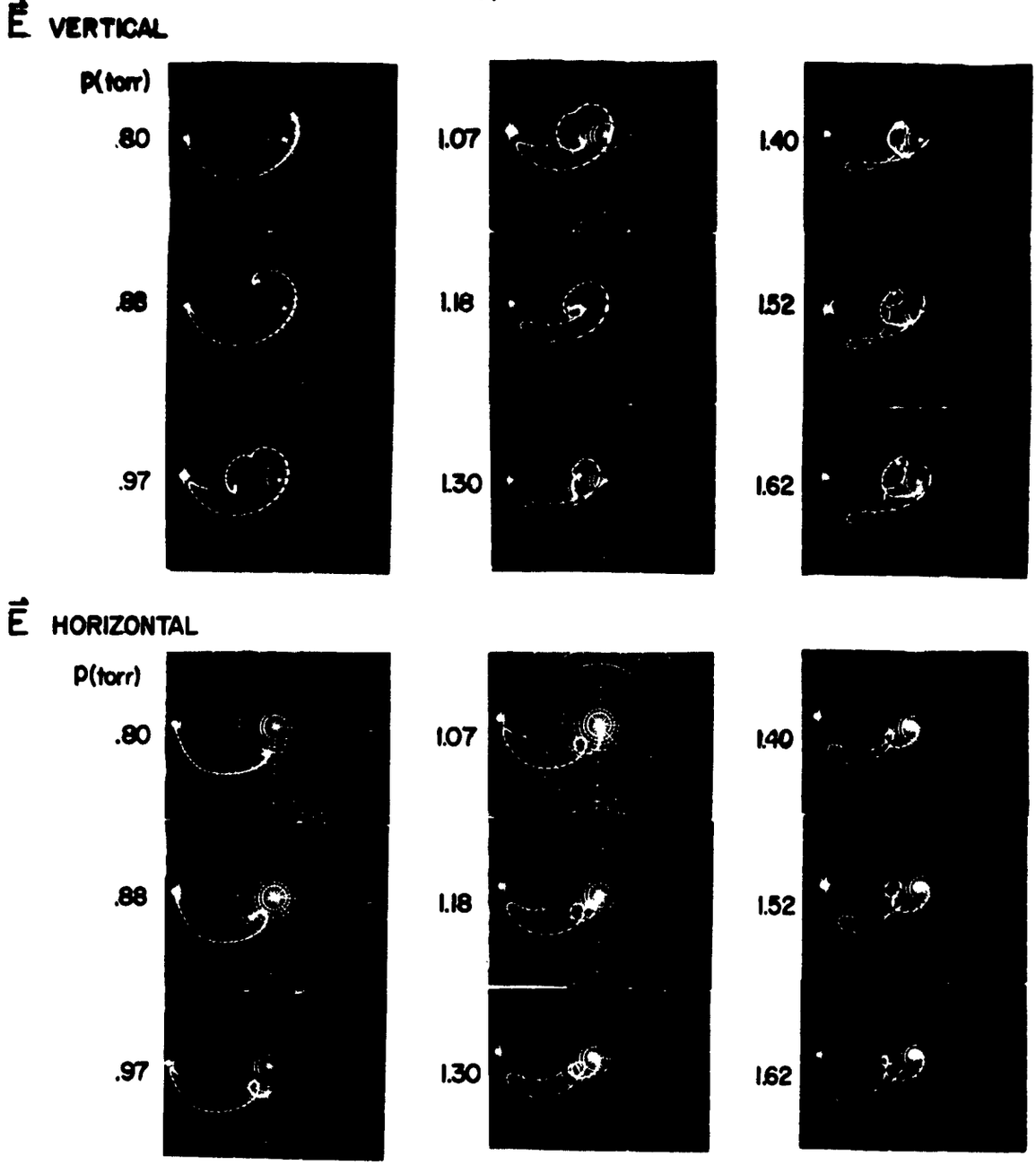

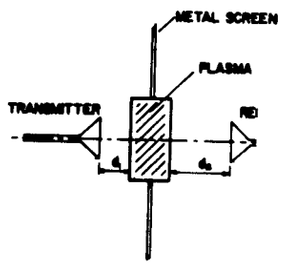

HELIUM
V_{P_0} = 2335 volts, $d_1 = 5\lambda$, $d_2 = 17\lambda$.

Fig. 31a Series of microwave transmission measurements made on a slab of plasma generated in Helium using a microwave system consisting of transmitting and receiving horn antennas located some distance from the plasma container.

$\vec{E}$ VERTICAL

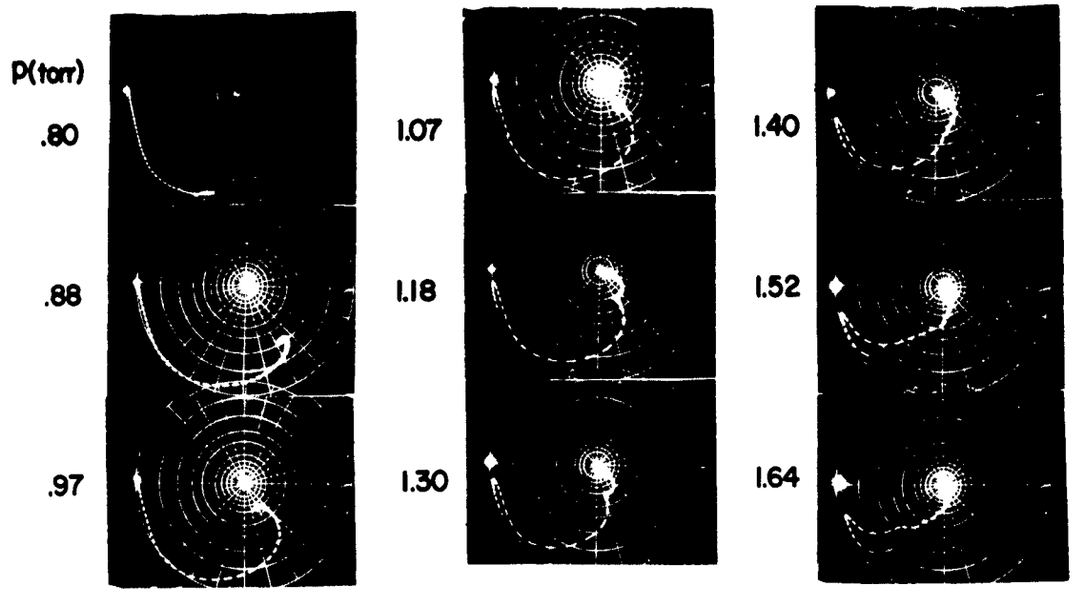

$\vec{E}$ HORIZONTAL

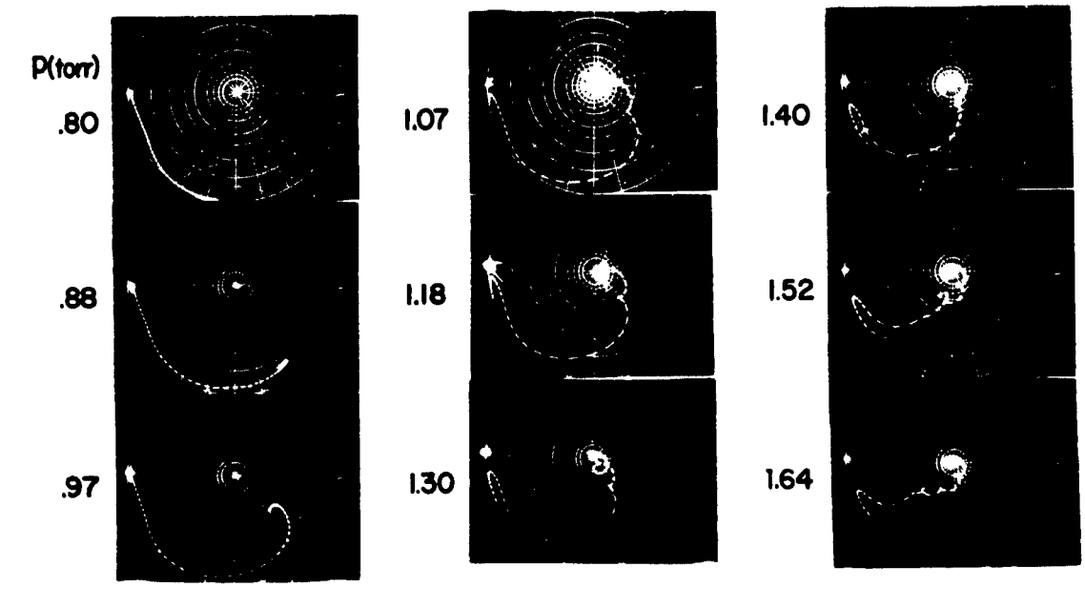

HELIUM
$Vp_o = 2335$ volts, $R_1 = 14.7\lambda$, $R_2 = 14.7\lambda$, $d_1 = 6.3\lambda$, $d_2 = 6.3\lambda$.

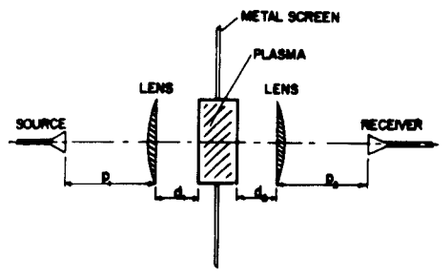

Fig. 31b Series of microwave transmission measurements made on a slab of plasma generated in Helium using a microwave system consisting of transmitting and receiving microwave lenses.

wave resulting in a strong dependence of the measurements on the orientation of the incident fields relative to the electrodes.

These effects can be eliminated or minimized by using an incident plane wave through the use of auxiliary lenses on both transmitting and receiving portions of the measurement system. The refractive defocussing (due to a uniform slab of plasma) is eliminated as are the polarization effects of the orientation of the incident fields relative to the electrodes. The effect of multiple reflections though not completely eliminated is greatly reduced and are present only as the plasma becomes relatively dense.

In Fig. 32 are compared measurements made when a parallel beam of energy (through the use of lenses) is incident on the plasma and the receiver is a simple short horn. In this arrangement a lens is used on the transmitting portion of the microwave arrangement but not on the receiving end. As seen from Fig. 32 when the receiver is near the plasma container then significant multiple reflections can occur between the receiving antenna aperture and the plasma resulting in violent "cusps" in the measurements and in erroneous values for the amplitude and phase of the wave transmitted through the plasma. As the distance between the plasma container and the receiving antenna is increased, the measurements approach more and more those obtained with a lens receiver. It is not until the receiver is more than 12λ from the plasma container that the measurements approach the lens values and even yet they show more pronounced "cusps" due to the multiple reflections. Thus if the receiving antenna is not very well matched to free space or if its "match" is uncertain it is necessary to use a lens as well on the receiving portion of the microwave arrangement if reliable measurements of the plasma are to be performed.

Thus of the three systems, only the two lens arrangment appears to be acceptable for measuring plasma properties by free-space propagation of e-m waves through the plasma.

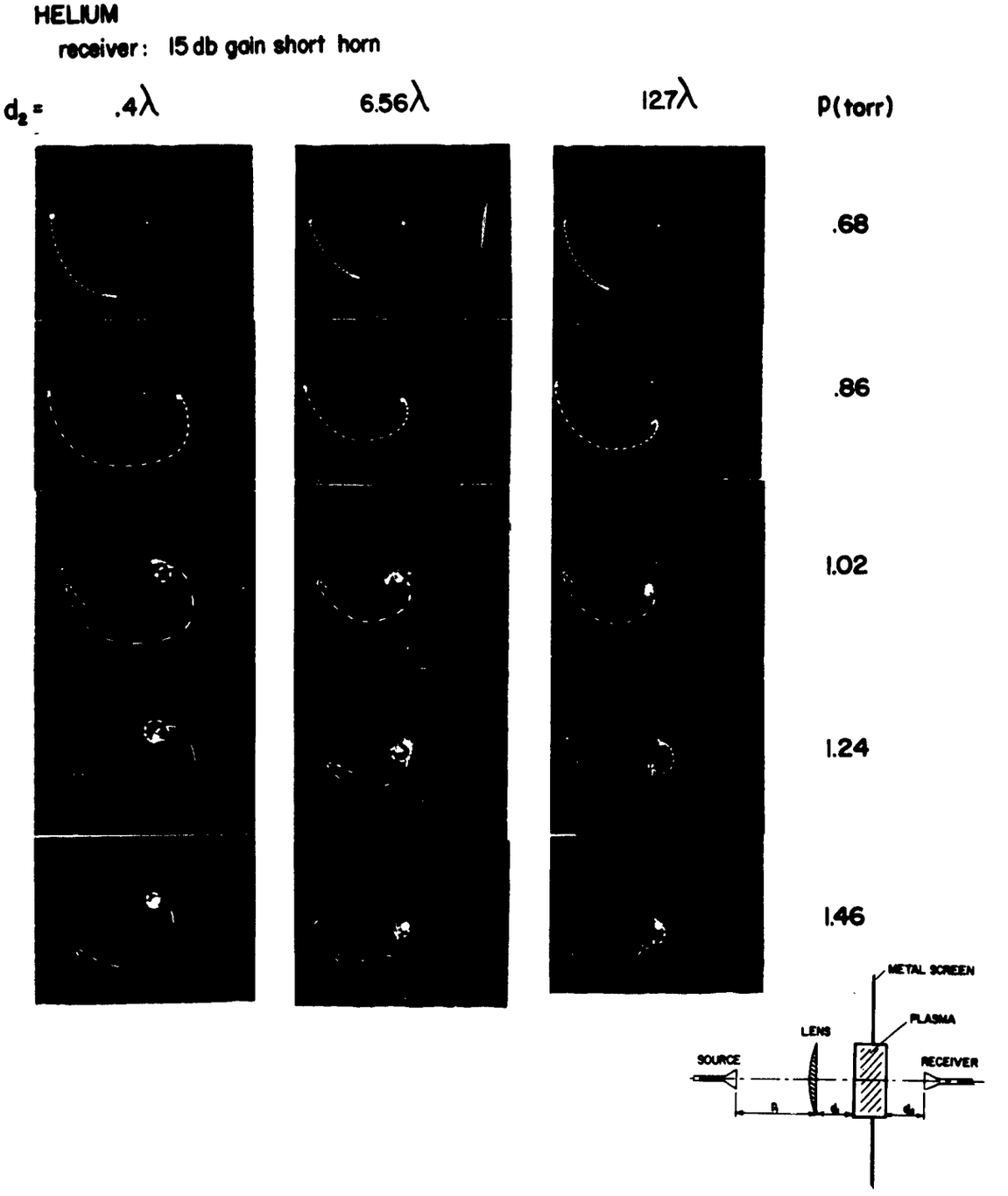

Fig. 32 Microwave transmission measurements made on a Helium plasma using a microwave system consisting of a microwave lens on the transmitting portion and a 15db gain horn as a receiver.

Free Space Microwave Determination of Plasma Properties in Helim and Argon

(i) Helium: The results of the previous section indicate that the best microwave arrangement for measuring the properties of plasmas by free-space transmission or reflection techniques is one in which a microwave lens is used to obtain a plane wave incident upon the plasma. In transmission measurements a second microwave lens is desirable on the receiving portion of the microwave arrangement to receive the e-m waves after they pass through the plasma and to collimate them into the aperture of a receiving horn located at the focus of the lens.

When matching plates are used on the flat-face of the microwave lens then the effect of multiple reflections which arise from reflection off the lens surface is greatly reduced. One still must, however, ascertain the "match" of the microwave system to the plasma container in order to make a proper interpretation of the measurements in the presence of the plasma.

The system mismatch does NOT affect the phase change introduced by the plasma (and hence has little effect on the determination of total electron density) but it does affect the attenuation and hence any estimate of collision frequency.

The measurements shown in Fig. 33 have been analysed in detail in order to ascertain the properties of the plasma generated in Helium by the use of free-space microwave techniques. The "reduced" experimental points for various pressures have been plotted in attenuation constant vs. phase constant (α vs. β) co-ordinates as shown in Fig. 34. Contours of constant voltage as determined by the timing markers are also shown. (Note that in order to clarify the presentation the attenuation scale has been displaced by 2db for each pressure so that to arrive at the true attenuation the appropriate value at $\beta = 0$ must be subtracted from each plot.)

When the experimental measurements formed "cusps", these were smoothed out since the cusps are a result of unwanted internal reflections from the plasma.

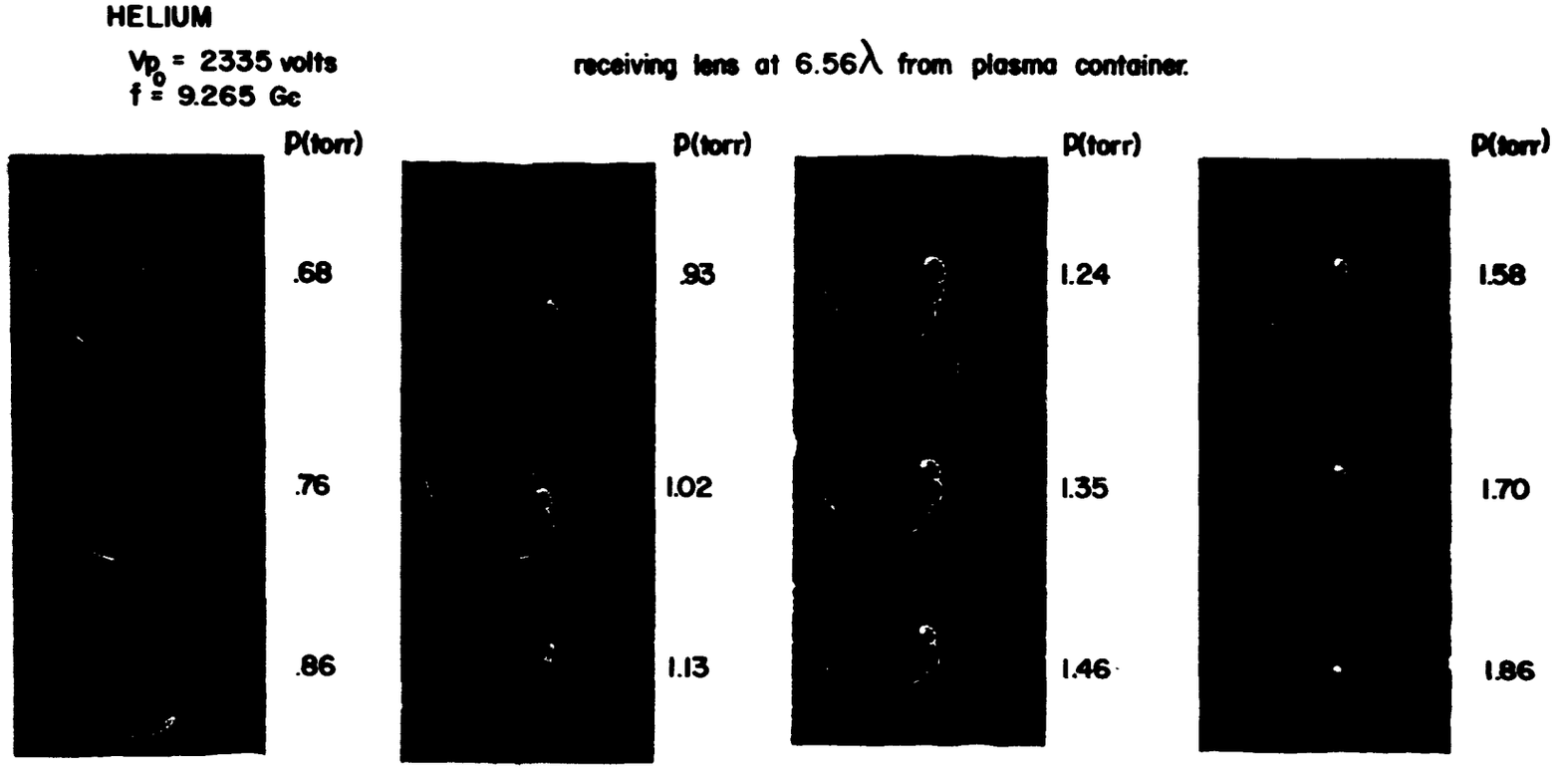

Fig. 33 Microwave transmission measurements made on a Helium plasma when the receiving lens is 6.56λ from the plasma container.

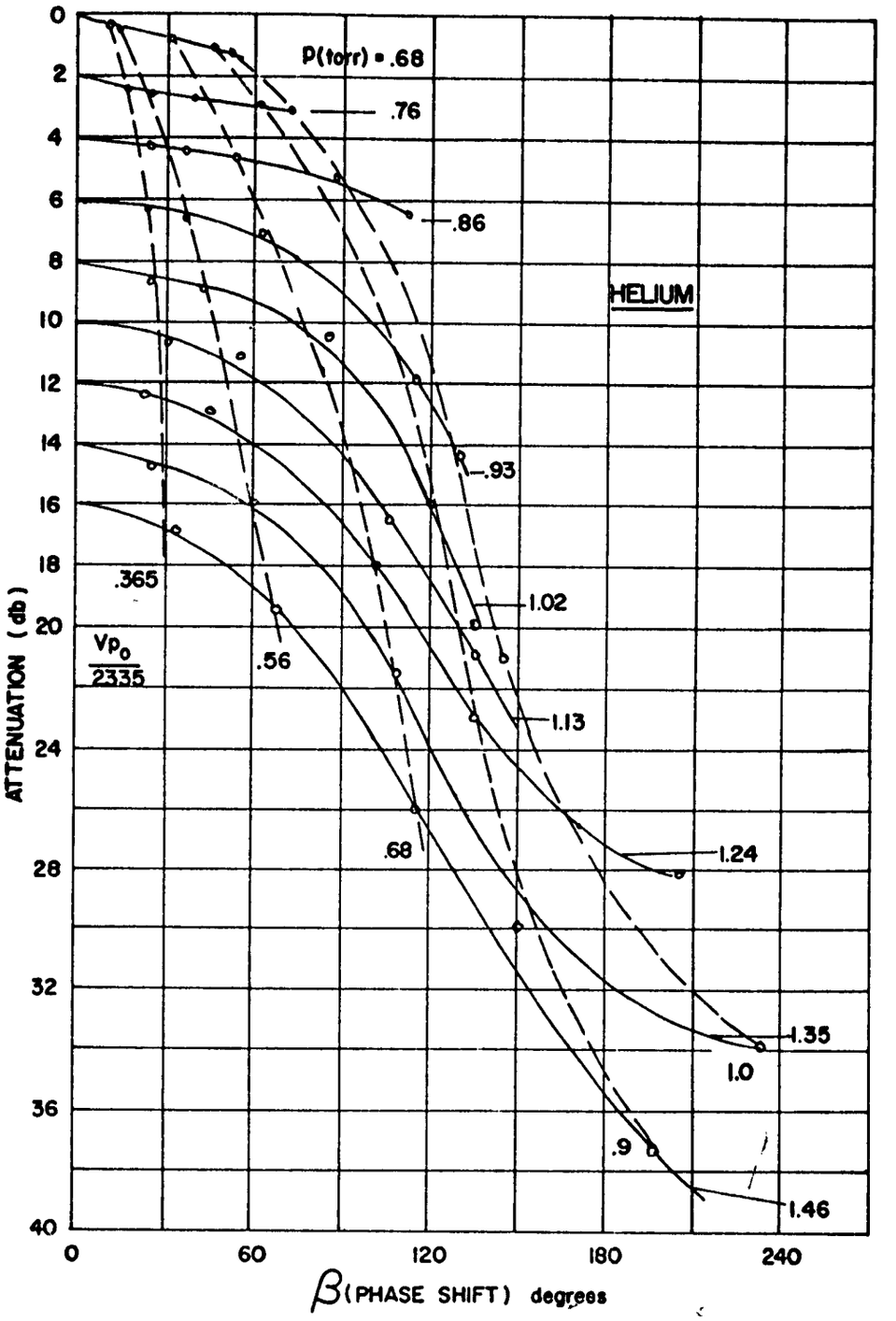

Fig. 34 Attenuation and phase shift measured by transmission of a plane e-m wave through a 60c/s Helium plasma as function of pressure and applied voltage.

From the $\alpha - \beta$ presentation, the values of normalised electron density and collision frequency could be obtained. The justification for using this "bounded" plasma model and neglecting the effect of the dielectric boundaries is that the dielectric plots comprising the plasma container are nearly an integral number of half-wavelength in optical thickness and hence the reflections from the container boundary are negligible.

A plot of the build-up of electron density during the voltage cycle is shown in Fig. 35. As the pressure is increased a greater and greater electron concentration is generated in the plasma. As noted earlier the phase shift is fairly insensitive to multiple reflections and other measurement system effects. Hence the phase shift is a good indication of the total electron density through which the incident microwave beam passed. The theoretical model used for interpretation of the measurements of phase shift and attenuation is based on a uniform slab of plasma of the same thickness as the experimental plasma. Thus the phase shift measured at a single frequency cannot give any information on the non-uniformity of the plasma in the direction of propagation but only the average electron density for a uniform slab. The phase shift results are very reproducible and there is no reason to doubt their validity or their interpretation in terms of electron density.

The variation of collision frequency with the voltage cycle at various pressures is shown in Fig. 36. The theoretical value for collision frequency is given by

$$\nu = \frac{4}{3}\sqrt{\frac{8\kappa T_e}{\pi m}}\; n_m Q_m \text{ sec}^{-1} \qquad (46)$$

where:

κ is the Boltzmann's constant

T_e is the electron temperature

m is the electronic mass

Q_m is the collision cross-section

$n_m = \frac{6.02 \times 10^{23}}{22,400} \cdot \frac{P_{mm}}{760}\left(\frac{273}{T_g}\right) = 9.66 \times 10^{18} \frac{P_{torr}}{T_g}$ is the concentration of the neutral species

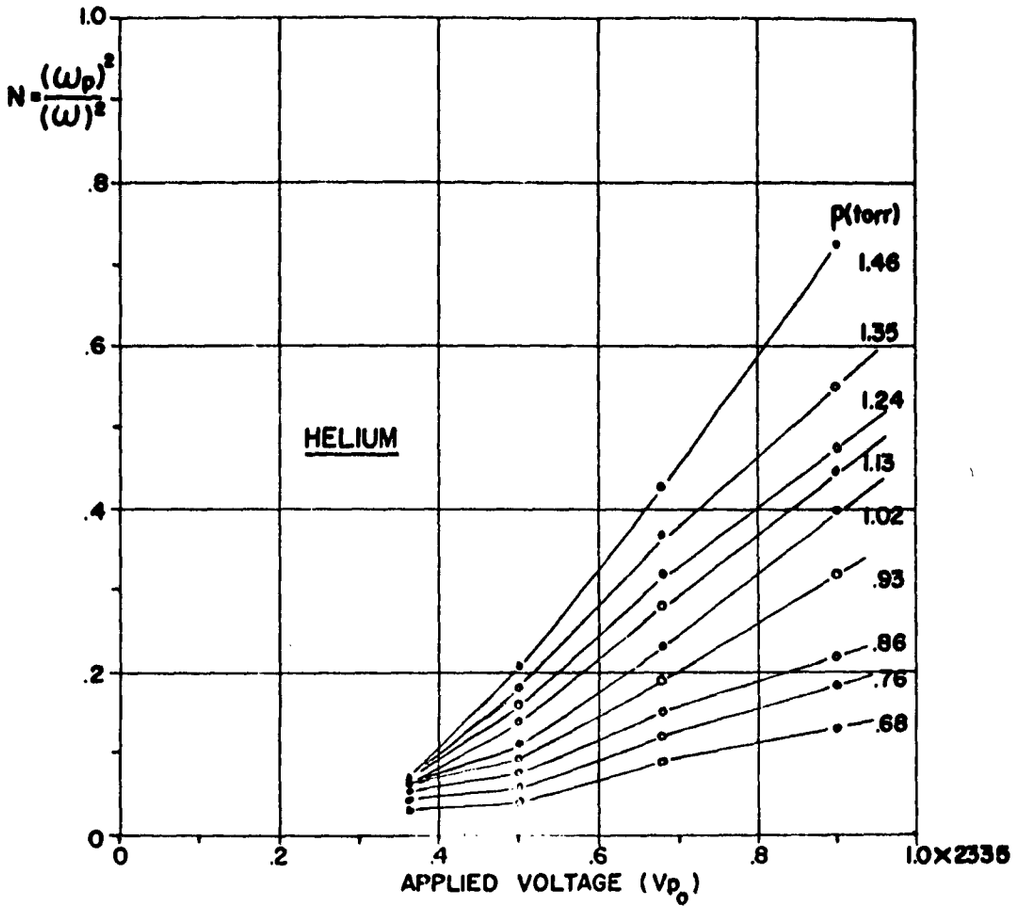

Fig. 35 Electron density in a Helium plasma as function of applied voltage and pressure (V_{po} in the voltage between the electrodes without plasma).

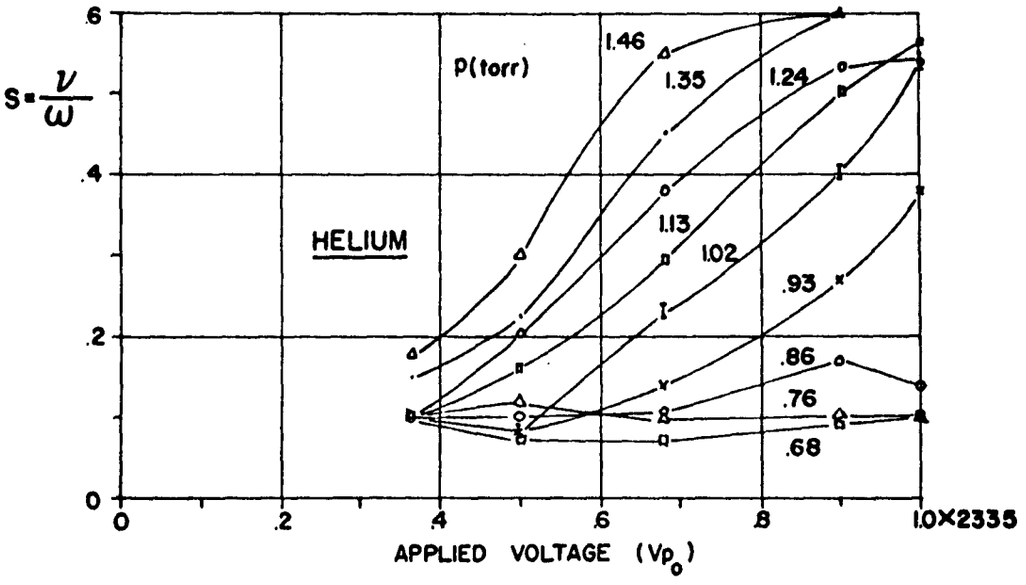

Fig. 36 Apparent collision frequency in a Helium plasma as function of applied voltage and pressure.

and T_g is the gas temperature.

Putting all the constants into Eqn. 46 yields

$$\nu = 8.10 \times 10^{24} \sqrt{T_e} \frac{P_{torr}}{T_g} Q_m \text{ sec}^{-1} \qquad (47)$$

Choosing "reasonable" estimates for the remaining quantities:

$$Q_m = 5.25 \times 10^{-16} \text{cm}^2; \qquad T_g = 300^\circ\text{K}; \qquad T_e = 60{,}000^\circ\text{K}$$

yields:

$$\nu = 3.47 \times 10^9 \, P_{torr}$$

Hence:

$$\frac{\nu}{\omega} = \frac{3.47 \times 10^9}{2\pi \times 9.265 \times 10^7} P_{torr} = 0.06 \, P_{torr}$$

Thus for values of the pressure between 0.8 and 1.0 torr the ratio of collision frequency to r-f radian frequency is of the order of .05. If we look at the experimental values in the pressure range 0.7 - 0.9 torr the ratio ν/ω is of the order of 0.07 to 0.10 a reasonable agreement with theory.

However, at higher values of pressure the collision frequency is considerably greater and can be up to an order of magnitude greater than that predicted by theory. The high values of collision frequency measured may thus be ascribed to three variables describing the kinetics of the plasma.

Electron Temperature - When the discharge in helium is actively driven as was the case in the experiments described, it is expected that the electron temperature will increase during the applied voltage cycle. For these large voltages, relatively short distance

between the electrode and the low gas pressures (long mean free path) the electrons in the plasma probably do not reach thermal equilibrium and in fact many of the collisions may be inelastic collisions. To explain the enhanced collision frequency solely on the basis of an increase in electron temperature would reuqire an increase of 5^2 or 25 in the electron temperature from the start to the end of the applied voltage cycle. This would correspond to final electron temperatures of the order of 300,000°K which is highly unlikely. There is no doubt that there should be an effect due to an increase of electron temperature but it is not likely to be as great as this. It is thus necessary to do independent electrical probe measurements of electron temperature in order to clarify this point.

Gas Temperature - In the computation, the gas was taken to be at room temperature - 300°K. Although the gas may heat up slightly, it is unlikely to change by a large amount. Furthermore the dependence on gas temperature is such that the collision frequency would be expected to decrease with increasing gas temperature.

Collision Cross-Section - The collision cross-section for helium has been established by experimental measurement at both d-c (zero frequency) and at very high frequencies (microwave range). For these conditions it is found to depend only very slightly on electron energy (for low electron energies < 2 ev) and a value of about 5.25×10^{-16} seems to be the presently accepted value. However, the collision cross-section for helium has not been measured for a slowly driven (such as 60c/s) discharge. Thus the value of the collision cross-section and its dependence upon electron temperature for such a plasma as generated in the experiments has not as yet been definitely established. It is possible that these values may be different for a discharge in the present mode of excitation. An increase of collision cross-section with electron temperature combined with the effect of the high electron temperature could explain the type of behaviour for the collision frequency that is measured. Also, only electron-neutral collisions have been considered. Electron-ion collisions may be important as well and should be considered.

Other Effects - A non-uniformity of the plasma in some manner not treated in Section III(a) which gives rise to refractive defocussing could result in a large measure of attenuation and hence in an increased value for the collision frequency. Similarly sheath potentials may possibly build up on the plasma container and influence the nature of the discharge. At present there is no definite indication of such effects. In addition contamination from the polystyrene container plates is possible, although optical spectrophotometer measurements were done and shoed only the characteristic spectrum of helium.

(ii) Argon: Due to the large values of attenuation and hence collision frequency measured in a helium discharge, an independent set of measurements were also performed for an argon plasma.

The experimental measurements of phase and attenuation for a variety of pressures are shown in Fig. 37. From these experimental values the attenuation-phase diagram showing lines of constant pressure and constant applied voltage shown in Fig. 38 was constructed. (As before the value of attenuation for each pressure is displaced by 2db in order to clarify the display).

The variation of electron density with applied voltage at different pressures based on a bounded, uniform slab of plasma is shown in Fig. 39. Again a regular variation of the electron concentration as determined from the phase measurements is evident.

The dependence of ν/ω on discharge voltage is shown in Fig. 40. The behaviour is markedly different from that obtained with helium showing no major change with the applied voltage. This may be due to a Ramsauer type effect. At low pressures (< 0.3torr) more or less reasonable values for the collision frequency are obtained - i.e. the measured collision frequencies are only slightly higher than that calculated theoretically. At higher pressures, large attenuation and hence large collision frequencies are measured. At these high pressures, the discharge in argon is visibly non-uniform taking the form of two intersecting cones whose common apex is in the centre of the discharge

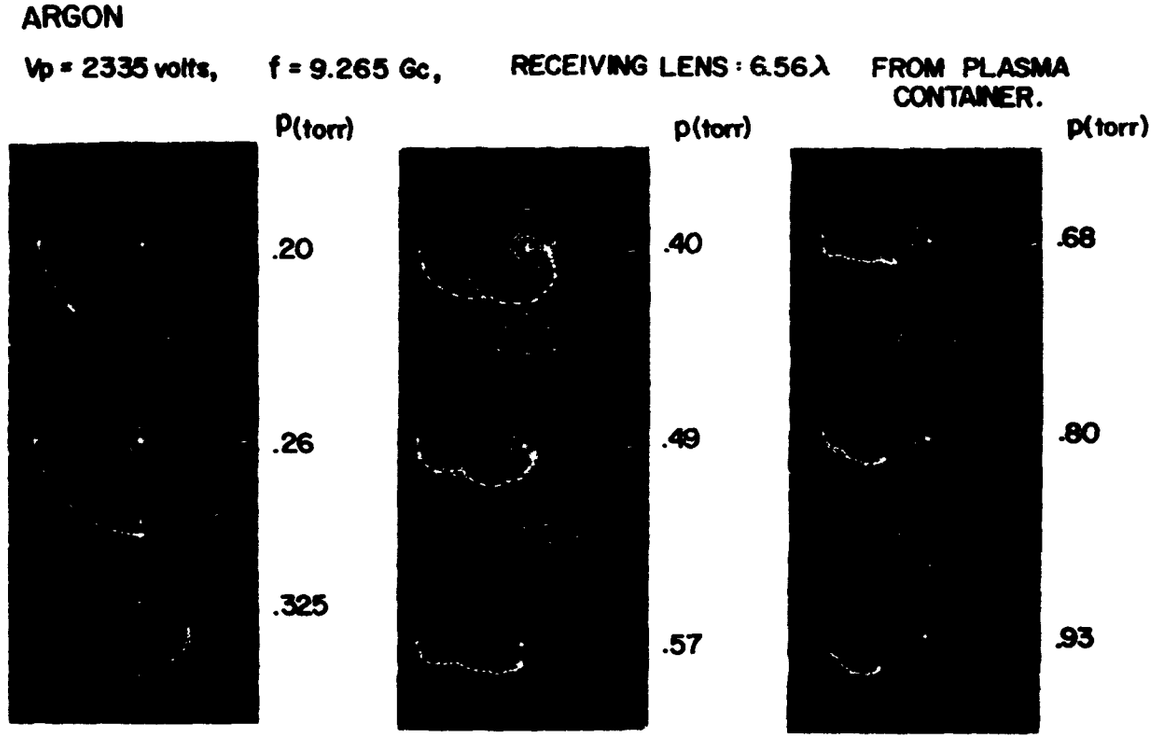

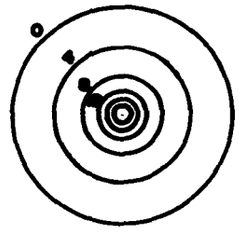

Fig. 37 Microwave transmission measurements made on an Argon plasma using a microwave system consisting of transmitting and receiving microwave lenses.

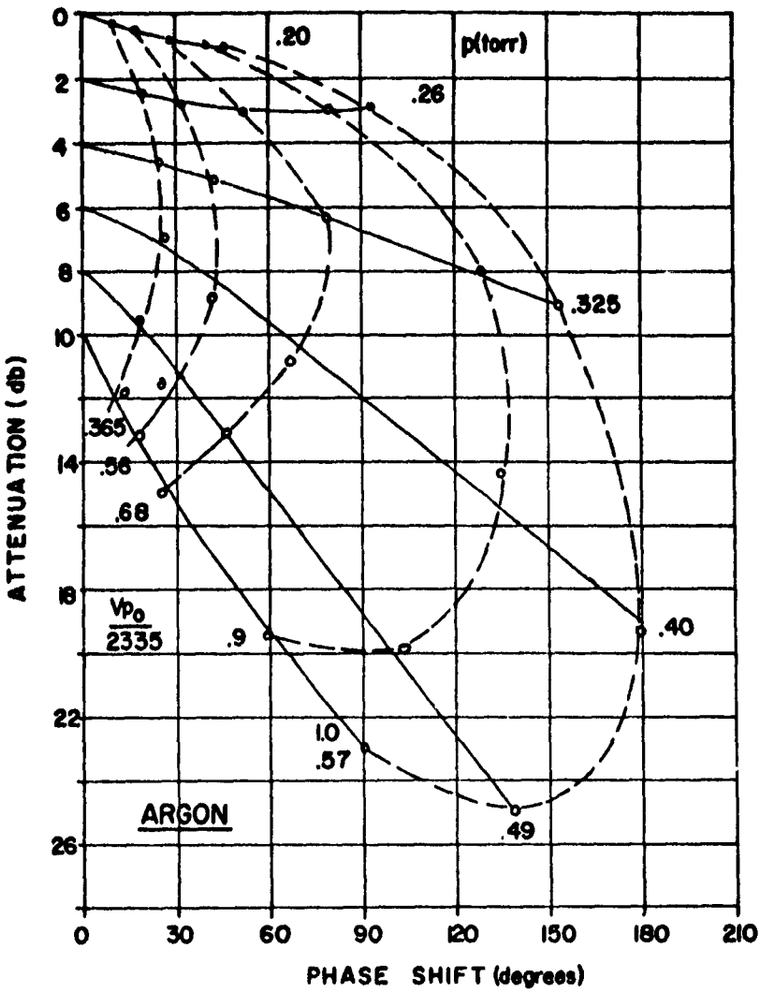

Fig. 38 Attenuation and phase shift measured by transmission of a plane e-m wave through a 60c/s Argon plasma as function of pressure and applied voltage.

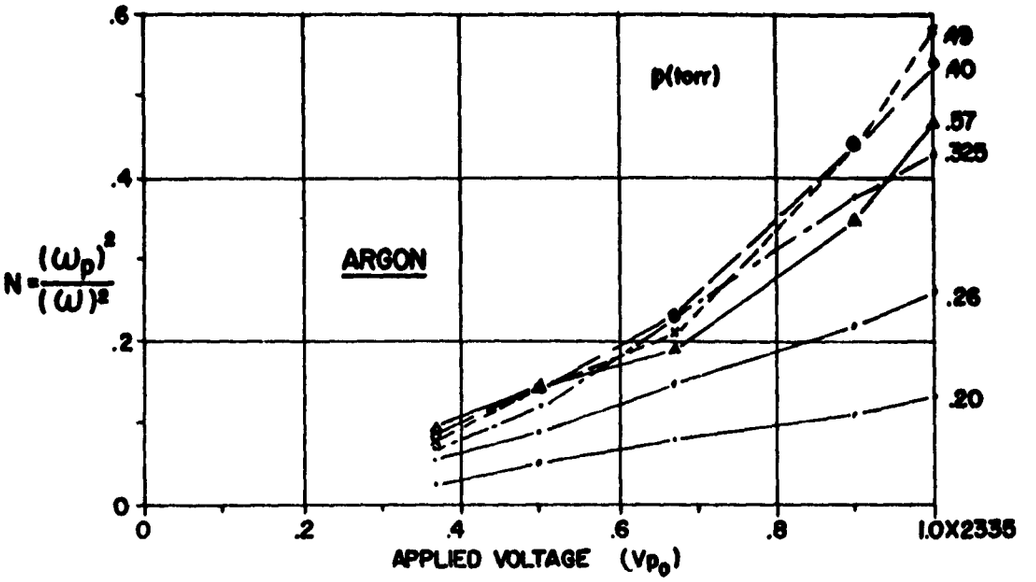

Fig. 39 Electron density in an Argon plasma as function of applied voltage and pressure (V_{po} is voltage between the electrodes without plasma).

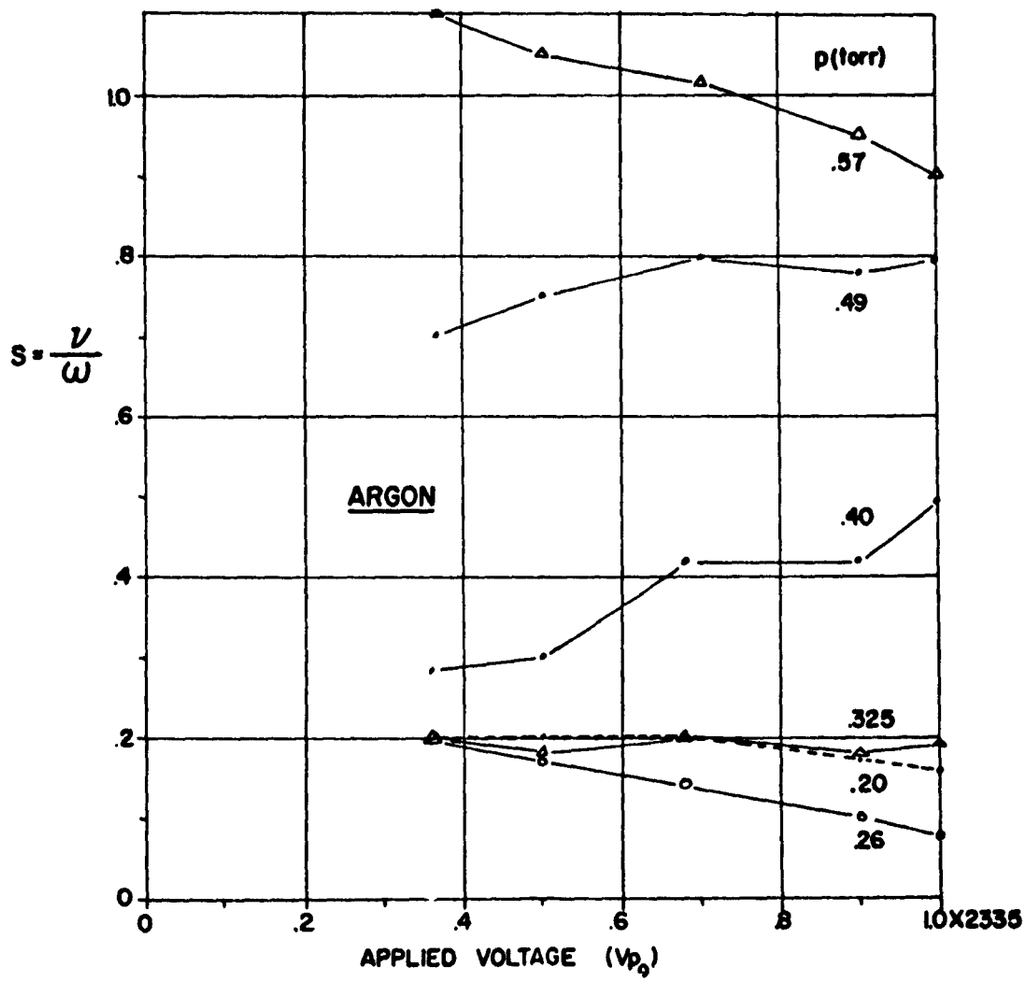

Fig. 40 Apparent collision frequency in an Argon plasma as function of applied voltage and pressure.

and whose bases are the respective electrodes. This increased attenuation at high pressures can thus be attributed to the non-uniformity of the discharge.

IV PRELIMINARY CONSIDERATIONS AND FACILITY FOR INVESTIGATION OF ANTENNA PROPERTIES IN THE PRESENCE OF ANISOTROPIC IONIZED MEDIA

(a) Preliminary Considerations

In the presence of a magnetic field, a plasma becomes anisotropic and simultaneously can support two wave modes. The 'transparency' of the plasma depends on the strength of the magnetic field and its direction relative to the direction of propagation as well as on the electron number density and collision frequency. For a magnetic field oriented in the direction of propagation of an incident electromagnetic wave, the dielectric coefficient of the plasma is given by:

$$K_{\pm} = 1 - \frac{\omega_p^2}{\omega} \frac{1}{\omega_{\pm}\omega_b} \tag{48}$$

where:

ω_p is the plasma frequency

ω is the radio frequency

ω_b is the electron cyclotron frequency

The K_+ value of the dielectric coefficient is associated with a wave mode with a circularly polarized electric field vector which rotates in the same direction as positive particles gyrate in the presence of the static magnetic field. This is the "ordinary wave" in ionospheric terminology. The phase velocity of this wave ($\beta_+/k = K_+^{\frac{1}{2}}$) is finite only for:

$$\omega \geq \sqrt{(\omega_b/2)^2 + \omega_p^2} - \omega_b/2$$

so that this wave propagates in the plasma only for frequencies in excess

of those given by the above expression.

The K- value of the dielectric coefficient corresponds to a circularly polarized wave mode whose electric vector rotates in the same direction as electrons move under the influence of the static magnetic field. This is the "extra-ordinary" wave which will not propagate in the frequency region:

$$\omega_b \text{ to } \sqrt{\left(\frac{\omega_b}{2} + (\omega_b/2)^2 + \omega_p^2\right)}.$$

The general behaviour of the "stop" and "pass" frequency regions of these wave modes is shown in Fig. 41.

It is seen that, depending on the strength of the imposed static magnetic field, frequencies well below the plasma frequency can penetrate through the plasma for one of the wave modes, a highly desirable situation in regard to re-entry communications. In the ideal case (no collisions or boundary effects) transmission along a static magnetic field is the most feasible since in this direction it is much easier to attain the required conditions for which at least half the power is transmitted using linearly polarized waves and full transmission using the approriate circular polarization. It is also realized, in this case, that the higher the intensity of the magnetic field the narrower are the stop-band regions.

Investigations of the radiation characteristics of a microwave antenna in the presence of an anisotropic sheath of plasma are not only of value in ascertaining the nature of the "pass-region" or "r-f windows" for radio frequencies below the plasma frequency but also since the properties of anisotropic plasma are functions of direction (angle) the shaping and scanning of antenna beam by using magnetic fields is another possibility.

The parameters of interest in such an investigation are the plasma frequency (ω_p) and the cyclotron frequency (ω_b) where:

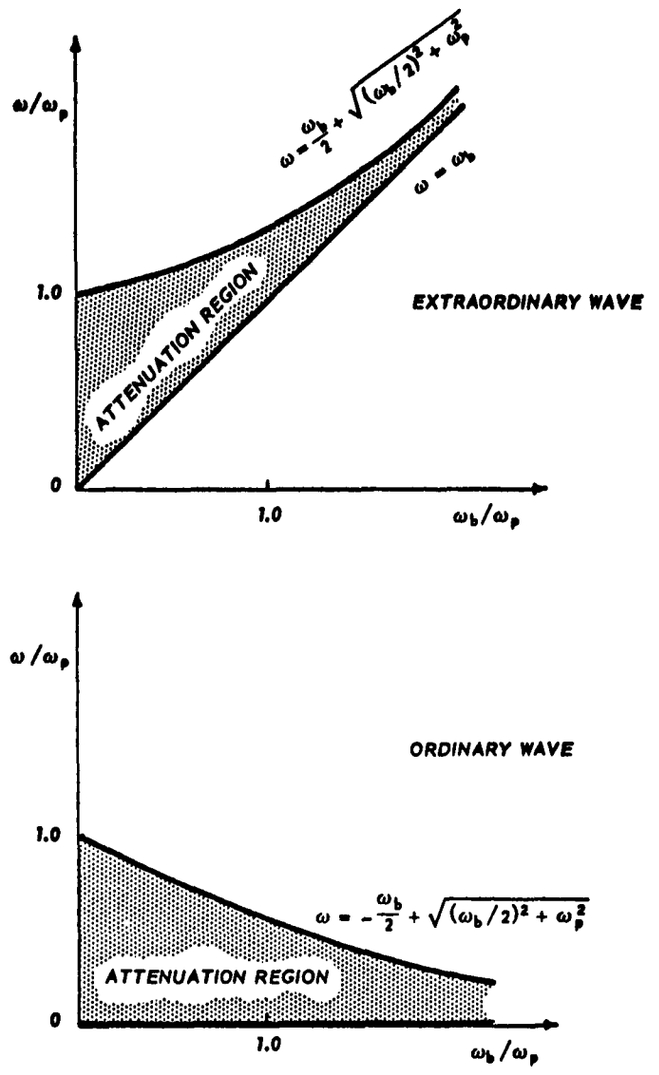

Figure 41 Variation of attenuation regions of a plasma for propagation of electromagnetic waves along the direction of the magnetic field.

$$\omega_p = (ne^2/m\,\varepsilon_o)^{\frac{1}{2}} = 5.64\times 10^4\ n^{\frac{1}{2}}$$

$$\omega_b = \frac{e}{m} B_o = 1.795\times 10^7\ B_o$$

n is the electron concentration in number/cm^3

B_o is the static magnetic field in Gauss

e,m are the electronic charge and mass respectively

ε_o is the permittivity of free space.

The critical regions of interest for the "extra-ordinary" wave mode are those for which:

$$\omega \sim \omega_b$$

$$\omega \sim \omega_b/2 + \sqrt{(\omega_b/2)^2 + \omega_p^2}$$

If the experimental frequency is chosen to be in the x-band range then:

$$\omega \sim 5.8\times 10^{10}\text{cps}$$

This will require a magnetic field of the order of 3.2kg so that $\omega \sim \omega_b$ and an electron density of $\sim 10^{12}$electrons/cc in order that $\omega \sim \omega_p$. These are the range of parameters desired for a laboratory experiment and will fulfill the conditions listed above.

(b) Experimental Facilities

For such experimental investigations, facilities have been set up capable of generating magnetic fields in excess of 4500 Gauss and with a working area of 7inches in diameter.

The apparatus consists basically of two "Plasmaflux" magnetic coils, model PF 7-275-455 (Fig. 42). These coils are precision, water-cooled, air core electromagnets designed to operate at 20 kilowatts per coil. They are mounted on a heavy metal framework with facility for varying the coil spacing to adjust the field shape and uniformity and

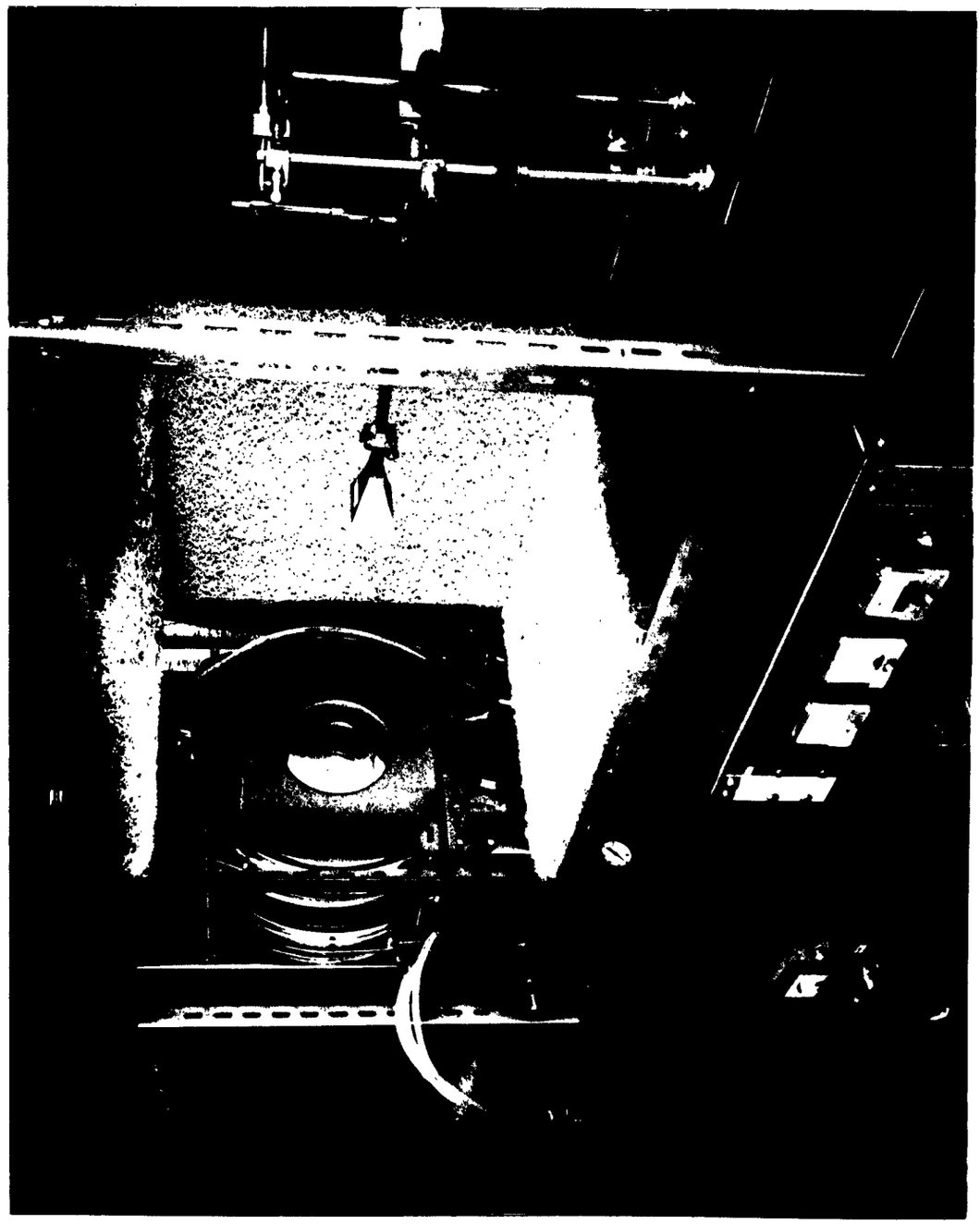

Fig. 42: Magnetic field apparatus capable of generating magnetic fields in excess of 4500 gauss in a working area of 7 inches in diameter.

further, to allow radial access for experimental apparatus and probes.

Water-cooling for the coils is provided by inlet and outlet water manifolds equipped with suitable temperature and pressure controls. A maximum inlet water pressure of 20psi can be maintained. The total water flow for two coils in parallel, operating at 20 kilowatts per coil, is 16 gpm. This hydraulically requires a differential pressure of 12 psi.

The electrical power for the magnets is provided by two "Regent" d-c arc welding supplies. These welders are each capable of delivering an open circuit potential of 70 volts, a 100% duty cycle current of 375 amps and a 35% duty cycle current of 625 amps. The magnetic coils are wired in parallel and the power supplies in series A maximum potential of 78 volts was measured across the electromagnets with this configuration. A summary of the specifications of the magnetic field facilities are given in Fig. 43.

The vacuum pumping and gas handling system is built into the supporting framework of the magnetic coils. A symmetrical input and output manifold arrangement with pressure gauges, vacuum valves and diffusion pump provide a suitable high-vacuum system and at the same time a convenient support for the plasma bottle.

Magnetic probe measurements were taken to determine the strength and uniformity of the field across the internal diameter of the magnetic coils. A precision, R.F.L. model 1890, gaussmeter with a coaxial probe was used. The probe was moved, along an axis parallel to the axis of the magnetic coils at intervals of $\frac{1}{2}$-inch across the 7-inch internal diameter. The results were traced on an X-Y recorder (Fig. 44). With a potential of 78 volts across the magnets and an intercoil spacing of $2\frac{1}{2}$-inches, a field of more than 4.5 kilogauss was measured. The uniformity of the magnetic field over a length of 3-inches was in the order of 4%.

The electromagnets together with the plasma bottle and vacuum system are positioned on a rotary turntable in such a manner that either free-space transmission of electromagnetic waves through

MECHANICAL

Working Inside Diameter	7 inches
Width	2.75 inches
Weight	135 lbs.

ELECTRICAL & MAGNETIC

Number of Turns/Coil	422
Resistance (at 20°C)/Coil	0.44 Ohms
Maximum Current/Coil	213 Amps
MCR* Single Coil	17.55
MCR* Helmholtz Pair (3" Intercoil Spacing)	25
MCR* Long Solenoid Array (Zero Intercoil Spacing)	79

COOLING

Water Requirement/Coil	0.4 GPM/Kilowatt
Maximum Inlet Manifold Press	20 PSIG.
Maximum Inlet Water Temperature	25°C

* Magnetic Conversion Ratio (Gauss per Ampere)

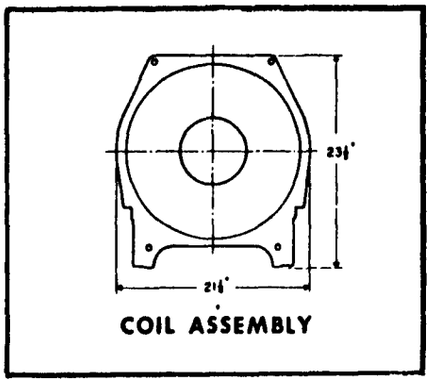

Figure43: Specification for Model PF7-275 Plasmaflux Magnetic Coil Assembly.

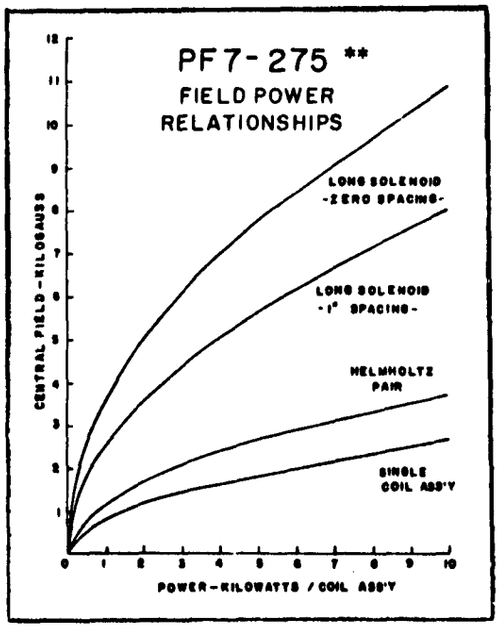

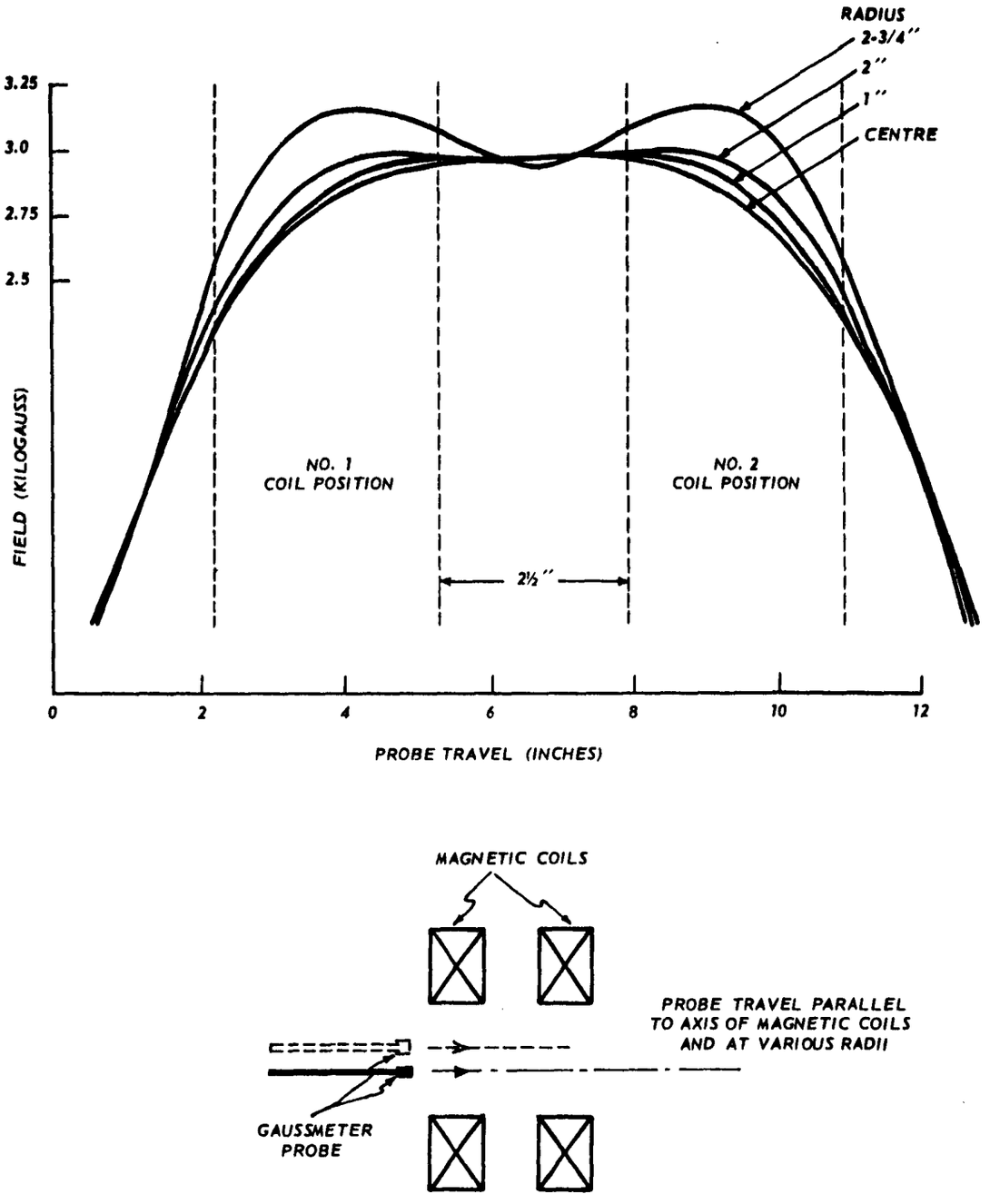

Figure 44: Magnetic Field Measurements - Helmholtz Pair.

the anisotropic plasma (Fig. 45a) or the far-field radiation of an antenna in the presence of an anisotropic slab of plasma can be made (Fig. 45b).

The water pipes, electrical cables, waveguides and vacuum lines, leading to the apparatus are fed in through rotary joints and flexible cables to allow the turntable to rotate freely through 180°.

The entire system is situated in an anechoic chamber. The apparatus itself is surrounded with microwave absorbing material to eliminate reflections.

A natural extension of the work under contract AF 19(604)-7334 would be to use the above facilities for the investigation of antenna properties in the presence of anisotropic ionized media.

V CONCLUSION

A laboratory experimental investigation has been conducted on the behaviour of a horn antenna in the presence of a plasma sheath. The effects of the plasma sheath on the radiation pattern and impedance of the antenna were determined at x-band (9.7Gc) frequencies using a fast acting microwave phase and amplitude measuring system. Using plasmas generated under controlled conditions, electron densities as high as corresponding to the plasma frequency at x-band could be obtained. It is found that at normal incidence the radiated power falls off rapidly (by as much as 25 decibels as "cut-off" is approached) with increasing electron density. The power radiated in the direction corresponding to large scanning angles increases with plasma density and may exceed the power radiated in these directions in the absence of the plasma. The presence of the plasma makes the phase front in the far-field become more plane (or may possibly reverse the curvature) than when the plasma is absent. Impedance measurements indicate that the plasma is not highly reflecting (VSWR less than 1.7) even when the plasma is very dense and hence does not present a very great mismatch to the antenna.

A theoretical model which considers the plasma as a uniform, infinite slab and takes into account diffraction around the outer edge of the plasma container has been formulated for comparison with experiment.

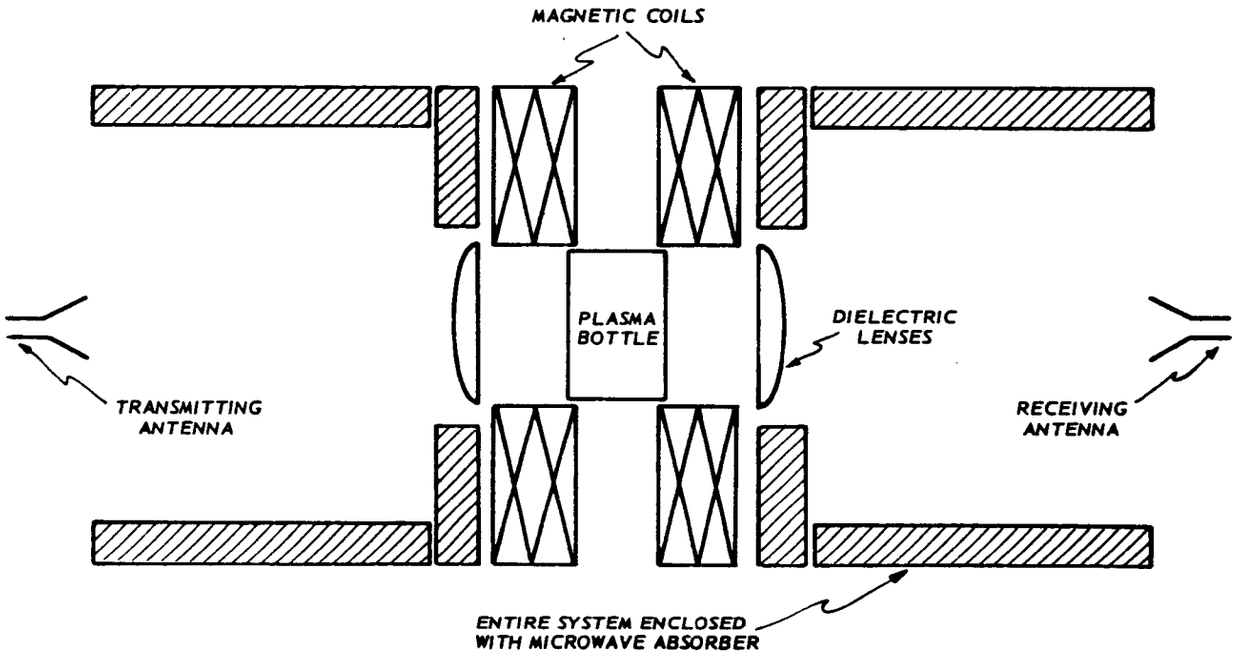

Figure 45a: Experimental Set-up for Transmission Tests on Anisotropic Media.

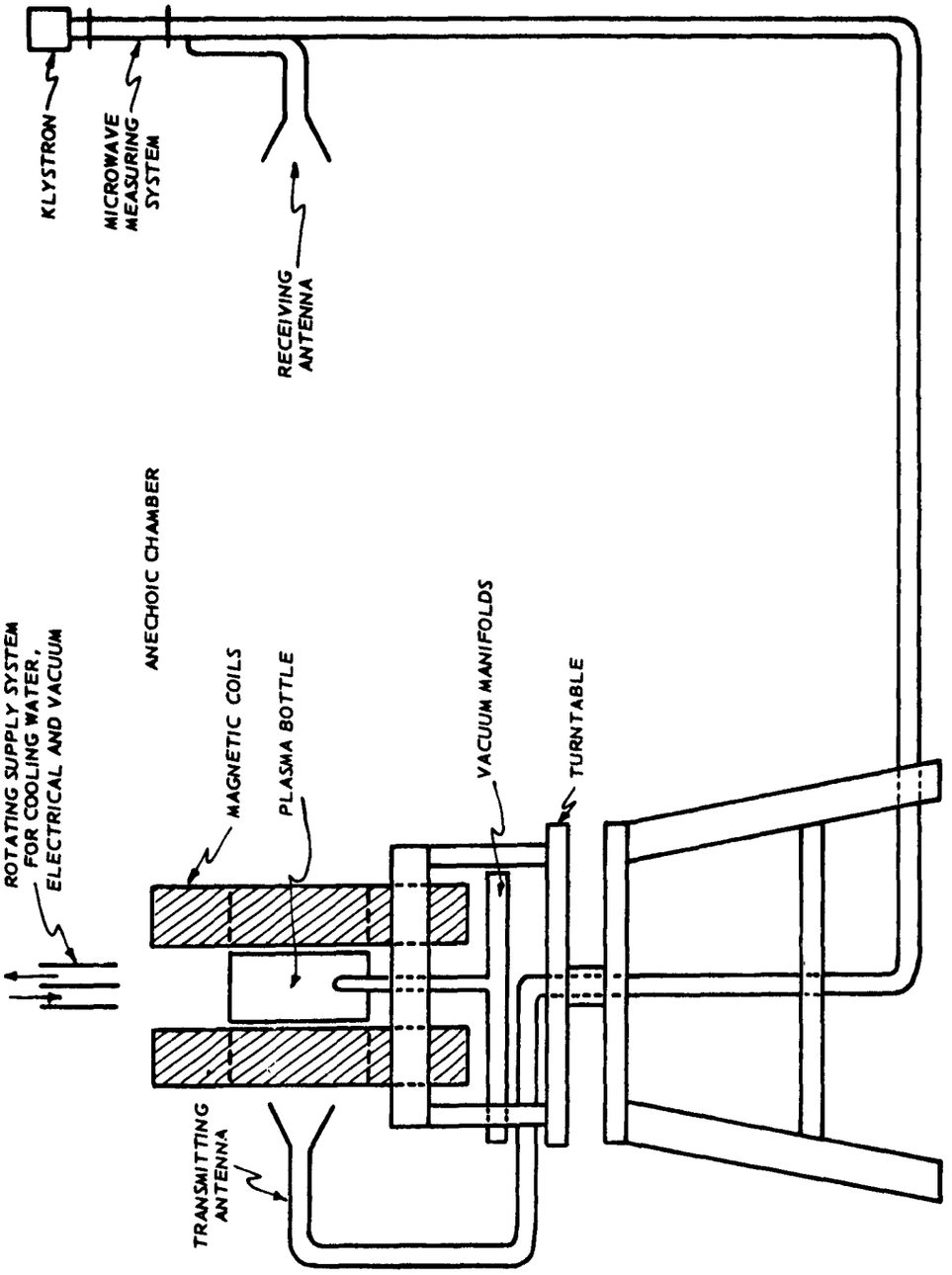

Figure 45b: Apparatus to Study Antenna Properties in the Presence of Anisotropic Media.

Some of the important features observed can be accounted for by using this model.

The influence of diffraction, refraction and reflection effects is very significant for any laboratory experiments with plasmas involving free-space microwave techniques. In many instances these phenomena predominate over the effect of the parameters of the plasma which are being determined and limit the amount (accuracy and detail) of information regarding the plasma which can be obtained. It is, therefore, essential to either minimize these effects (where possible) or to take them into account in any quantitative interpretation of experimental measurements.

Thus a comprehensive series of investigations designed to test the validity of different theoretical treatments of plasma properties and to assess the accuracy of measuring the properties of plasmas which are finite in extent using transmission or reflection of microwaves have been conducted.

Analytic results have been obtained showing the effect of the boundaries of the plasma, refractive defocussing by the plasma, non-uniformity of the plasma both in the direction of propagation and normal to the direction of propagation and diffraction due to the finite size of the plasma on the properties of electromagnetic waves transmitted through (and in some cases reflected from) a plasma.

Measurements on various experimental geometries demonstrate the influence of the dielectric boundaries of the plasma container, the effect of multiple reflection within the measurement system and the precautions which must be exercised both in the measurements and interpretation of the results. It is shown that the use of microwave lenses to obtain a plane wave incident on the plasma and a microwave lens in the receiving portion of the measurement system is essential if meaningful measurements are to be made.

The properties of a plasma generated in helium and in argon were measured using the "optimum" microwave arrangement. High values of the collision frequency were found in helium. These are attributed

to variations in electron temperature and collision cross-section due to the type of excitation used in generating the plasma.

As a result of the above investigation, it is now possible to design and conduct more quantitative experiments on the properties of antenna in ionized media. A natural extension of this study is the investigation of the properties of antennas in the presence of anisotropic ionized media. A major requirement for such investigations are suitable magnetic field facilities. Such an apparatus has been set-up and tested.

VI REFERENCES

1. F.J.F. Osborne, "A Versatile Microwave Diagnostic System for Plasma Studies", Proc. of the 3rd Symp. on Engineering Aspects of MHD (to be published).

2. M.P. Bachynski, G.G. Cloutier, "Antenna Radiation Patterns in the Presence of a Plasma Sheath", Proc. of Symp. on the Plasma Sheath, Plenum Press (to be published).

3. M.P. Bachynski, G.G. Cloutier, K.A. Graf, "Antenna Properties in the Presence of Ionized Media", AFCRL Report 62-191 March (1962).

4. M.P. Bachynski, G. Bekefi, "Investigation of Aberrations in Microwave Lens Systems", Eaton Electronics Laboratory, McGill University Technical Report No. 35 (1955).

5. R.J. Jahn, "Microwave Probing of Ionized-Gas Flows", Phys. Fluids 5, 678-686, June (1962).

6. P.W. Kuhns, "Microwave Measurements of Steady-State and Decaying Plasmas" Trans. IRE SET-8, 173-178, June (1962).

7. R. Buser, W. Buser, "Determination of Plasma Properties by Free-Space Microwave Techniques", J. Appl. Phys. 33, 2275-2282, July (1962).

8. R. Warder, M. Brodwin, A.B. Cambel, "Sources of Error in the Microwave Diagnostics of Plasmas", J. Appl. Phys. 33, 2868-2870, Sept. (1962).

9. G.R. Nicoll, J. Baser, "Comparison of Microwave and Langmuir Probe Measurements on a Gaseous Plasma", J. Elect. Cont. XII, 23-29, June (1962).

10. L. Talbot, J.E. Katz, C.L. Brundin, "Comparison Between Langmuir Probe and Microwave Electron Density Measurements in an Arc-Heated Low-Density Wind Tunnel", Phys. Fluids 6, 559-565, April (1963).

11. I.P. French, G.G. Cloutier, M.P. Bachynski, "The Absorptivity Spectrum of a Uniform Anisotropic Plasma Slab", Can. J. Phys. 39, 1273-1290 (1961).

12. K.A. Graf, M.P. Bachynski, "Transmission and Reflection of Electromagnetic Waves at a Plasma Boundary for Arbitrary Angles of Incidence", Can. J. Phys. 39, 1544-1562 (1962).

13. M.A. Heald, "The Application of Microwave Techniques to Stellarator Research", Princeton University Project Matterhorn Report MATT-17, August (1959).

14. C.B. Wharton, "International Summer Course in Plasma Physics", Danish Atomic Energy Commission Report No. 18, 579-582 (1960).

15. C.B. Wharton, D.M. Sleger, "Microwave Determination of Plasma Density Profiles", J. Appl. Phys. 31, 428-430 (1960).

16. R. Motley, M.A. Heald, "Use of Multiple Polarizations for Electron Density Profile Measurements in High Temperature Plasmas", Proc. Symp. on Millimetre Waves, Polytechnic Press N.Y., 141-154 (1960).

17. M.P. Bachynski, I.P. Shkarofsky, T.W. Johnston, "Plasmas and the Electromagnetic Field" (in press).

18. K.G. Budden, "Radio Waves in the Ionosphere", Cambridge Univ. Press (1961).

19. G.R. Nicoll, J. Basu, "Reflection and Transmission of an Electromagnetic Wave by a Gaseous Plasma", IEE (London) Monograph No. 498E, January (1962).

20. F.A. Albini, R.G. Jahn, "Reflection and Transmission of Electromagnetic Waves at Electron Density Gradients", J. Appl. Phys. 32, 75-82, January (1961).

21. F.A. Albini, R.G. Jahn, "Reflection and Transmission of Electromagnetic Waves at Electron Density Gradients", Tech. Note No. 3, Guggenheim Jet Propulsion Center, Calif. Inst. of Tech. Pasadena, October (1960).

22. M.P. Bachynski, G.G. Cloutier, K.A. Graf, "Microwave Measurements of Finite Plasmas", AFCRL-63-161, May (1963).

23. J. Morita, S.B. Cohn, "Microwave Lens Matching by Simulated Quarter-Wave Transformers", Trans. IRE, AP-4, 33-39, January (1956).

ACKNOWLEDGEMENTS

The author is indebted to Mr. B.W. Gibbs for development of much of the experimental apparatus and for carrying out most of the experimental measurements.

The research described in this report was conducted jointly by the author and Dr. G.G. Cloutier and Mr. K.A. Graf.